NASA/CR-20205001147

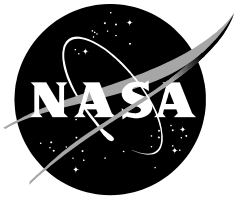

Model Rotor Hover Performance at Low Reynolds Number

Franklin D. Harris
F. D. Harris & Associates
Ames Research Center, Moffett Field, California

May 2020

NASA STI Program ... in Profile

Since its founding, NASA has been dedicated to the advancement of aeronautics and space science. The NASA scientific and technical information (STI) program plays a key part in helping NASA maintain this important role.

The NASA STI program operates under the auspices of the Agency Chief Information Officer. It collects, organizes, provides for archiving, and disseminates NASA's STI. The NASA STI program provides access to the NTRS Registered and its public interface, the NASA Technical Reports Server, thus providing one of the largest collections of aeronautical and space science STI in the world. Results are published in both non-NASA channels and by NASA in the NASA STI Report Series, which includes the following report types:

- TECHNICAL PUBLICATION. Reports of completed research or a major significant phase of research that present the results of NASA Programs and include extensive data or theoretical analysis. Includes compilations of significant scientific and technical data and information deemed to be of continuing reference value. NASA counterpart of peer-reviewed formal professional papers but has less stringent limitations on manuscript length and extent of graphic presentations.

- TECHNICAL MEMORANDUM. Scientific and technical findings that are preliminary or of specialized interest, e.g., quick release reports, working papers, and bibliographies that contain minimal annotation. Does not contain extensive analysis.

- CONTRACTOR REPORT. Scientific and technical findings by NASA-sponsored contractors and grantees.

- CONFERENCE PUBLICATION. Collected papers from scientific and technical conferences, symposia, seminars, or other meetings sponsored or co-sponsored by NASA.

- SPECIAL PUBLICATION. Scientific, technical, or historical information from NASA programs, projects, and missions, often concerned with subjects having substantial public interest.

- TECHNICAL TRANSLATION. English-language translations of foreign scientific and technical material pertinent to NASA's mission.

Specialized services also include organizing and publishing research results, distributing specialized research announcements and feeds, providing information desk and personal search support, and enabling data exchange services.

For more information about the NASA STI program, see the following:

- Access the NASA STI program home page at http://www.sti.nasa.gov

- E-mail your question to help@sti.nasa.gov

- Phone the NASA STI Information Desk at 757-864-9658

- Write to:
  NASA STI Information Desk
  Mail Stop 148
  NASA Langley Research Center
  Hampton, VA 23681-2199

NASA/CR-20205001147

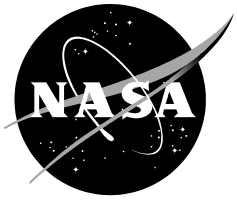

Model Rotor Hover Performance at Low Reynolds Number

Franklin D. Harris
F. D. Harris & Associates
Ames Research Center, Moffett Field, California

National Aeronautics and
Space Administration

Ames Research Center
Moffett Field, CA 94035-1000

May 2020

Available from:

NASA STI Support Services
Mail Stop 148
NASA Langley Research Center
Hampton, VA 23681-2199
757-864-9658

National Technical Information Service
5301 Shawnee Road
Alexandria, VA 22312
webmail@ntis.gov
703-605-6000

This report is also available in electronic form at

http://ntrs.nasa.gov

TABLE OF CONTENTS

LIST OF FIGURES

LIST OF FIGURES (cont.)

LIST OF TABLES

MODEL ROTOR HOVER PERFORMANCE AT LOW REYNOLDS NUMBER

Franklin D. Harris*

Ames Research Center

SUMMARY

Hover performance data from four key experiments has been analyzed in detail to shed some light on model rotor hover performance at low Reynolds number. Each experiment used the simplest blade geometry. The blades were constant chord and untwisted. Three experiments used blades with the NACA 0012 airfoil from root to tip. The NACA 0015 was used in the earliest test. The four experiments provide data spanning a Reynolds number range of 136,500 to 548,700.

The specific objective of this report is to ask and answer two questions:

1. Does blade aspect ratio influence hover performance or is rotor solidity the fundamental rotor geometry parameter for practical engineering purposes? ANSWER: Rotor solidity is the fundamental rotor geometry parameter for practical engineering purposes. Any effect of blade aspect ratio appears to be such a secondary variable that its effect lies within the range of experimental error.
2. Is Reynolds number a significant factor in scaling up hover performance to full-scale rotor performance? The answer is twofold. ANSWER: (a) Reynolds number effects on the increase of power with thrust do not appear to be a significant factor for practical engineering purposes, and (b) Reynolds number effects on minimum profile power at or very near zero rotor thrust could not be clearly established primarily because the low torque levels could not be accurately measured with the test equipment used. This has led to significant data scatter.

A number of other observations can be made based on the analysis provided herein. For instance:

1. The test matrices used in the four key references contained far too few data points. A collective pitch variation of four or five data points is insufficient to establish experimental accuracy and data repeatability.
2. A common property of the power-versus-thrust (raised to the 3/2 exponent) graphs was that this curve was linear below the onset of blade stall.
3. The blade-to-blade interference at or near zero thrust may, in fact, be creating a turbulent flow field such that the effective Reynolds number at a blade element is considerably greater than what theories using two-dimensional (2D) airfoil properties at a blade element would calculate.
4. Definitive experiments answering the two key questions have yet to be made.

* F. D. Harris & Associates, 15505 Valley Drive, Piedmont, Oklahoma 73078.

INTRODUCTION

Over the last eight decades, four key experiments have been conducted dealing with the question of the effect of the number of blades on thrust versus power behavior in hovering flight. The tests used untwisted rectangular blades. In three of the experiments the blades used the NACA 0012 airfoil from blade root to tip. The earliest experiment, reported in 1937, used blades having the NACA 0015 airfoil from root to tip. Taken together, the four model rotor experiments also shed some light on the effect of Reynolds number because the tip Reynolds numbers varied from a low of 139,000 up to 525,000. The diameters of these small rotors varied from 52 to 60 inches.

This report uses the reported experimental data from the following four tests (Refs. 1-4) to examine what influence Reynolds number has on the hovering performance of these small rotors. Appendix A provides the experimental data examined herein in tabulated form.

Ref. 1. Montgomery Knight and Ralph Hefner, *Static Thrust Analysis of the Lifting Airscrew*, NACA TN 626, Dec. 1937.

Ref. 2. Anton Jack Landgrebe, *An Analytical and Experimental Investigation of Helicopter Rotor Performance and Wake Geometry Characteristics*, USAAMRDL TR 71-24, June 1971.

Ref. 3. Manikandan Ramasamy, *Hover Performance Measurements Toward Understanding Aerodynamic Interference in Coaxial, Tandem, and Tilt Rotors*, AHS Journal, vol. 60, no. 3, June 2015.

Ref. 4. Mahendra Bhagwat and Manikandan Ramasamy, *Effect of Blade Number and Solidity on Rotor Hover Performance*, AHS Specialists' Conference on Aeromechanics Design for Transformative Vertical Flight, San Francisco, CA, Jan. 16-18, 2018.

A fifth document (Ref. 5) not available to the public when written (but still in the author's possession because of its historical value) is included at the very end of this report. This Boeing Company – Vertol Division, Interoffice Memorandum was prepared by Ron Gormont in June of 1970.

The four hover performance experiments were conducted with rather similar blades as Tables 1, 2, and 3 show. Even the range in tip Reynolds number and tip Mach number covers many experiments with small, model rotor systems as Figure 1 below shows. It should be noted, however, that Landgrebe's experiment was conducted with Mach scaled blades, which is quite typical of the rotorcraft industry's requirements. On the other hand, the experiments conducted by Knight and Hefner at Georgia Tech and Ramasamy and Bhagwat at NASA Ames Research Center were more along the lines of basic research.

This report (1) examines the four experimental data bases following Knight and Hefner's 1937 finding that solidity (whether changed by blade number or blade aspect ratio) is key, (2) compares blade element momentum theory (BEMT) to test data, (3) provides a semi-empirical equation to estimate the hover power required for a given thrust, and (4) offers recommendations for additional experiments.

Table 1. Number of Blades Tested

Ref.	b = 2	3	4	5	6	7	8	Reynolds Number Range
1	Yes	Yes	Yes	Yes	No	No	No	267,825 Only
2	Yes	No	Yes	No	Yes	No	Yes	411,200 to 548,720
3	Yes*	Yes	Yes*	Yes*	Yes	No	No	221,560 to 329,984
4	Yes	Yes	Yes	Yes	Yes	No	No	139,528 to 334,866

* Note: Tabulated data not currently available.

Table 2. Blade Geometry

Ref.	Diameter (in.)	Chord (in.)	Twist (deg.)	Blade Aspect Ratio	NACA Airfoil	Hub Diameter (in.)	Flap Hinge (in.)	Root Cutout (% R)
1	60.00	2.000	0	15.00	0015	3.00	1.000	16.7
2	53.50	1.470	0	18.20	0012	na	1.816	14.8
3	52.10	2.290	0	11.37	0012	??	??	19.1
4	52.25*	2.297	0	11.37	0012	??	??	19.0

* Note: Reduced diameter blades were tested.

Table 3. Baseline Solidity Comparison

Ref.	b = 2	3	4	5	6	7	8
1	0.0424	0.0637	0.0849	0.1061	No	No	No
2	0.0350	No	0.0700	No	0.1050	No	0.1400
3	0.0560*	0.0840	0.1120*	0.1400*	0.1680	No	No
4	0.0586	0.0880	0.1172	0.1466	0.1759	No	No

* Note: Tabulated data not currently available

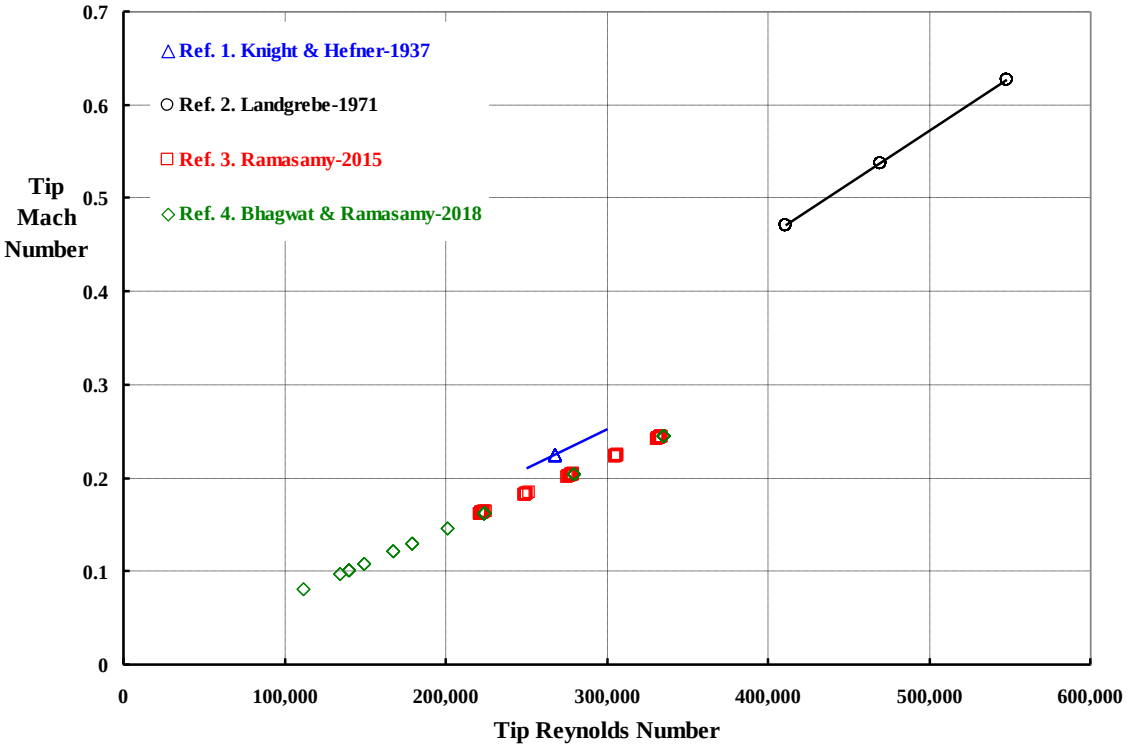

Figure 1. Test data range for the four key experiments studied in this report.

USE OF SOLIDITY

The four experiments used a number of blades (Table 1) to investigate hover performance. However, each referenced experiment differed in the blade aspect ratio that was selected (Table 2). Therefore, keep in mind that the use of solidity as an important rotor system characteristic might be better defined as

$$\text{Solidity} = \sigma = \frac{b}{\pi(R/c)} \quad \text{where } R = \text{radius and } c = \text{chord} \qquad \text{Eq. (1)}$$

When solidity is viewed in this manner, the following question is frequently raised: If solidity is obtained with a few, low aspect ratio blades, will that give the same hover performance obtained with many, high aspect ratio blades? Asking this question in another way: At equal solidity, does the hover performance *really* depend on just the ratio of blade number to blade aspect ratio? Table 3 show that the four experiments taken together did, in fact, provide experimental data to examine this question.

This fundamental question about the use of solidity was addressed quite specifically by Landgrebe (Ref. 2, page 16). He summarized the question with these words:

> Effect of Aspect Ratio at Constant Solidity
>
> Of particular interest to the rotor designer is the trade-off in performance between chord and number of blades while maintaining constant rotor solidity (total blade area and disc area held constant). The experimental results comparing the hover performance for eight, 18.2-aspect-ratio blades (c = 1.47 in.) and six 13.6-aspect-ratio blades (c = 1.96 in.) at a constant solidity of 0.140 are presented in Figure 21 [see Figure 2 below]. Over the thrust range tested (i.e., up to the stall flutter boundary), the results are essentially equivalent for the two configurations. The existence of the stall flutter boundary prohibited the investigation of the trade-off of number of blades and chord at conditions associated with deep penetration into stall. The eight narrow-chord blades exhibited stall flutter at lower performance levels than the six wide-chord blades. This implies that the aeroelastic, rather than the aerodynamic, characteristics of the blades may ultimately be the determining factor in selecting blade aspect ratio.

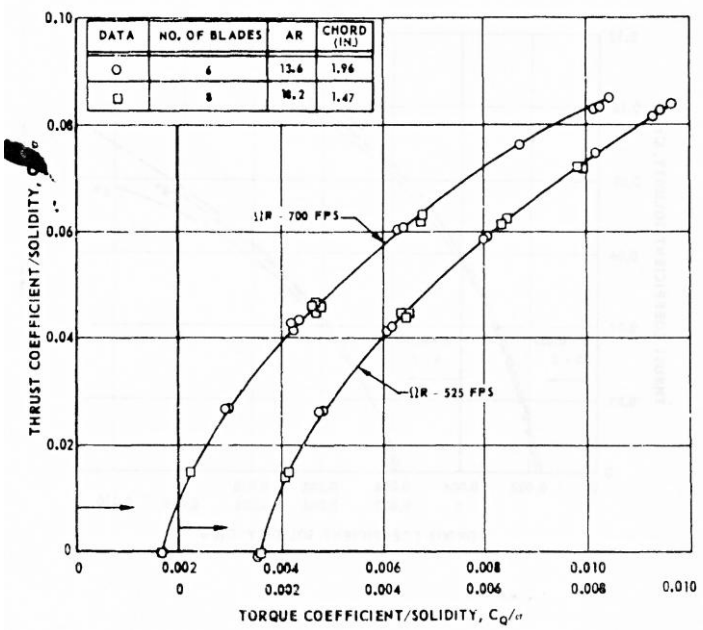

Figure 2. Landgrebe's experiment reinforces the use of solidity as the nondimensional parameter when comparing two different rotor system geometries. The blade twist in this experiment was a linear –8 degrees for both blade sets.

A very important point to note about Landgrebe's example is that the tip Reynolds number varied considerably (548,000 to 959,500). But two sets of data were tested at a tip Reynolds number of 548,000 (i.e., b = 8, AR = 10.2, V_t = 700 and b = 6, AR = 10.2, V_t = 525). Landgrebe's example therefore suggests that in this tip Reynolds number range there is no effect of Reynolds number or blade aspect ratio.

A second example of the just how fundamental solidity can be became available in 2017 (Ref. 6, pages 19–22). Harris wrote:

> **Blade Number at Equal Solidity**
>
> During May of 1994, Bell Helicopter Textron Inc. (BHTI) conducted checkout of two 0.15-Mach-scaled JVX model proprotors. This initiated subsequent testing in the NASA Langley Research Center 14- by 22-Foot Subsonic Wind Tunnel from June 13 to July 29, 1994. The purpose of the wind tunnel test was to quantify and compare acoustic, aerodynamics, and Blade Vortex Interaction (BVI) characteristics of two similar tiltrotor rotor systems with different numbers of blades but of equal solidity.
>
> The debugging and checkout of BHTI's Power Force Model was conducted at Bell's facility. This provided hover performance data for both the three- and the four-bladed configurations (fig. 22 and table 2), which was included in the complete data report (ref. 20). The performance data is provided in Appendices F and G and shown in figures 23 to 25 herein.

The experimental evidence of this second example is shown here with Figure 3. In this example, the tip Reynolds number was well above one-half million because of the high tip Mach number at which the test was conducted.

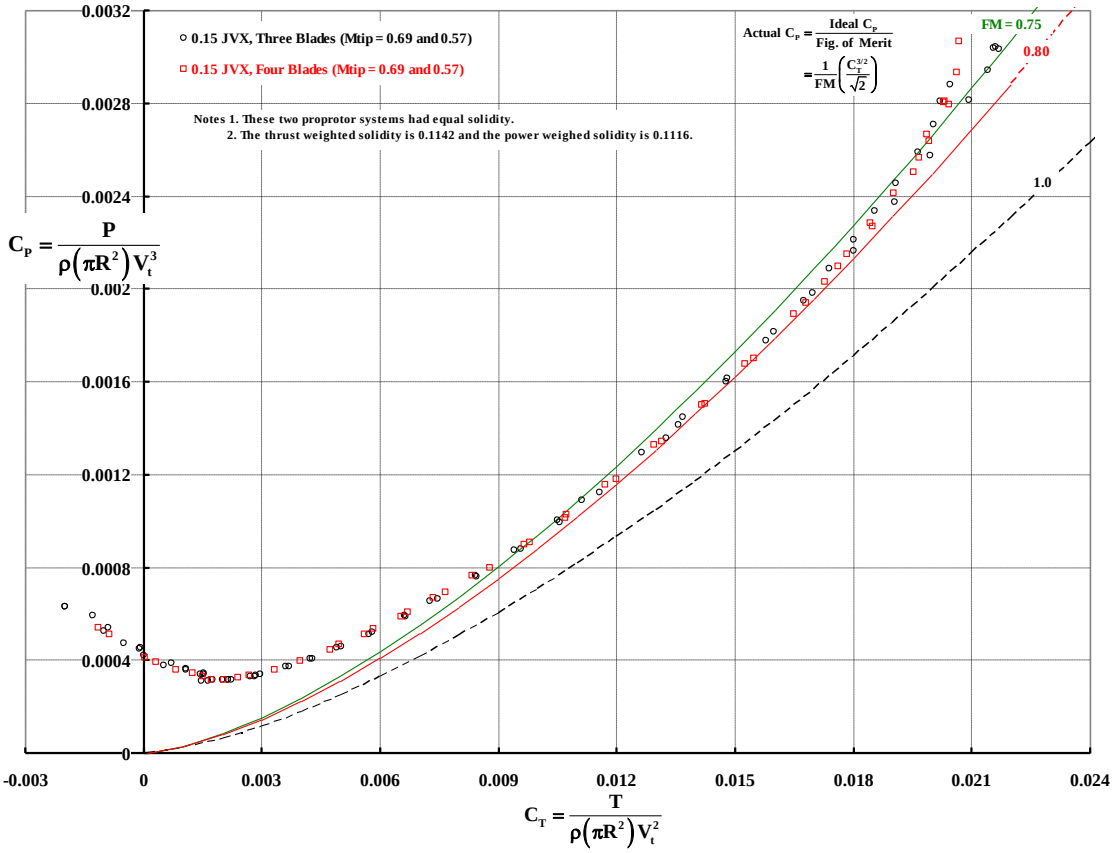

Figure 3. Bell's experiment reinforces the use of solidity as the correct parameter when blade aspect ratio and number of blades are being studied.

A third example of just how fundamental solidity can be became available in October of 2012 (Ref. 7, pages 172–178). When applied to hover performance of some 40 odd full-scale, single rotor helicopters, Harris wrote (on page 175):

> The results of applying equation 2.120 are shown in Fig. 2-74. This figure reflects modern results based on hover engine power required (out of ground effect) obtained with 40 single rotor helicopters [see Figure 4 below]. This group does not include results where compressibility was an obvious factor, such as those reported by Ritter [207]. A little statistical analysis plus educated guessing shows that the average constants for the 40 helicopters are:
>
> - Main rotor minimum airfoil drag coefficient (C_{do}) = 0.008.
> - Tail rotor minimum airfoil drag coefficient ($C_{do\text{-}tr}$) = 0.016.
> - Tail rotor induced-power correction factor (k_{tr}) = 1.35.
> - Main rotor transmission efficiency (η_{mr}) = 0.96.
> - Tail rotor transmission efficiency (η_{tr}) = 0.95.
>
> Because the flight test reports give little or no information about accessory power, I lumped SHP_{acc} and error into one constant horsepower for each individual helicopter. This lumped sum yielded 28 results with less than 5 percent error, 10 results with between 5 and 10 percent error, and 2 results with between 10 and 15 percent error when the blade element results were compared to experiment. These are percentages of the lowest-recorded engine shaft horsepower of the respective helicopter.

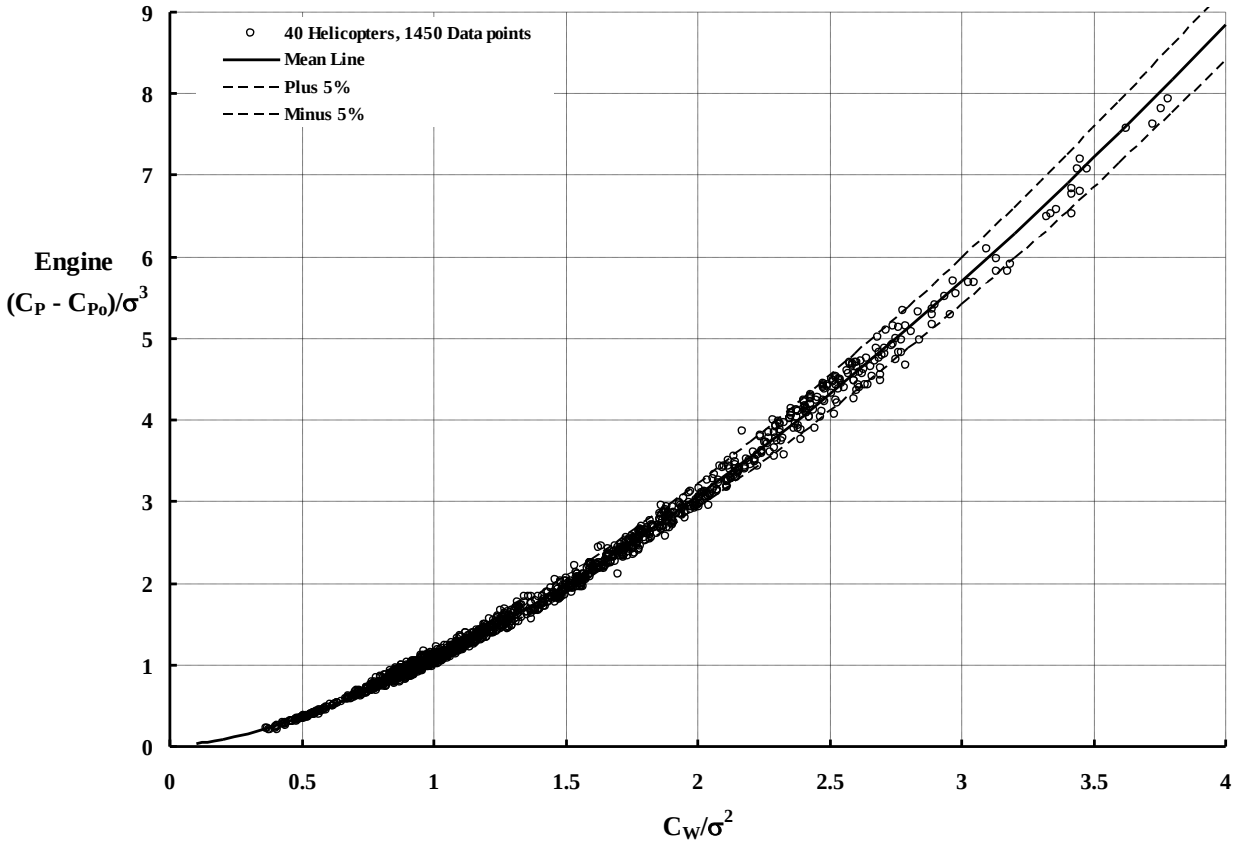

Figure 4. Flight test data from 40 full-scale, single rotor helicopters show that Knight and Hefner's similarity parameters remove solidity as a variable for engineering purposes (Ref. 7, page 175).

KNIGHT AND HEFNER'S BLADE ELEMENT MOMENTUM THEORY

The use of solidity as a nondimensional parameter became quite clear to Knight and Hefner as they reported in 1937 (Ref. 1). They presented blade element momentum theory (BEMT) in quite a different form than that shown in highly respected text books such as References 8 and 9. Knight and Hefner's form is provided in more detail in Appendix B herein. In summary, they began BEMT with the classical assumption that a blade element has an angle of attack (α) that can be calculated as

$$\alpha = \theta - \phi \qquad \text{Eq. (2)}$$

where (θ) is the geometric blade pitch angle and (ϕ) is the inflow angle.[1] Knight and Hefner clearly stated that all angles were assumed to be small. Now, applying BEMT yields the result that the inflow angle is calculated from

$$\phi = \frac{\sigma a}{16x}\left(\sqrt{1+\frac{32\theta x}{\sigma a}}-1\right) \qquad \text{Eq. (3)}$$

where (a) is the lift curve slope of the airfoil commonly taken as 5.73 per radian and (x) is the nondimensional blade radius station, calculated as x = r/R. Knight and Hefner saw that the blade element of attack would then appear as

$$\alpha = \theta - \frac{\sigma a}{16x}\left(\sqrt{1+\frac{32\theta x}{\sigma a}}-1\right) \qquad \text{Eq. (4)}$$

To Knight and Hefner, it was a simple step to factor ($\sigma a/16$) out in Eq. (4) to show that the blade element of attack could be written as

$$\alpha = \frac{\sigma a}{16}\left[\frac{16\theta}{\sigma a} - \frac{1}{x}\left(\sqrt{1+\frac{32\theta x}{\sigma a}}-1\right)\right] = \frac{\sigma a}{16}\left[\Theta - \frac{1}{x}\left(\sqrt{1+2\Theta x}-1\right)\right] \qquad \text{Eq. (5)}$$

and that the blade geometric angle (θ) should be used in their BEMT analysis as ($\Theta = 16\theta/\sigma a$). They used Eq. (5) as the basis for their derivation of hover performance thrust and power equations. In this regard they approached the classical problem by calculating the primary blade element force coefficients of lift and drag assuming

$$C_\ell = a\alpha \quad C_d = C_{do} + \delta\alpha^2 \qquad \text{Eq. (6)}$$

when a symmetrical airfoil such as the NACA 0012 or 0015 was under consideration.

The calculation of a thrust coefficient (C_T), induced power coefficient ($C_{P\text{-ind}}$), minimum profile coefficient (C_{Po}), and delta profile power due to lift (ΔC_{Po}) was a relatively simple matter of radial integration as Appendix B shows. In summary, the results are

$$C_T = \frac{\sigma^2 a^2}{32}F_T \quad C_{P-ind} = \frac{\sigma^3 a^3}{512}F_{P-ind}$$
$$C_{Po} = \frac{\sigma C_{do}}{8} \quad \Delta C_{Po} = \frac{\delta}{a}\frac{\sigma^3 a^3}{512}F_{\Delta Po} \qquad \text{Eq. (7)}$$

[1] The cover of recent AHS Journals (with the equation at the top of the cover page) provides the more complete solution to BEMT theory for the inflow ratio (λ). The inflow angle is then calculated as $\phi = \lambda/x$.

The last step Knight and Hefner took was to state that if the minimum profile power coefficient is subtracted from the total power coefficient (i.e. $C_P - C_{Po} = C_{P\text{-ind}} + \Delta C_{PO}$) then the correct way to begin studying hover performance *with rectangular blades having zero twist using the same airfoil from blade root to tip* would be to graph

$$\frac{C_P - C_{Po}}{\sigma^3} \text{ versus } \frac{C_T}{\sigma^2} \quad \text{and} \quad \frac{C_T}{\sigma^2} \text{ versus } \frac{\theta}{\sigma} \ . \qquad \text{Eq. (8)}$$

They assumed that any variations in airfoil lift curve slope (a = 5.73 per rad.) would be small.

EXPERIMENTAL DATA AND COMPARISON TO BEMT

The four hover performance experiments were conducted with rather similar blades as Tables 1, 2, and 3 confirm. Even the range in tip Reynolds number and tip Mach number covers many experiments with small, model rotor systems as Figure 1 showed. It should be noted, however, that Landgrebe's experiment was conducted with Mach scaled blades, which is quite typical of the rotorcraft industry's requirements. On the other hand, the experiments conducted by Knight and Hefner at Georgia Tech and Ramasamy and Bhagwat at NASA Ames Research Center were more along the lines of basic research.

The following discussion presents the four experiments studied in this report and the comparison to BEMT in chronological order.

Reference 1. Montgomery Knight and Ralph Hefner, 1937.

These researchers conveyed the background and purpose for their study in the introduction to their 1937 60-page report, writing:

> The problem of greater safety in flight is today commanding more and more attention. Two different methods of attack are being developed at present. One of these consists of improving the conventional fixed-wing airplane through such modifications as Handley Page slots, wing profiles giving smooth maximum lift characteristics, methods of obtaining more complete rolling and yawing control in stalled flight, and other special devices. The alternative method is that of developing a type of aircraft in which there will always be relative motion between the lifting surfaces and the air, regardless of the motion or attitude of the aircraft as a whole. This type is exemplified by the autogiro and the various experimental helicopters, of which the Breguet–Dorand is the most outstanding recent example (reference 1).
>
> In order to investigate the possibilities of the rotating-wing type of aircraft, a general study of the vertical motion of the lifting airscrew has been undertaken at the Daniel Guggenheim School of Aeronautics of the Georgia School of Technology. This project is receiving financial support from the National Advisory Committee for Aeronautics and the State Engineering Experiment Station of Georgia.
>
> The purpose of this report is to present the results of the first part of this investigation, which covers the phase of static thrust or hovering flight of the helicopter. Glauert's assumptions (reference 2) furnish the background for the theoretical portion of the study. However, the induced velocity through the rotor is determined on the basis of vortex theory rather than by using the concept of the "actuator disk." This change has been made because the vortex theory offers a much clearer picture of the mechanism of airscrew thrust without materially complicating the derivation of the induced velocity equation, which is identical for both methods.
>
> The experimental part of the analysis provides numerical values of such parameters as are essentially empirical and serves to show the agreement between the calculated and actual values of thrust and torque for four different rotor models.

Knight and Hefner proved their point that the most informative way to deal with solidity variations was to plot $\frac{C_T}{\sigma^2}$ versus $\frac{\theta}{\sigma}$ and $\frac{C_P - C_{Po}}{\sigma^3}$ versus $\frac{C_T}{\sigma^2}$ as Figures 5 and 6 below clearly show. The balance system used to obtain such very accurate data is described in considerable detail in their report. For instance, blade pitch angle was set to within ±0.05 degrees. Their few paragraphs on this and other aspects of the test should be of interest even to today's researchers.

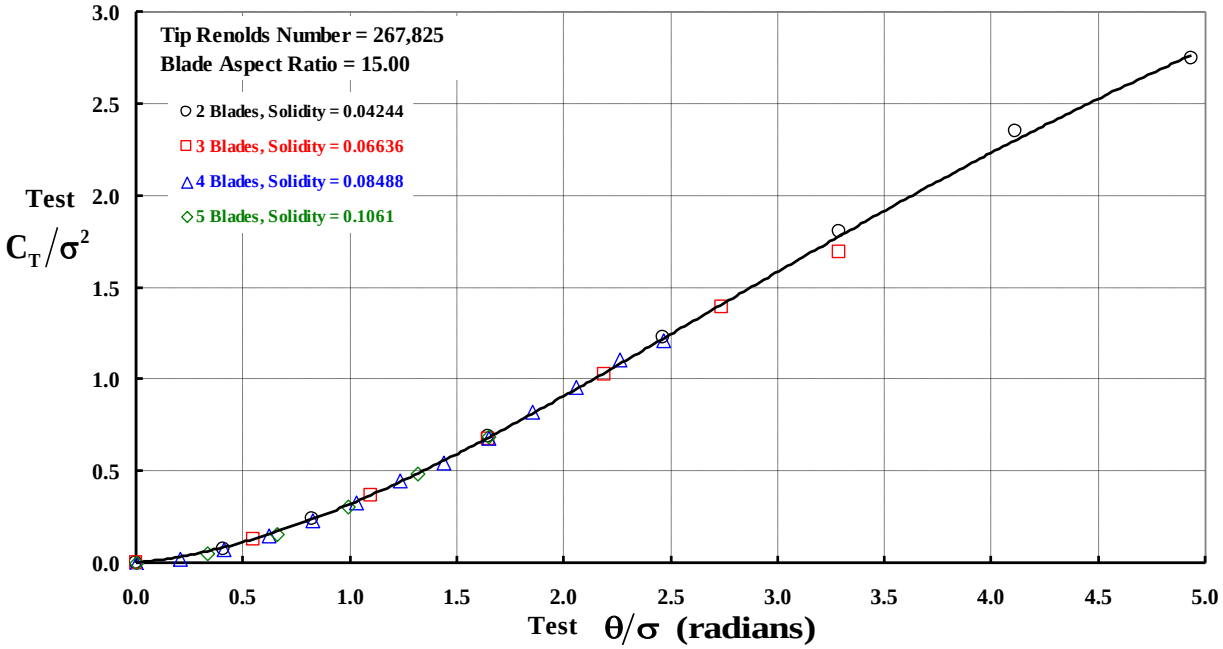

Figure 5. Knight and Hefner proved experimentally that thrust versus collective pitch should be nondimensionized as shown here. However, solidity was varied with only one blade aspect ratio. Note that their experiment was conducted at a relatively low tip Reynolds number.

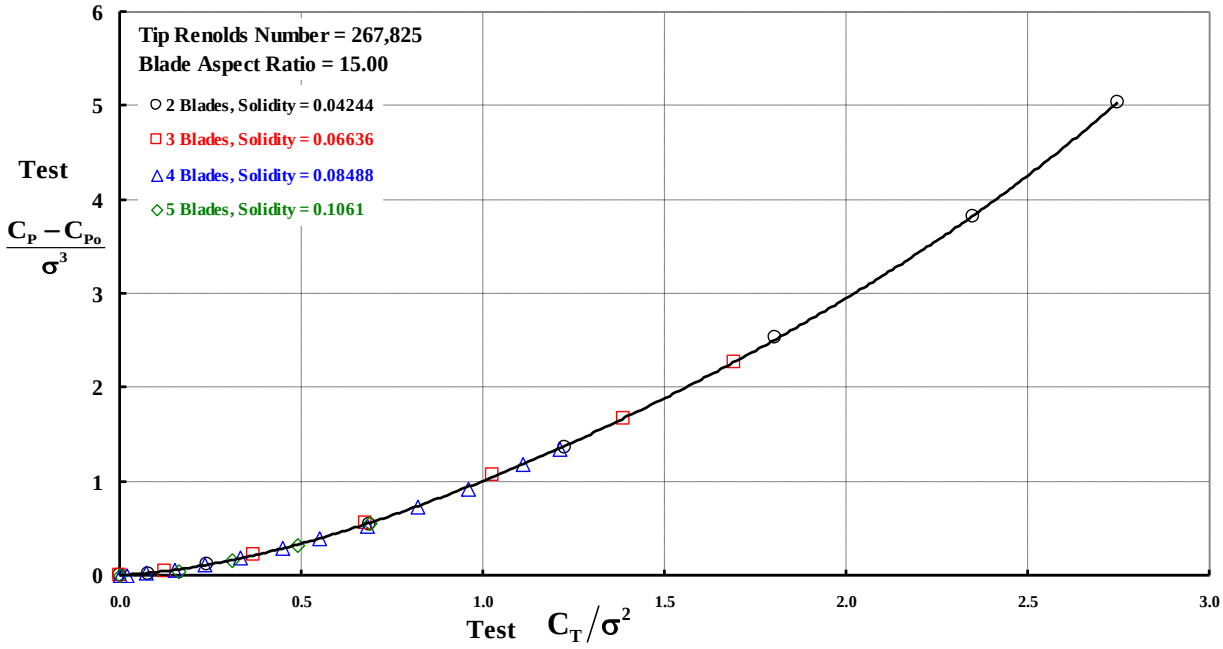

Figure 6. The use of solidity *changed by either blade number or blade aspect ratio* in power-versus-thrust performance calculations was generally accepted for over four decades.

To prepare for the comparison of their of BEMT form, they needed reasonable values of the airfoil's lift curve slope (a) and the airfoil drag coefficient's increase due to angle of attack (δ) as required by Eq. (6). Their results for a 6-foot-span and 6-inch-chord wing in the Georgia Tech wind tunnel are provided here as Figure 7. The test of the NACA 0015 was conducted at a Reynolds number of 242,000. They concluded that an airfoil's lift curve slope (a) should be about 5.75 per radian and the airfoil drag coefficient's increase due to angle of attack (δ) was on the order of 0.75 for a Reynolds number of 242,000. Note that the maximum lift coefficient appears (from Figure 7) to be somewhat above 0.9. The excessive drag rise with airfoil angle of attack due to stall onset begins at an angle of attack of about 11 degrees (0.192 radians). In fact, an approximate drag coefficient versus angle of attack up to 12 degrees would be

$$\text{Airfoil}\, C_d = 0.0113 + 0.75\alpha^2 + 1{,}000\left(\alpha - 0.192\right)^{11/4} \text{ with } \alpha \text{ in radians, RN} = 242{,}000 \quad \text{Eq. (9)}$$

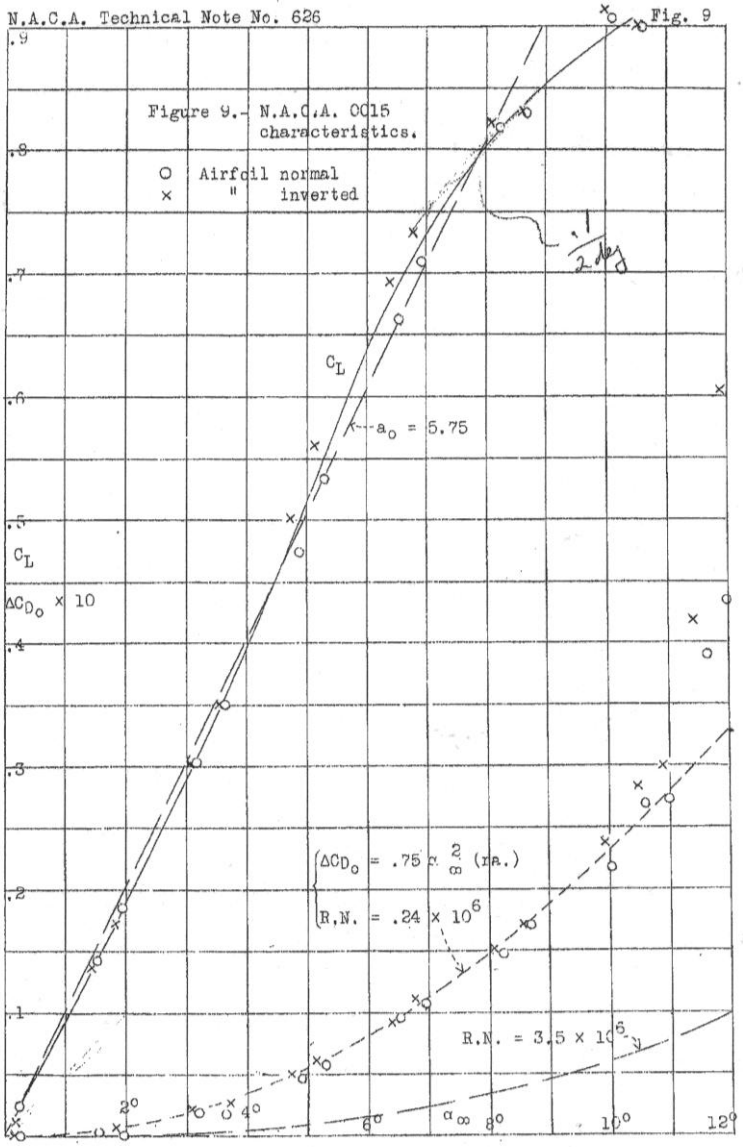

Figure 7. NACA 0015 lift and drag coefficients at a Reynolds number of 242,000. Note that at a Reynolds number of 3.5 million, $\Delta C_{do} = 0.228\ (\alpha \text{ in rad.})^2$.

The accuracy with which Knight and Hefner's use of BEMT predicts their experimental data is shown in Figures 8 and 9. The author has rarely seen such an accurate comparison for thrust versus collective pitch as Figure 8 displays. On the other hand, Figure 6 indicates that BEMT does not predict measured $(C_P - C_{Po})/\sigma^3$ by a first-order factor of about 1.126. The immediate question is this: Is the error in induced power ($C_{P\text{-ind}}$) or delta profile power (ΔC_{Po}) OR in both power elements? As of mid-2019, the author has not found a definitive answer.

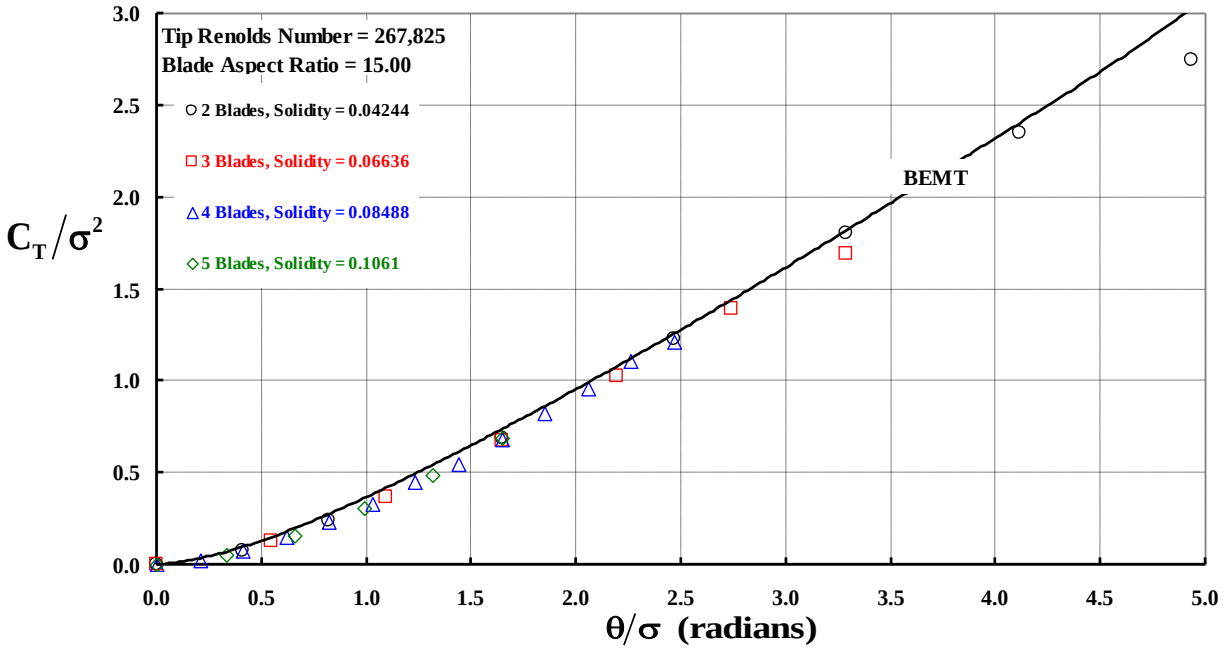

Figure 8. BEMT and experiment for Knight and Hefner's thrust coefficient vs. collective pitch are in rarely seen agreement.

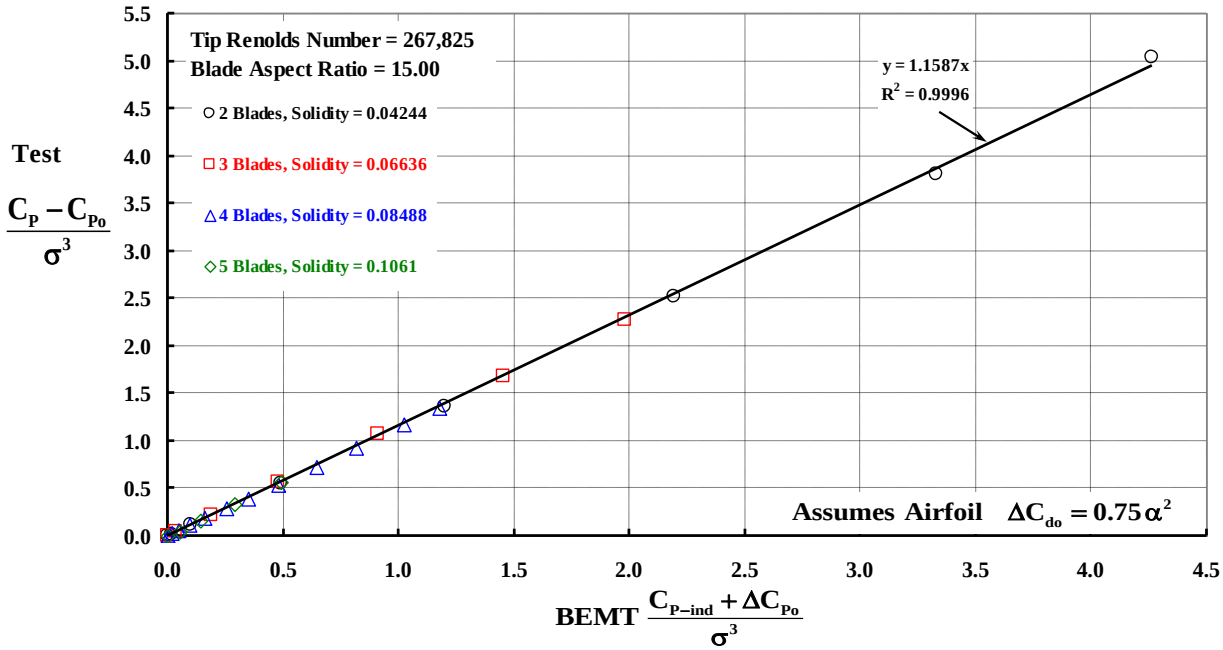

Figure 9. Knight and Hefner's experiment showed that BEMT gave a very poor prediction of the hover power required for a given thrust regardless of the number of equal aspect ratio blades.

Reference 2. Jack Landgrebe, June 1971.

Landgrebe's introduction provides a glimpse of the intermediate steps taken between the BEMT of 1937 and the completely free wake in common use today. He began his 1971 report by writing:

> The need for attaining peak lift system performance is greater with rotary-wing VTOL aircraft than with conventional aircraft. This results directly from the generally lower payload to gross weight ratio of such aircraft, which, in turn, increases the payload penalty associated with any unexpected deficiencies in performance that might arise as a result of shortcomings in the design analyses employed. For example, since the payload is typically 25% of the gross weight, a performance deficiency of 1% in lift capability can result in a 4% reduction in payload.
>
> As described in Reference 1, commonly used theoretical methods become inaccurate as number of blades, blade solidity, blade loading, and tip Mach number are increased. The discrepancies noted appear to stem from simplifying assumptions made in the analyses regarding the geometric characteristics of the rotor wake. In Reference 1, a method for considering the effects of wake contraction on hover performance was introduced. This computerized method developed at the United Aircraft Research Laboratories (UARL) and termed the UARL Prescribed Wake Hover Performance Method, requires a prior knowledge of the wake geometry. However, at the time Reference 1 was written (1967), available wake geometry data were extremely limited. Due to the expense involved, systematic wake geometry data on full-scale rotors were almost nonexistent. Available model results, on the other hand, were limited to rotors having three blades or less and operating at low tip Mach numbers. Thus, two methods of approach were initiated under this investigation to obtain the required wake geometry information. In the first an experimental investigation, using model rotors, was conducted in which a systematic, self-consistent set of data on rotor performance and associated wake geometry characteristics was obtained for a wide range of blade designs and operating conditions. In the second, an available analytical method for predicting rotor wake geometry in forward flight, described in Reference 2, was extended to the hover condition. Briefly, the method developed involves the establishment of an initial wake model comprised of finite vortex elements and the repeated application of the Biot-Savart law to compute the velocity induced by each vortex element at the end points of all other vortex elements in the wake. These velocities are then integrated over a small increment of time to determine the new positions of the wake elements, and the entire process is repeated until a converged wake geometry is obtained.
>
> The incorporation of the experimental and analytical wake geometry in the Prescribed Wake Method results in two analyses (the Prescribed Experimental Wake Analysis and the Prescribed Theoretical Wake Analysis) for computing hover performance. The availability of model rotor data permits the evaluation of these analyses by (1) providing experimental wake data both for input to the Prescribed Experimental Wake Analysis and for comparison with predicted wake geometry results of the Prescribed Theoretical Wake Method, and (2) providing consistent experimental performance data for comparison with predicted performance results. Thus, the principal objectives of this investigation were to:
>
> (a) Provide experimental information on the performance and wake geometry characteristics of hovering model rotors as influenced by number of blades, blade twist, blade aspect ratio, rotor tip speed, and blade collective pitch setting
>
> (b) Modify an existing forward–flight distorted wake program to permit the prediction of the wake geometry characteristics in hover
>
> (c) Evaluate the accuracy of various hover performance theories having differing rotor wake geometry assumptions
>
> Included in this report are: (1) a description of the model rotor experimental program, (2) a discussion of the experimental rotor performance and wake geometry results, (3) comparisons of the experimental wake geometry results with other experimental sources, (4) descriptions of the theoretical methods for predicting wake geometry and hover performance, (5) a discussion of the results of the evaluation of the wake geometry analysis, and (6) a discussion of the results of the evaluation of the theoretical methods for predicting hover performance.

Landgrebe's report provides the influence of blade number at three Reynolds numbers: 411,200; 469,950; and 548,720. Data at the highest Reynolds number, illustrated in Figures 10 and 11, clearly show that the early BEMT created a shortcoming that rotorcraft engineers had in dealing with blade aerodynamic stall and stall flutter. These deficiencies were in addition to the lack of a free-wake model, the problem Landgrebe was reporting on.

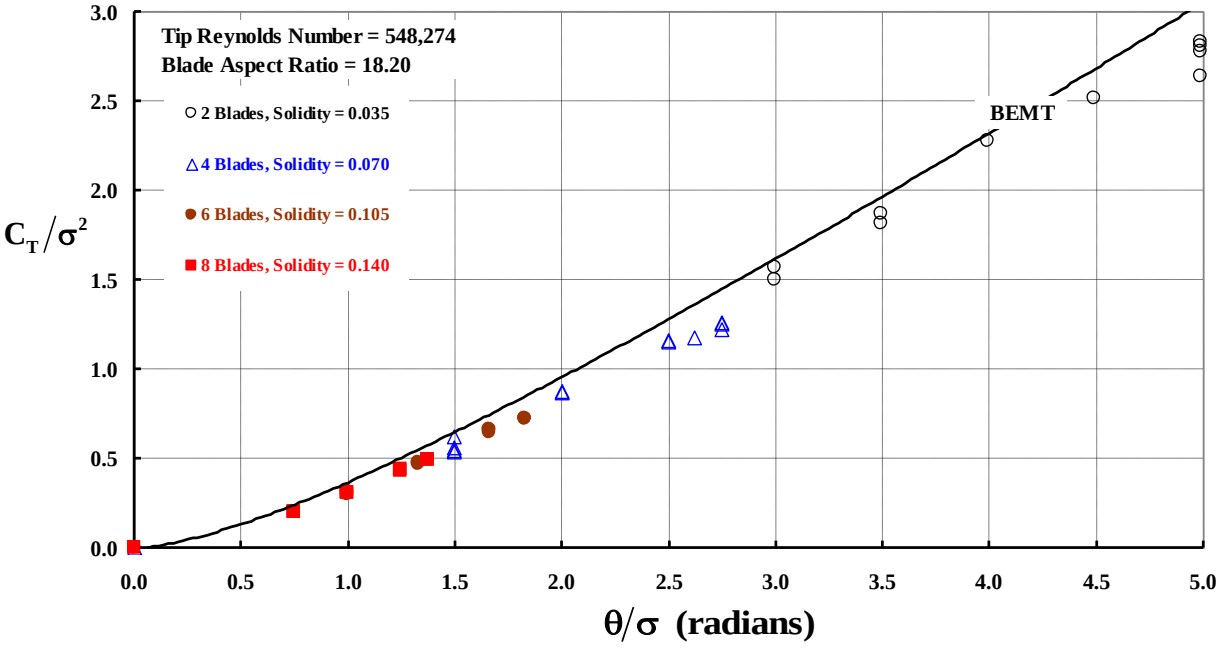

Figure 10. Evidence of blade stall appears in Landgrebe's thrust vs. pitch data.

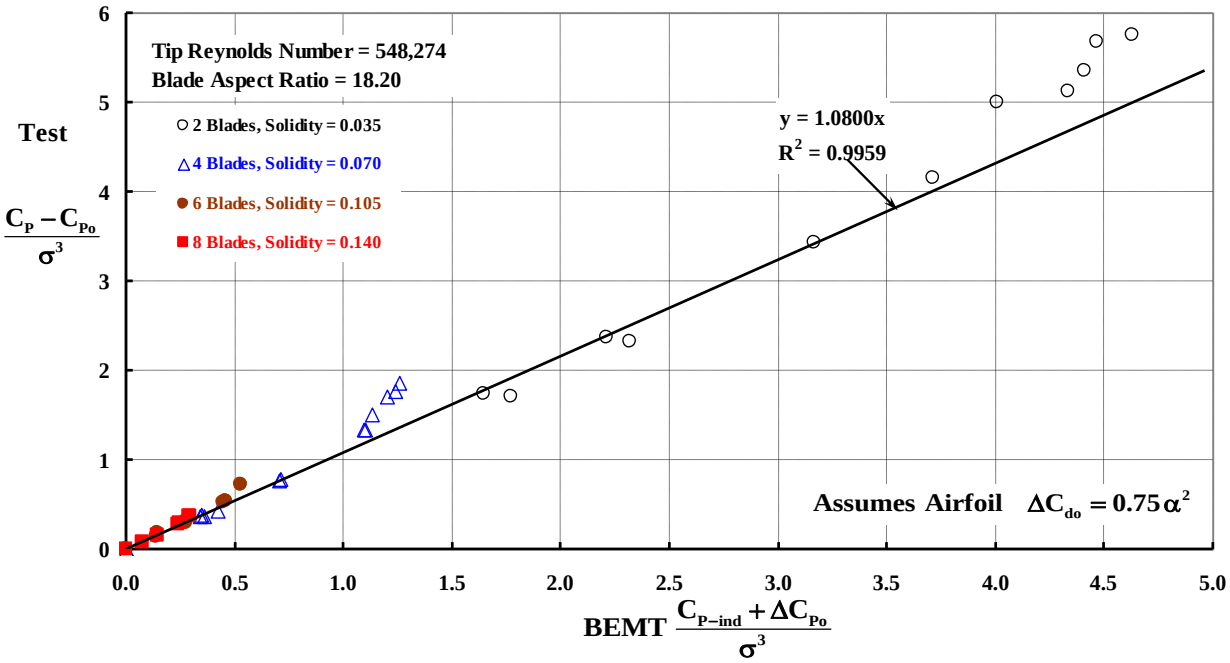

Figure 11. The tip Mach number at a tip Reynolds number of 548,274 was 0.627. Blade stall is clearly evident in this power vs. thrust data. Note that if $C_T/\sigma = 0.1$ is taken as the measure of blade stall onset, then in Knight and Hefner's notation stall onset would begin at $C_T/\sigma^2 = 0.1/\sigma$.

Landgrebe repeated his hover performance test at an intermediate Reynolds number of 469,949 and showed that solidity should be accounted for as Knight and Hefner determined and Figure 12 confirms. With respect to power, BEMT underpredicted the test data by a factor of 1.080 at a tip Reynolds number of 548,274 as shown in Figure 11. Test results shown at a Reynolds number of 469,949 in Figure 13 give an underprediction factor of 1.207.

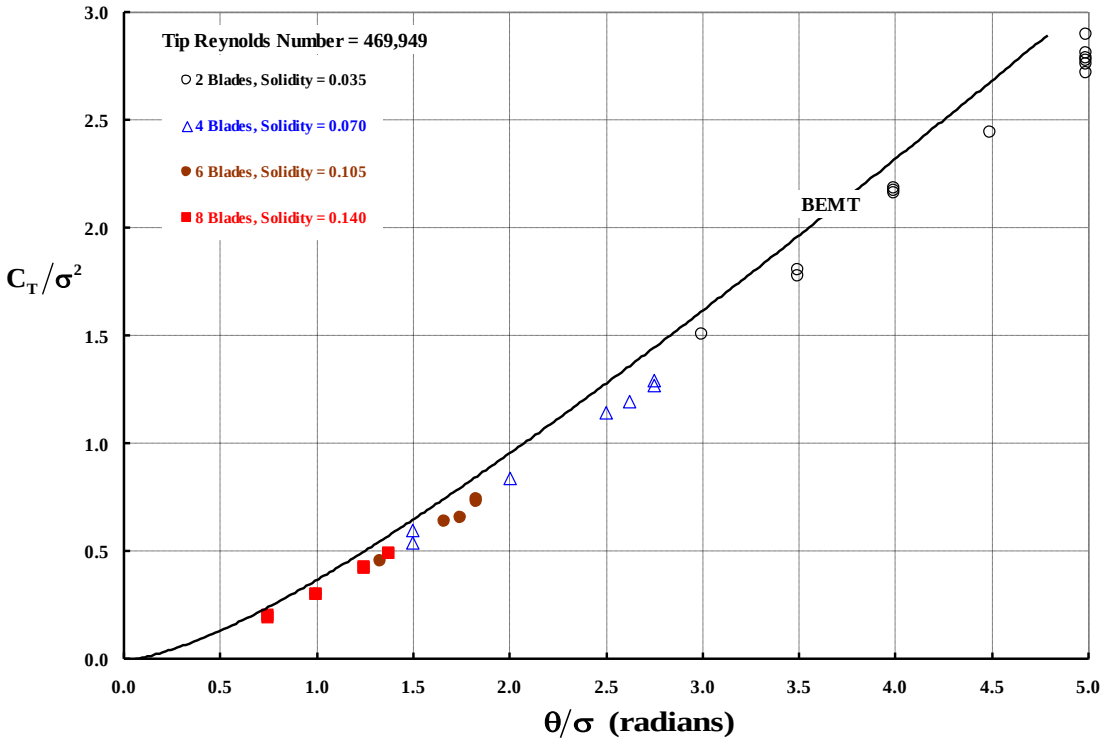

Figure 12. There is less evidence of blade stall at the tip Reynolds number of 469,949 and the lower tip Mach number of 0.537.

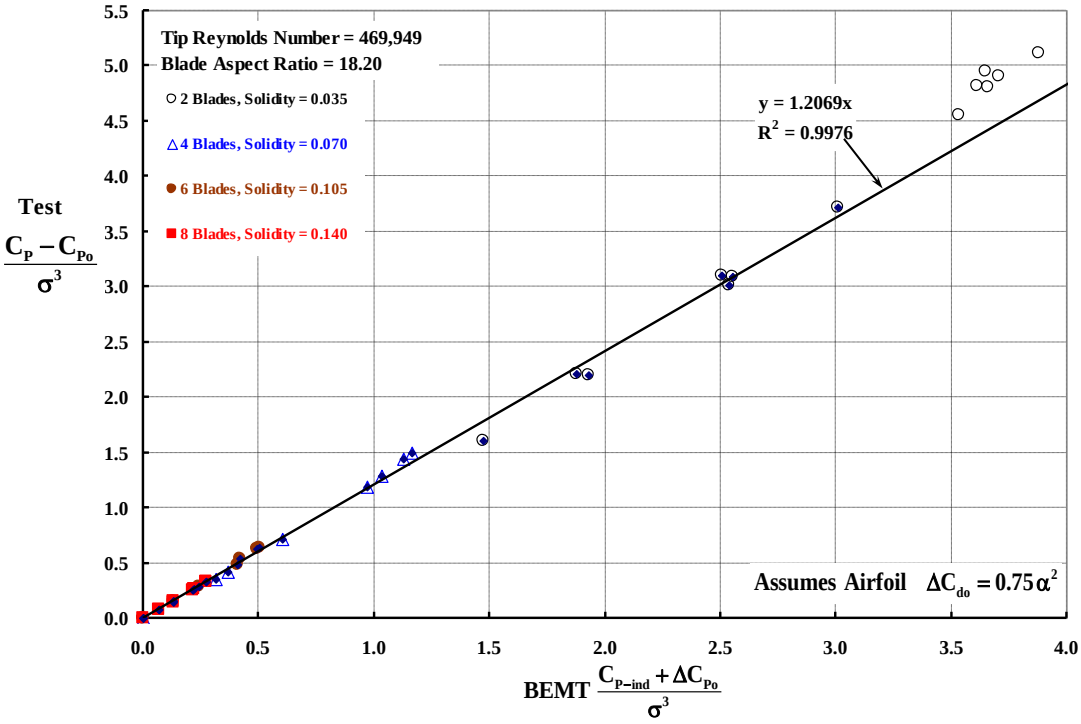

Figure 13. Only the two-bladed rotor shows clear evidence of blade stall.

Lastly, hover performance results at a third Reynolds number of 411,205 are shown in Figures 14 and 15. Figure 15 shows that BEMT's underprediction of power is by a factor of 1.1179. While tip Mach number for Landgrebe's experiments ranges from a low Mach number of 0.470 to 0.627, this does not seem to explain—to the author—just exactly why the three different underpredication factors do not form a logical trend with Reynolds number. Clearly, more detailed study of Landgrebe's experiment is required.

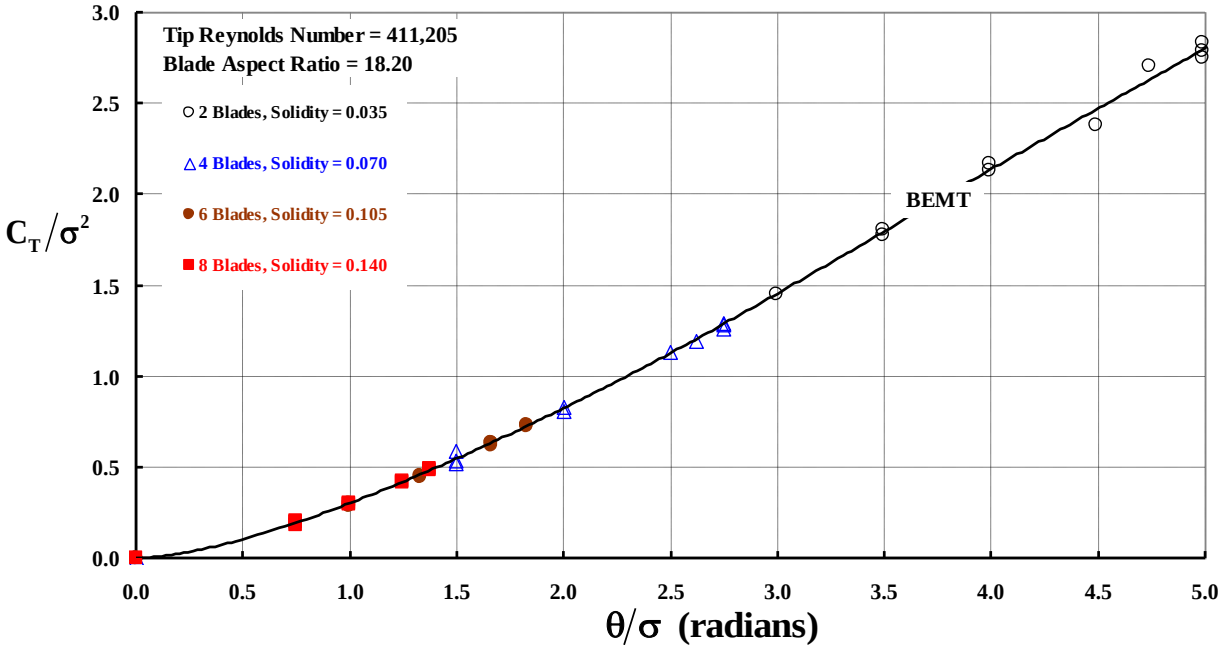

Figure 14. Landgrebe's thrust vs. pitch data at the lowest tip Mach number appears free of compressibility effects.

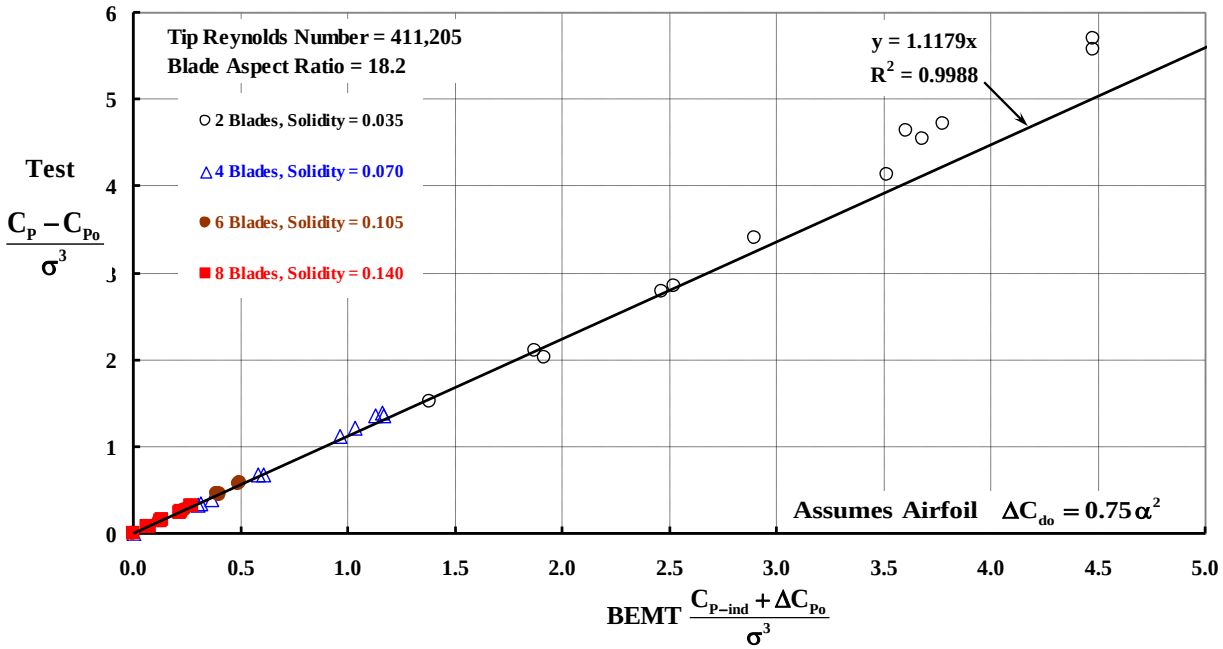

Figure 15. The two-bladed rotor was tested to a C_T/σ of 0.1575, and blade stall appears to be a factor in Landgrebe's power vs. thrust curve.

Reference 3. Manikandan Ramasamy, June 2015.

A portion of Ramasamy's AHS Journal paper from June 2015 was devoted to nearly a repeat of Landgrebe's work reported four decades earlier. Ramasamy wrote in the abstract of his paper, that

> The aerodynamic interference between rotors in a multirotor system in hover was analyzed using a series of experiments. *First, single-rotor measurements were acquired over a wide range of test conditions by varying thrust, tip speed, and number of blades (two to six).* [Author's emphasis]. Next, parametric studies were conducted methodically on torque-balanced coaxial-, tandem-, and tilt rotors. For coaxial rotors, the effects of axial separation distance, blade twist distribution, and rotor rotation direction on the system performance were studied. For the tandem rotors, the effect of overlap between rotors on the system performance was measured using untwisted and twisted blades. A unique aspect of the experiment was the ability to measure the performance of the individual rotors even when they were operated as part of a torque-balanced multirotor system. The multirotor measurements, when compared with isolated single-rotor measurements, revealed the influence of one rotor on the other, thereby enabling various interference loss factors to be quantified. Momentum theory and blade-element momentum theory were used to understand and explain the measurements.

At the present time, a data report from this comprehensive experiment has not been completed. However, Ramasamy generously forwarded tabulated data for the six-bladed configuration, tested at several tip Reynolds number range from 220,725 up to 329,659, to the author. (Ramasamy extracted this six-bladed data from his much larger data bank, as can be appreciated from reading his paper.) The corresponding tip Mach numbers range from 0.163 to 0.243. Note from Figure 1 that Mani's test operating range falls very close to what Knight and Hefner chose in 1937.

Ignoring the inaccurate collective pitch settings, Figure 16 shows that Reynolds number appears to have little (if any) effect on the thrust-versus-collective-pitch curve.

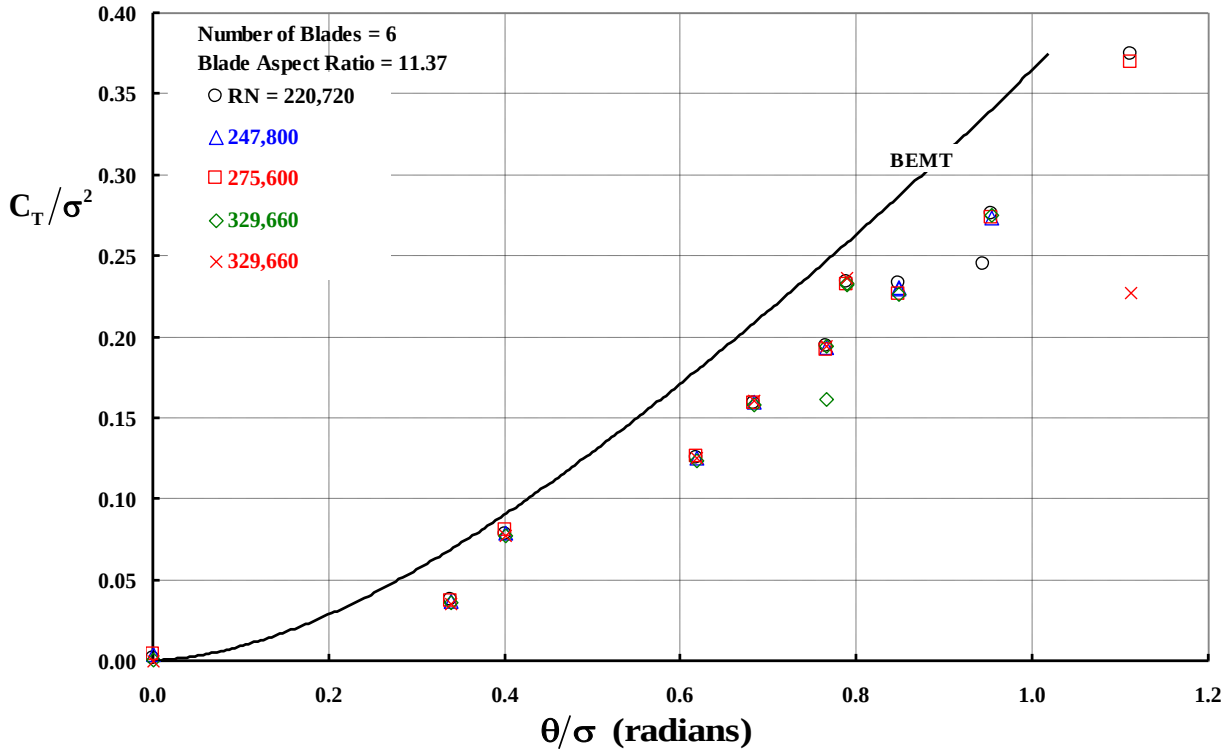

Figure 16. Blade pitch was not set very accurately in this experiment.

BEMT's view of Ramasamy's measured power is shown in Figure 17. The thrust levels are quite low, being on the order of C_T/σ = 0.062 as a maximum for the lowest Reynolds number. There does seem to be a Reynolds number effect—but this may only be a reflection of experimental accuracy.

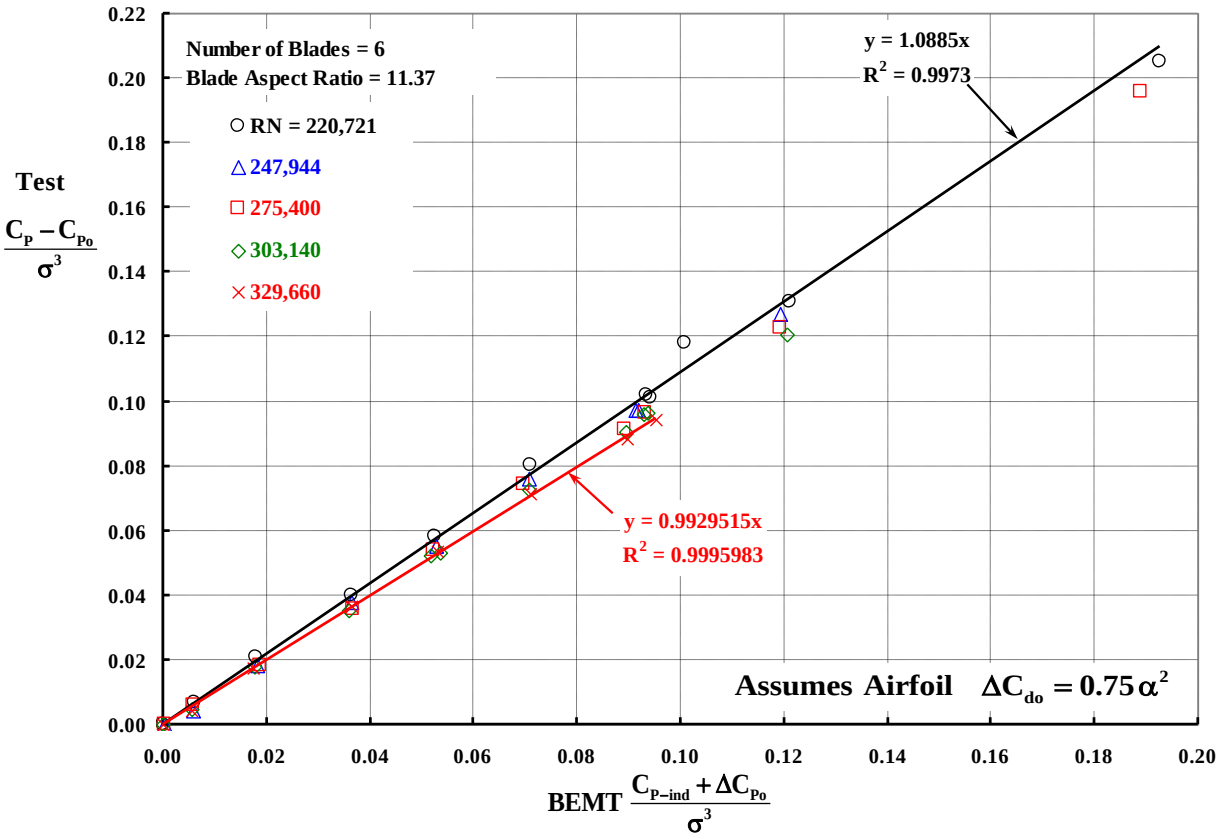

Figure 17. A slight influence of Reynolds number appears evident in Ramasamy's test with six blades. However, experimental accuracy cannot be dismissed as a factor.

Reference 4. Mahendra Bhagwat and Manikandan Ramasamy, January 2018.

Bhagwat and Ramasamy's AHS Specialists' Conference paper from January 2018 describes a unique experiment. They studied the effects of blade number at rotor RPM's from 500 to 1,200. To examine the effect of solidity, they simply cut off blade radius, which changed blade aspect ratio. Unfortunately, reducing bladed radius while holding RPM constant created a Reynolds number change as well as a solidity change. This approach also increased the root cutout. The author has been unable to separate the effects of the three simultaneous changes. Therefore, this report has studied the hover performance data where tip Reynolds number is varied with blade numbers 2, 3, 4, 5, and 6. *None of the cut-off blade data is used*. For the sake of completeness, Appendix A does provide the tabulated data for all configurations.

The abstract of Mahendra and Mani's paper is of particular interest because the question about the use of solidity as *the* key parameter has not been settled. In their paper, they wrote:

> Solidity plays an important role in rotor hover performance. Different rotors are typically compared in terms of the blade loading coefficient (thrust coefficient divided by solidity) and power loading coefficient (power or torque coefficient divided by solidity). This is analogous to fixed-wing where the wing efficiency is measured in terms of the mean lift to drag ratio, and allows comparison of different rotors operating at nominally the same average lift coefficient. It has even been suggested that based on blade element momentum theory, the blade number does not have any effect on performance while comparing rotors with the same solidity. Recent interest in proprotor performance has brought to focus some experimental results that appear to support this hypothesis. However, some of the authors' prior work showed that the blade number has a primary influence on the induced power in hover rather than the solidity. Blade aspect ratio, the other constituent in solidity, was shown to have a much smaller and secondary influence. This paper examines these results using simple analysis tools in an effort to better understand the seemingly anomalous behavior. This is complemented by a unique experimental undertaking involving hover performance measurements for several rotor configurations with two to six blades. These experiments should provide a large enough data base to provide further insights into the effects of blade number and solidity on hover performance.

Unfortunately, the experiment that Mahendra and Mani reported on in their January 2018 paper does not provided additional experimental evidence to answer the question. An additional disturbing situation has been observed: Figures 18 and 19 disagree in the slope of test $\frac{C_P - C_{Po}}{\sigma^3}$ versus BEMT $\frac{C_P - C_{Po}}{\sigma^3}$. That is, Ramasamy's result in June 2015 (Ref. 3) of the slope equaling 0.993 to 1.098 becomes 1.148 in the testing in January 2018 (Ref. 4). This difference— as of this study—cannot be explained simply by the small differences in blade geometry provided in Tables 1, 2, and 3.

Additional study of Reference 4 test data is provided in Figures 20 through 25 without discussion.

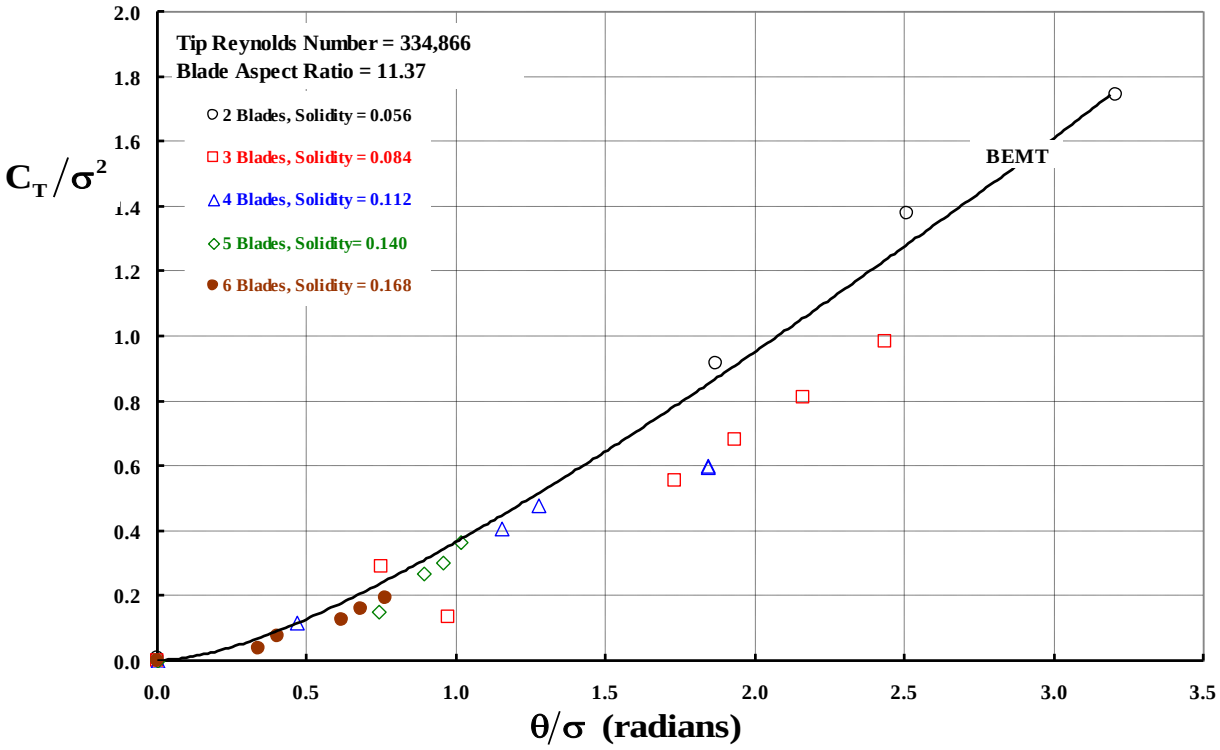

Figure 18. Blade collective pitch was not set very accurately in this experiment.

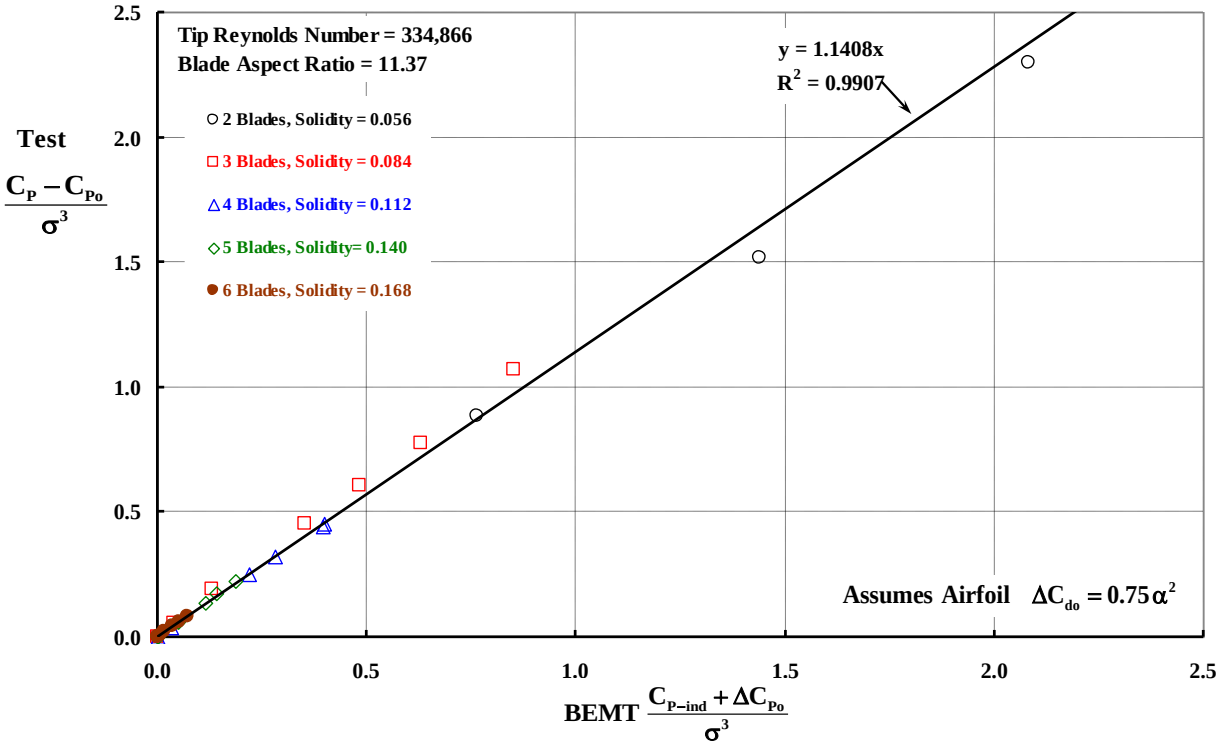

Figure 19. Bhagwat and Ramasamy proved experimentally that power versus solidity should be nondimensionized as Knight and Hefner found. However, solidity was varied with only the one blade aspect ratio (11.37).

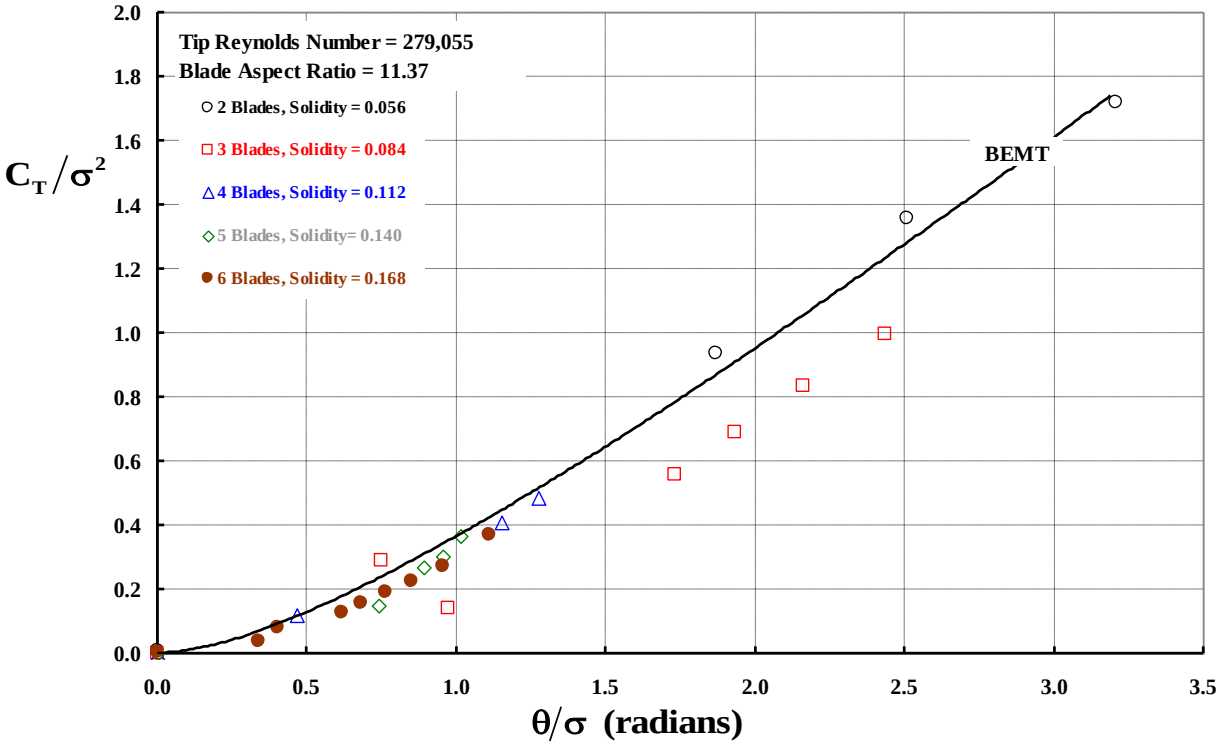

Figure 20. Blade collective pitch was not set very accurately in this experiment.

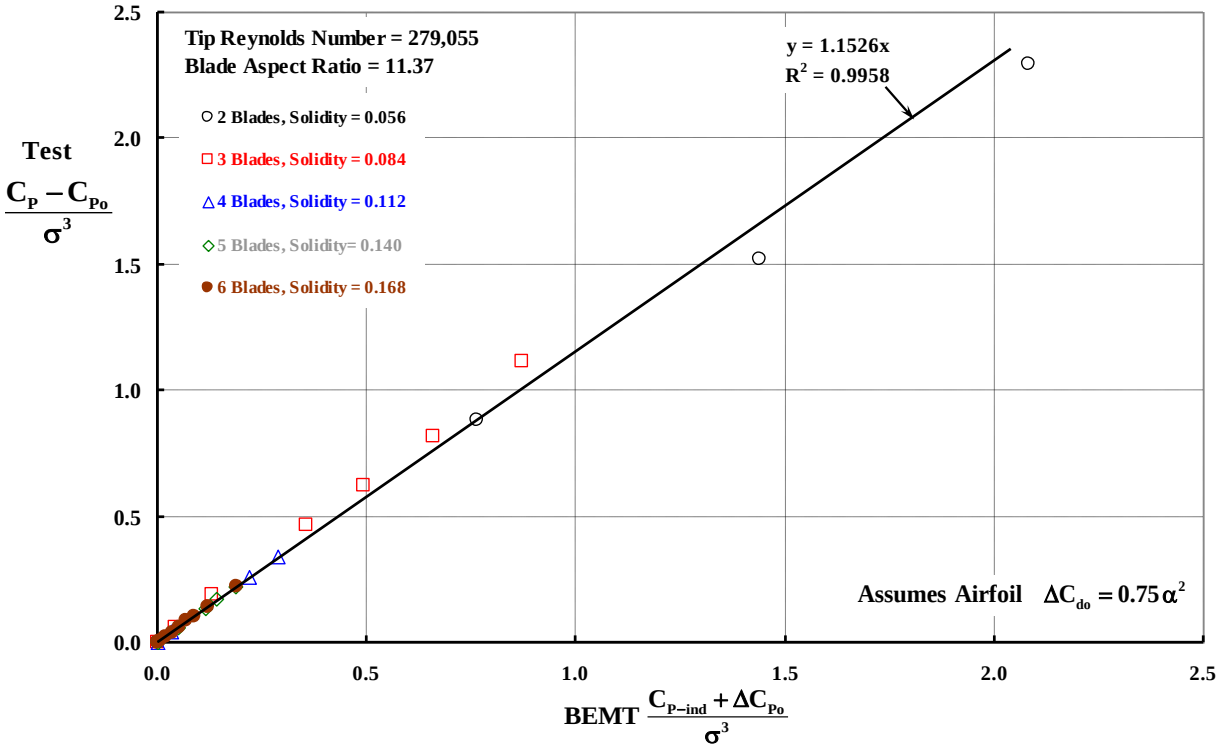

Figure 21. The three-bladed configuration continues to be out of line with data from the other test configurations.

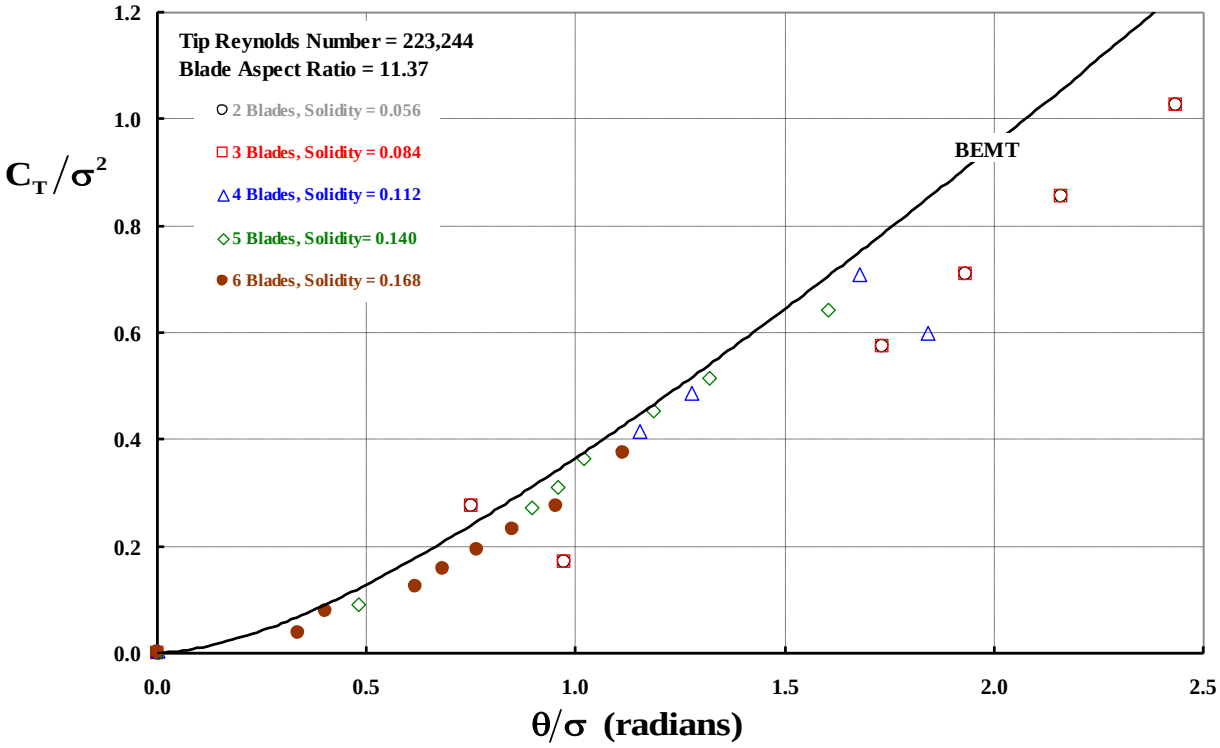

Figure 22. Blade collective pitch was not set very accurately in this experiment.

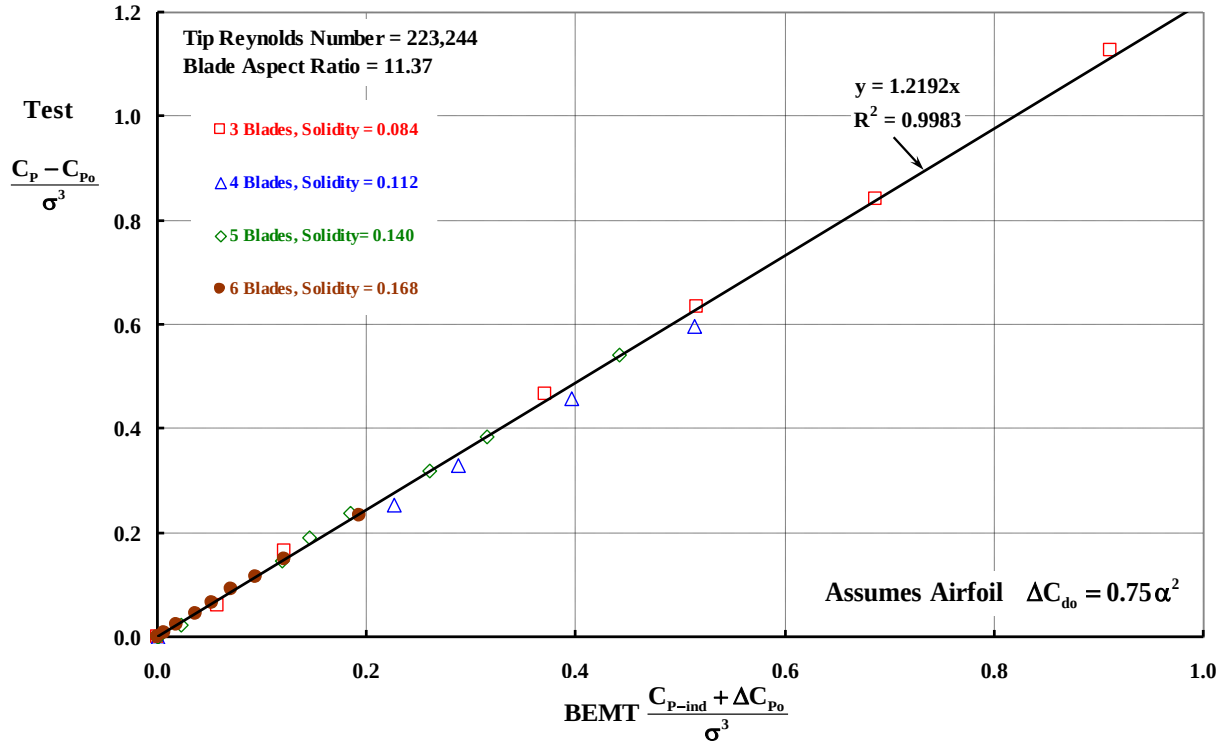

Figure 23. BEMT seriously underpredicts test results.

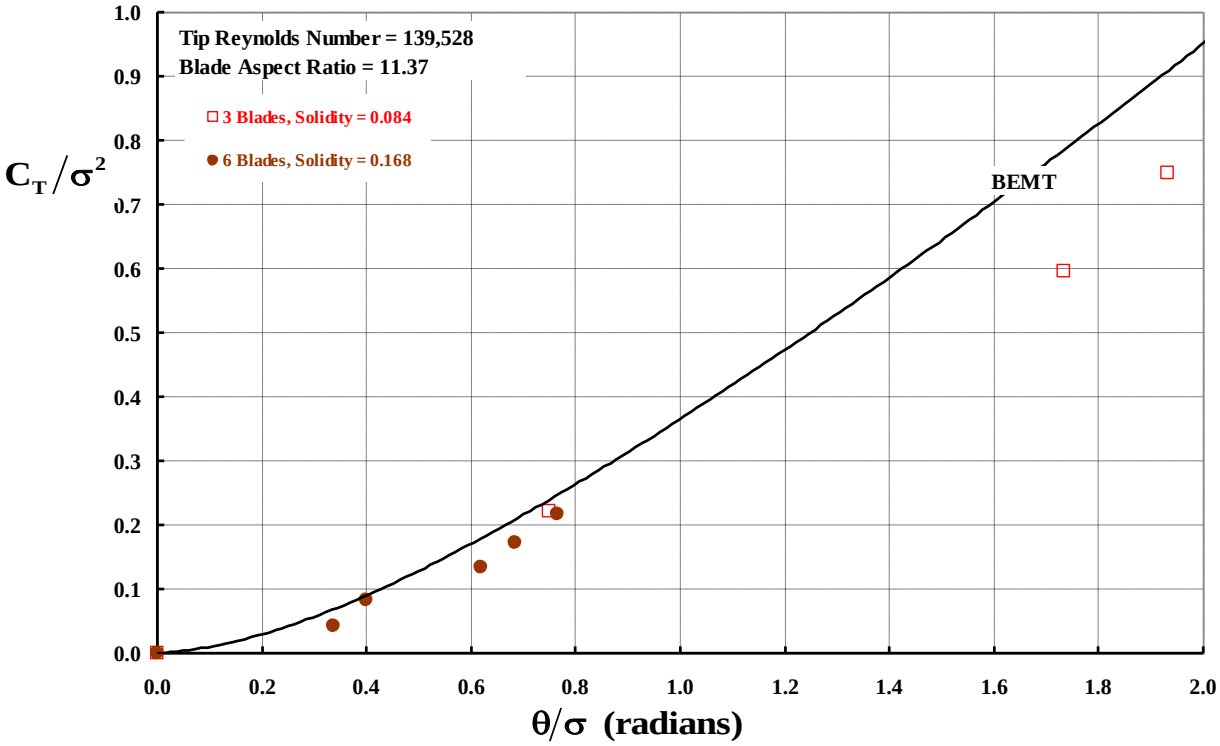

Figure 24. Blade collective pitch was not set very accurately in this experiment.

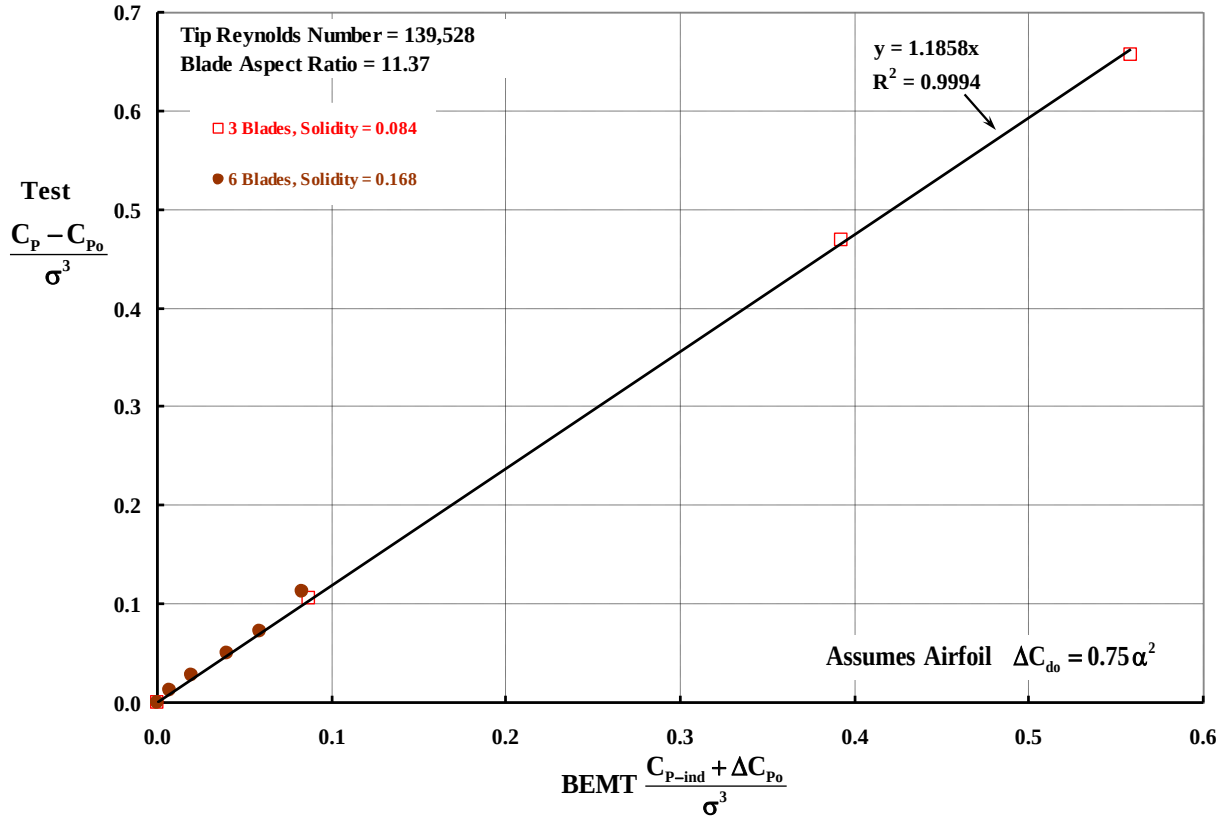

Figure 25. Only limited data was obtained at the lowest Reynolds number tested.

DATA ANALYSIS

Hover performance obtained from the four key experiments under discussion can be summarized with three fundamental graphs. The first is the basic graph showing the behavior of thrust versus collective pitch using Knight and Hefner's parameters. This result, shown in Figure 26, can be very useful in setting collective pitch (θ in radians) to obtain a desired thrust for a rotor having any solidity (σ)—*provided the blades are untwisted, have a constant chord, and the airfoil is a NACA 0012 from blade root to tip.*

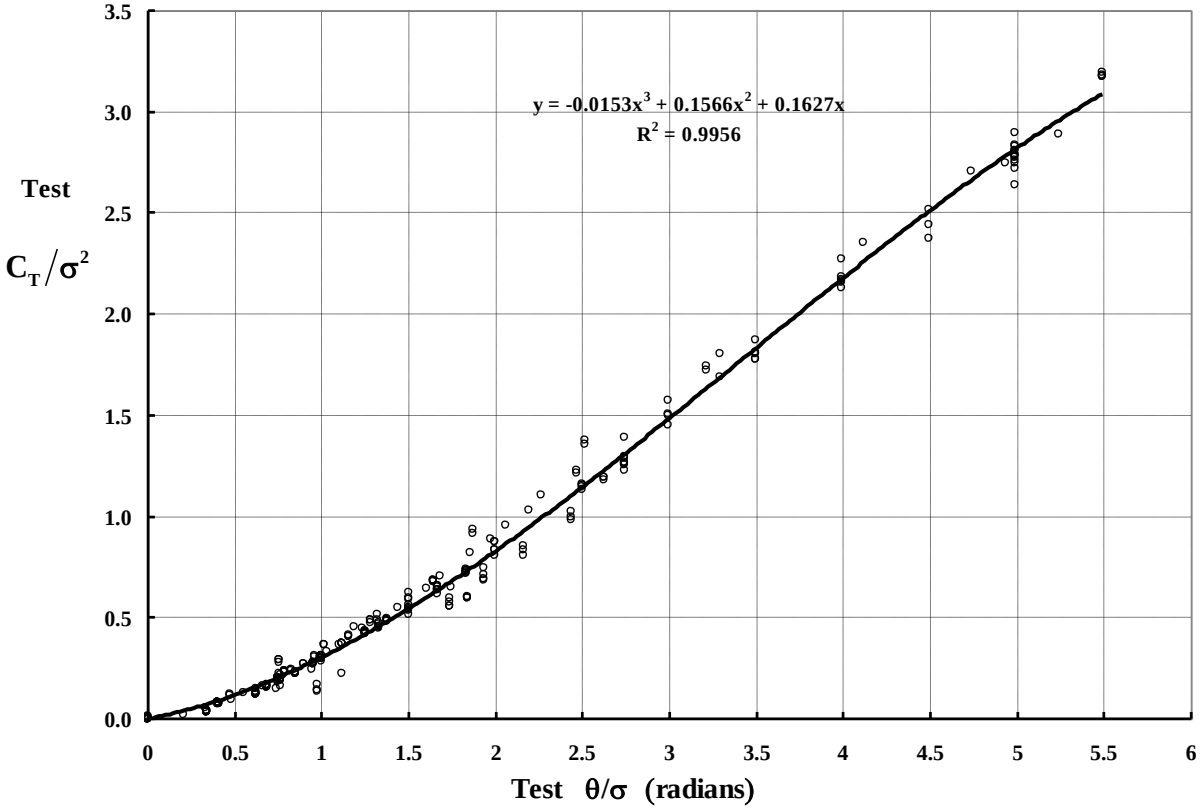

Figure 26. Knight and Hefner's BEMT parameters offer a useful engineering approximation to the test data from the four key experiments under discussion.

The second graph, provided here in Figure 27, indicates that Knight and Hefner's use of solidity is quite reasonable. However, their format for examining hover performance beyond the onset of stall and compressibility effects remains questionable. To illustrate this point, suppose, for example, that *onset of rotor stall in hover* generally begins when $C_T/\sigma = 0.10$ to 0.12, which has been the author's and others' experience. Then Knight and Hefner's format would say that rotor stall onset in hover should be expected when $C_T/\sigma^2 = 0.10/\sigma$.

The third graph, Figure 28, confirms the inadequacy of BEMT when the objective is to estimate power required to produce a given thrust. This fact has been known to rotorcraft industry engineers for several decades. The search for an improved hover performance prediction methodology has been ever ongoing, even before Knight and Hefner's 1937 report became available.

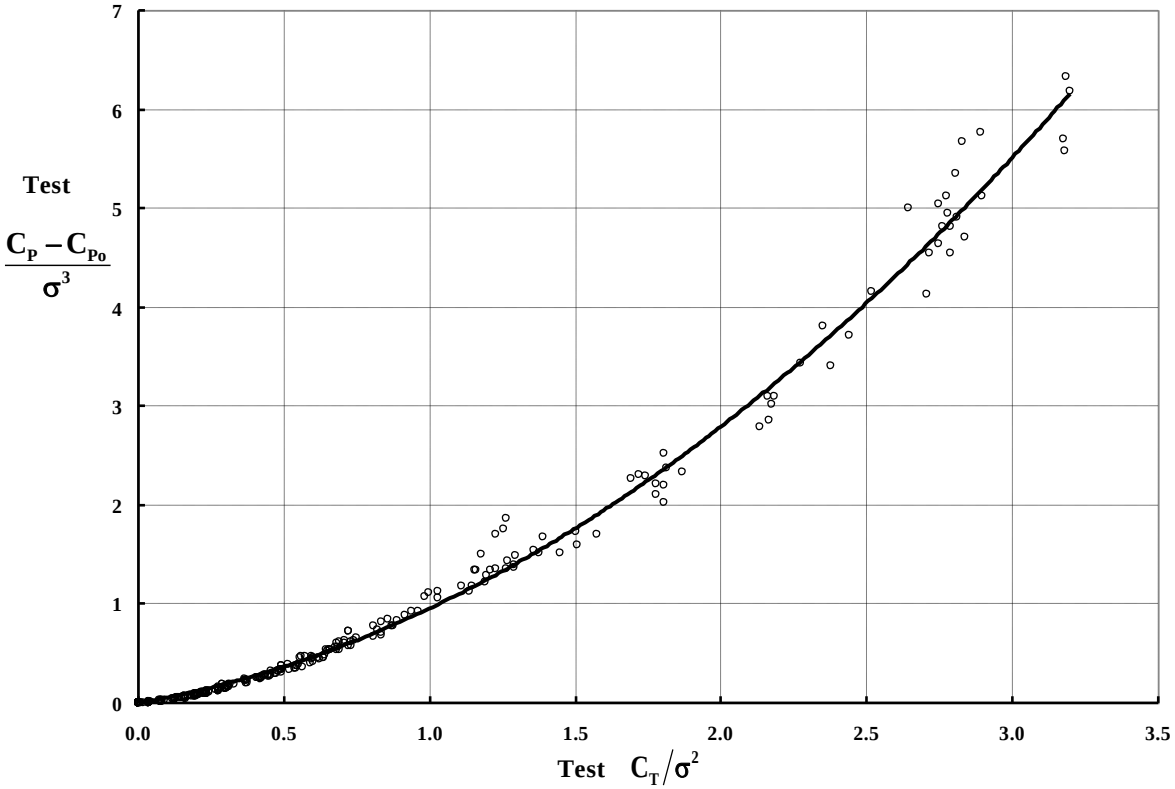

Figure 27. Knight and Hefner's BEMT parameters offer a useful way to collect experimental data for simple blade geometries.

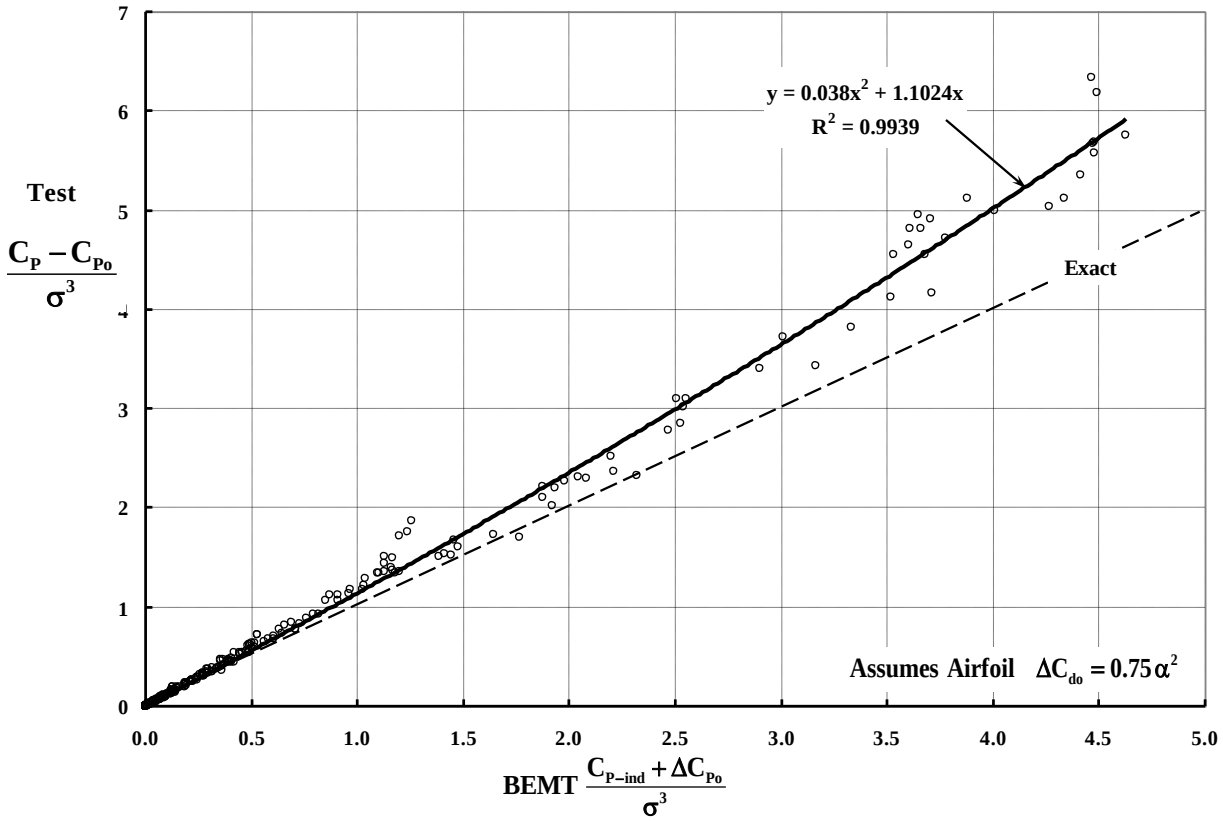

Figure 28. Knight and Hefner's BEMT is very optimistic when used to predict hover performance for simple blade geometries.

A First-Order Engineering Approximation

The preceding data bank from the four key experiments allows an empirical equation to be found using a linear regression analysis. The basis of the analysis is the relatively well known method of estimating hover performance that the author has used for decades. Applying what has been learned from the preceding discussion, the author assumes that

$$C_P = K_0 \frac{\sigma}{(\text{Tip RN}/1{,}000)^{1/8}} + K_1 \sigma \left(\frac{C_T}{\sigma}\right)^2 + K_2 \frac{C_T^{3/2}}{\sqrt{2}} \qquad \text{Eq. (10)}$$

The first term in Eq. (10) is simply the profile power at zero thrust. This minimum power depends on the Reynolds number, as discussed by Ron Gormont in Reference 5. The second term in Eq. (10) accounts for the airfoil drag coefficient rise with lift coefficient. The third term accounts for induced power. The linear regression analysis gives the result that

$$C_P = \frac{0.0032895\ \sigma}{(\text{Tip RN}/1{,}000)^{1/8}} + 0.09814\ \sigma \left(\frac{C_T}{\sigma}\right)^2 + 1.2923\left(\frac{C_T^{3/2}}{\sqrt{2}}\right) \qquad \text{Eq. (11)}$$

It appears from Figure 29 that the Appendix A data of C_P versus C_T from the four key experiments under discussion can be predicted to within ±10 percent by Eq. (11). Of course, Eq. (11) does not include the effects of stall. Therefore, the approximation offered by Eq. (16) must be restricted to a maximum C_T/σ of 0.10, or perhaps 0.11. Furthermore, the approximation assumes tip Reynolds numbers below 525,000 and tip Mach numbers below 0.45.

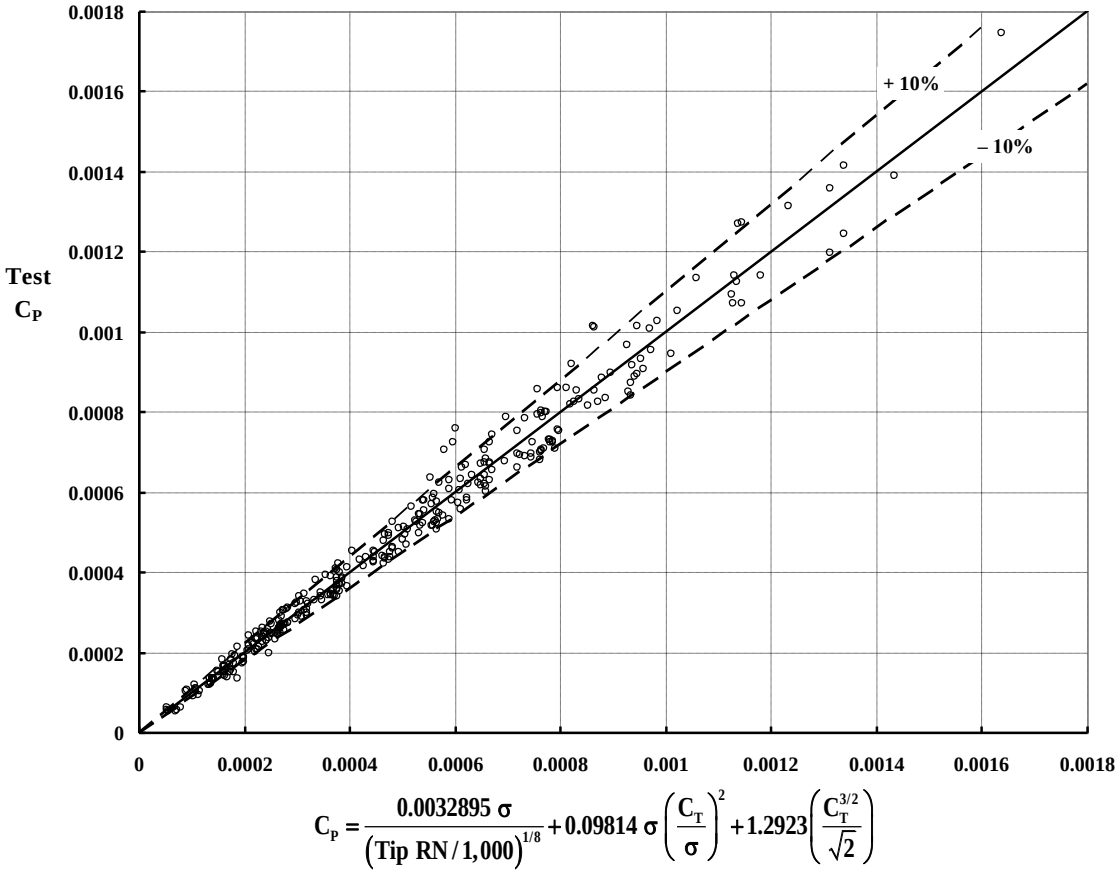

Figure 29. This first approximation can be of practical engineering use.

Both Eqs. (10) and (11) as well as Figure 29 make the assumption that the coefficients K_1 and K_2 are constant. However, when BEMT is examined in more detail, it becomes apparent that the *coefficients are not constant*. Rather, the two coefficients depend on Knight and Hefner's collective pitch parameter ($\Theta = 16\theta/\sigma\, a$) and therefore on C_T/σ^2 according to Figure 5. To illustrate, the coefficient $K_2 = 1.2923$ in Eq. (11) "empirically corrects" ideal induced power ($C_T^{3/2}/\sqrt{2}$) to agree with experiment. However, following BEMT and Eq. (7), the K_2 correction should be calculated as

$$K_2 = \frac{\text{BEMT } C_{P-ind}}{\text{Ideal } C_{P-ind}} = \frac{\frac{\sigma^3 a^3}{512} F_{P-ind}}{C_T^{3/2}/\sqrt{2}} = \sqrt{2}\,\frac{\frac{\sigma^3 a^3}{512} F_{P-ind}}{\left(\frac{\sigma^2 a^2}{32} F_T\right)^{3/2}} = \frac{1}{2}\frac{F_{P-ind}}{\left(F_T\right)^{3/2}} \qquad \text{Eq. (12)}$$

To a very close approximation, K_2 is seen, from Figure 30, to be

$$K_2 = \frac{1}{2}\frac{F_{P-ind}}{\left(F_T\right)^{3/2}} \approx \sqrt{\frac{54}{49}} + \frac{0.10836}{\sqrt{1+2\Theta}} - \frac{0.02679}{\left(\sqrt{1+2\Theta}\right)^2} \qquad \text{Eq. (13)}$$

Thus, at zero pitch where $\Theta = 16\theta/\sigma\, a = 0$, K_2 equals $\sqrt{32/25} \approx 1.31$. In the limiting case as Θ approaches infinity, K_2 equals $\sqrt{54/49} \approx 1.05$. This is a substantial change in K_2 as Figure 30 shows.

In a similar manner, the "constant" K_1 in Eq. (11) and using Eq. (7), is seen to be

$$K_1 = \frac{\text{BEMT } \Delta C_{Po}}{\left(C_T/\sigma\right)^2} = \sigma^2\,\frac{\frac{\delta}{a}\frac{\sigma^3 a^3}{512} F_{\Delta Po}}{\left(\frac{\sigma^2 a^2}{32} F_T\right)^2} = \sigma\delta\left[\frac{2}{a^2}\frac{F_{\Delta Po}}{\left(F_T\right)^2}\right] = \sigma\delta\left(\frac{2}{a^2}\right)\left[\frac{F_{\Delta Po}}{\left(F_T\right)^2}\right] \qquad \text{Eq. (14)}$$

Therefore, K_1 also varies with Θ and is approximated as

$$K_1 = \left[\sigma\delta\left(\frac{2}{a^2}\right)\right]\left[\frac{F_{\Delta Po}}{\left(F_T\right)^2}\right] = \sigma\delta\left(\frac{2}{a^2}\right)\left[\frac{9}{4} + \frac{0.5331}{\sqrt{1+2\Theta}} - \frac{0.1161}{\left(\sqrt{1+2\Theta}\right)^2}\right] \qquad \text{Eq. (15)}$$

At zero pitch, $F_{\Delta Po}/\left(F_T\right)^2$ equals $8/3 \approx 2.67$. In the limiting case as Θ approaches infinity, $F_{\Delta Po}/\left(F_T\right)^2$ equals $9/4 = 2.25$. This is also a substantial change in $F_{\Delta Po}/\left(F_T\right)^2$ as Figure 31 shows.

There is another interesting aspect to the use of BEMT. In first-order hover performance estimates, many engineers will use their experience by saying *during conceptual and perhaps even preliminary design* that

$$C_P = C_{Po} + K\left(\text{Ideal } C_P\right) = C_{Po} + K\left(\frac{C_T^{3/2}}{\sqrt{2}}\right) = C_{Po} + \left(K_2 + K_4\right)\left(\frac{C_T^{3/2}}{\sqrt{2}}\right) \qquad \text{Eq. (16)}$$

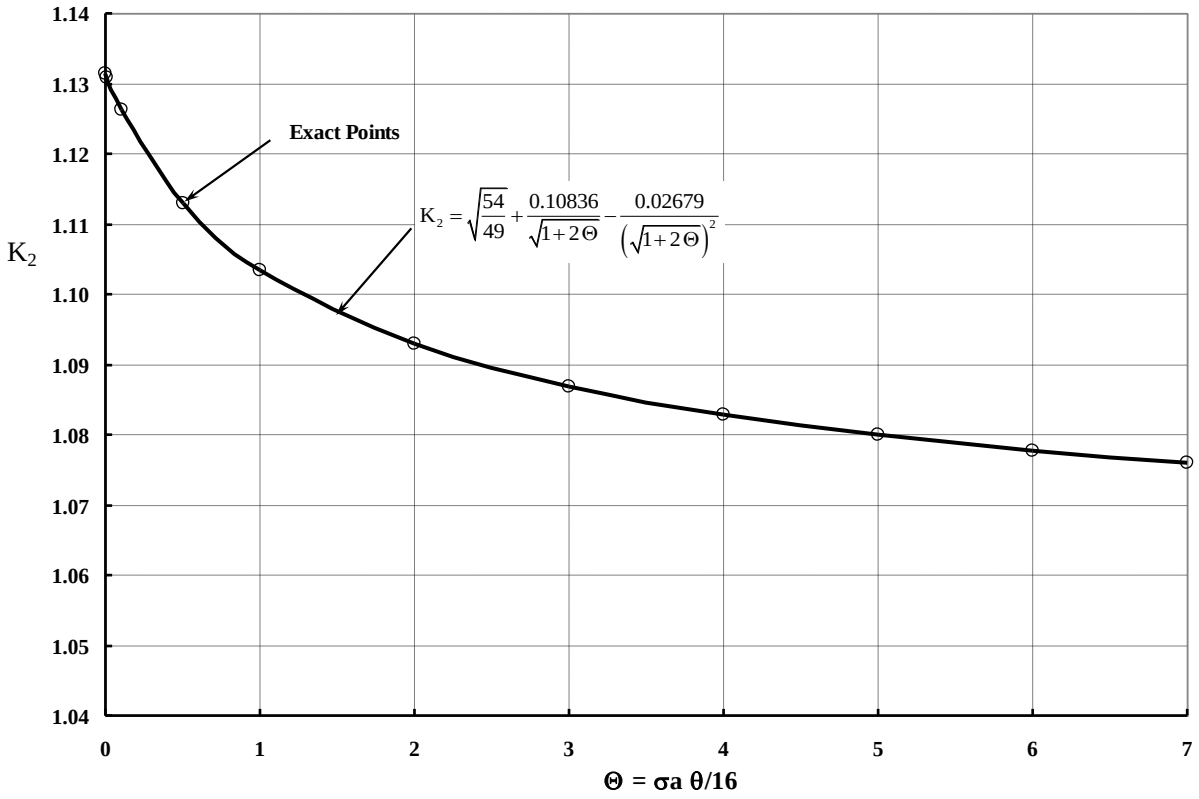

Figure 30. Some semi-empirical BEMT constants are not constant.

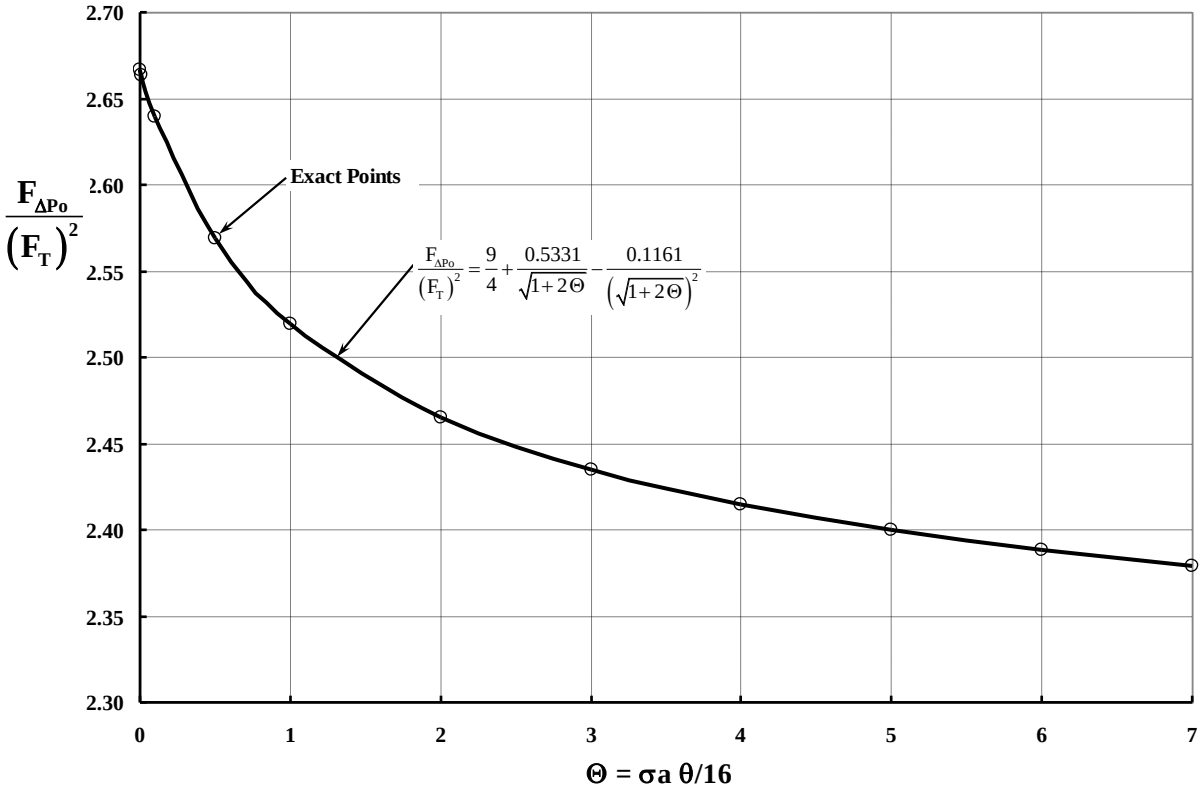

Figure 31. Some semi-empirical BEMT constants are not constant.

The value K in Eq. (16) can be obtained from experimental data by plotting test C_P versus ideal power $C_T^{3/2}/\sqrt{2}$ and then taking the slope of the curve, which is the K that Knight and Hefner were estimating.[2] BEMT can be used to estimate the constant K in the following manner.

The coefficient K_2 that corrects induced power was defined with Eq. (13). The change of ΔC_{Po} with ideal induced power ($C_T^{3/2}/\sqrt{2}$) creates a fourth constant, K_4, which is defined as

$$K_4 = \frac{\text{BEMT } \Delta C_{Po}}{\text{Ideal } C_P} = \frac{\frac{\delta}{a}\frac{\sigma^3 a^3}{512}F_{\Delta Po}}{C_T^{3/2}/\sqrt{2}} = \frac{\frac{\delta}{a}\frac{\sigma^3 a^3}{512}F_{\Delta Po}}{\left(\frac{\sigma^2 a^2}{32}F_T\right)^{3/2}/\sqrt{2}} = \frac{\delta}{a}\left[\frac{F_{\Delta Po}}{2\left(F_T\right)^{3/2}}\right] \qquad \text{Eq. (17)}$$

and $F_{\Delta Po}/2\left(F_T\right)^{3/2}$ also varies with $\Theta = 16\theta/\sigma a$ using the approximation

$$\frac{F_{\Delta Po}}{2\left(F_T\right)^{3/2}} \approx \frac{\delta}{a}\left[0.46328\sqrt{1+2\Theta}-1\right] \qquad \text{Eq. (18)}$$

Therefore, the coefficient $K = K_2 + K_4$ as used in Eq. (16) is

$$K = K_2 + K_4 \approx \left[\sqrt{\frac{54}{49}} + \frac{0.10836}{\sqrt{1+2\Theta}} - \frac{0.02679}{\left(\sqrt{1+2\Theta}\right)^2}\right] + \frac{\delta}{a}\left[0.46328\sqrt{1+2\Theta}-1\right] \qquad \text{Eq. (19)}$$

Thus, the range in K becomes dependent on the airfoil's drag coefficient parabolic rise with the airfoil lift coefficient denoted by δ in Eq. (6). This dependency is shown in Figure 32. Keep in mind that the BEMT value of K_2 is known to be considerably lower than what a modern, free-wake analysis would show.

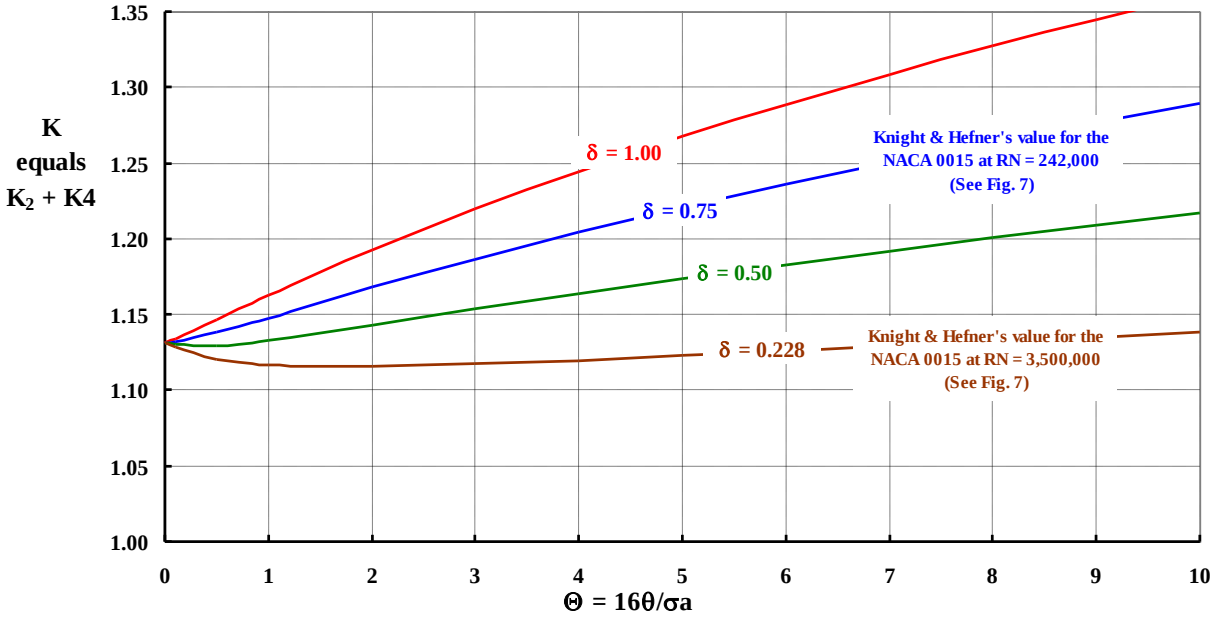

Figure 32. The K in C_P = K(ideal C_P) depends on the airfoil's $\Delta C_{do} = \delta\,(\alpha^2)$.

[2] This is a very handy estimating method and it is of value because the delta profile power due to thrust varies as C_T^2 and induced power varies as $C_T^{3/2}$. The method is reasonable because in the range of C_T of practical interest, profile power is roughly 20 percent of total power and induced power is the other 80 percent of the total power.

The Primary Observations

The four references under study hardly provide a definitive set of data to answer any number of questions that come to mind. *In fact, the four experiments form an eclectic data set that appears to have only one property in common.* This property is that the measured power varies linearly with the measured thrust raised to the 3/2 power. That is, the power coefficient (C_P) varies linearly with the thrust coefficient as $C_T^{3/2}$. Figure 33 illustrates this common property that many experimenters have found even before Knight and Hefner saw it in 1939.

The use of $C_T^{3/2}$ for the abscissa is, of course, an approximation because both profile power and induced power are increasing with thrust. The profile power is frequently analytically found to vary with thrust squared while induced power is approximated with thrust varying to the 3/2 power. But Knight and Hefner's coordinate transformation—*assuming that profile power varies with thrust squared*—showed that both power components could be captured correctly when the thrust coefficient and solidity were combined in their coefficient, C_T/σ^2. (This was discussed earlier in this report.)

Figure 33 shows that profile power at zero rotor thrust is increasing as the number of blades increases when blade aspect ratio remains constant, which is a well-known fact. And this data also shows—*at least visually*—that the slopes of the curves are approximately equal, probably within experimental accuracy. These two observations can be repeated again as

$$C_P = C_{P_o} + \frac{K}{\sqrt{2}} C_T^{3/2} \qquad \text{Eq. (20)}$$

an approximation that many practicing engineers have used for decades.

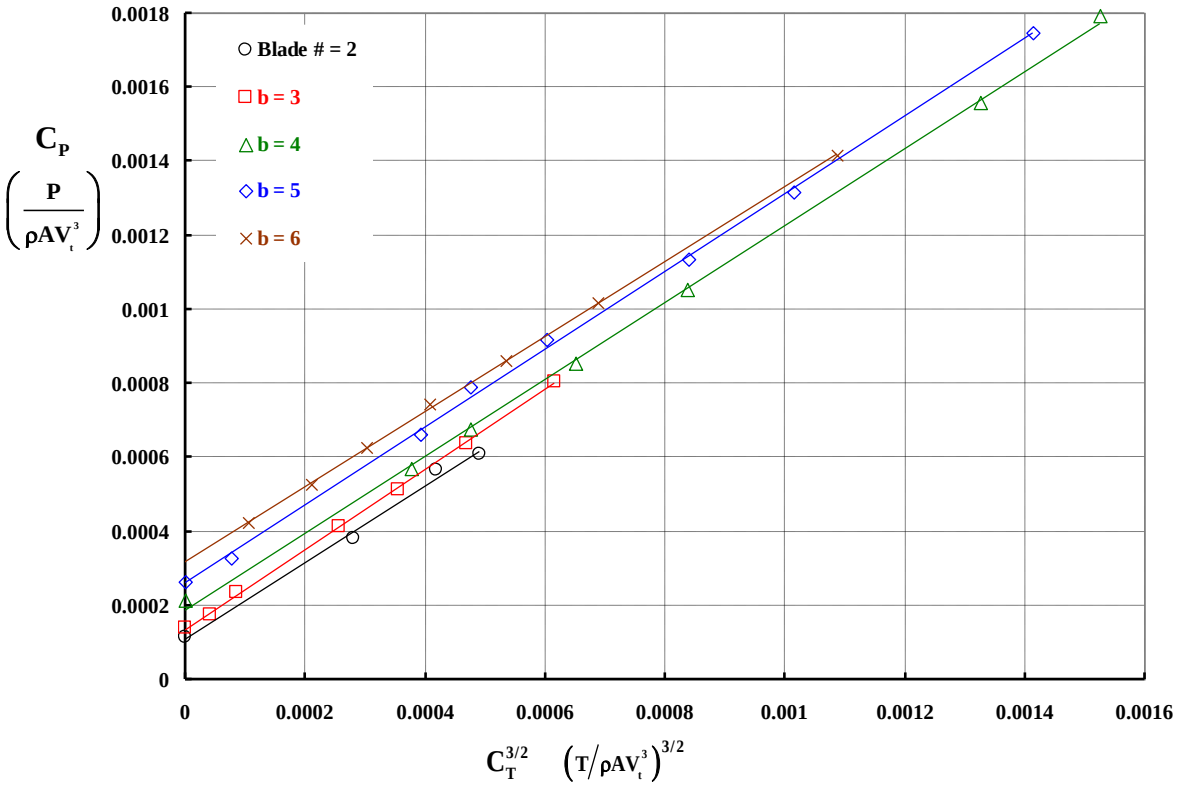

Figure 33. Hover C_P varies linearly with $C_T^{3/2}$ below blade stall onset provided the tip Mach number is in the incompressible range. (Blade AR = 11.37, Tip RN = 223,244, Ref. 4.)

Now, recall that Knight and Hefner's BEMT derivation led to the first-order parameters

$$\frac{C_P - C_{Po}}{\sigma^3} \text{ and } \frac{C_T}{\sigma^2}$$

when they assumed hover performance with rectangular blades having zero twist and using the same airfoil from blade root to tip. Thus, Eq. (20) should be divided through by solidity cubed, which leads to

$$\frac{C_P - C_{Po}}{\sigma^3} = K\left[\frac{1}{\sqrt{2}}\left(\frac{C_T}{\sigma^2}\right)^{3/2}\right] \qquad \text{Eq. (21)}$$

Re-graphing Figure 33 in the coordinates of Eq. (21) shows (in Figure 34) that the effect of blade number has been removed as a variable—at least to the first order and probably within experimental accuracy. This is a 2018 reaffirmation of Knight and Hefner's conclusion in 1937.

When all of the data from the four references are collected on a graph, as shown in Figures 35 and 36, it becomes reasonably clear that the effects of blade aspect ratio and Reynolds number cannot be unquestionably quantified, probably because of experimental accuracy.

The striking point to be made about this primary observation is that IF the common property is TRUE, then Figure 32 says that the delta profile power (ΔC_{Po}) increase with thrust as measured with δ must lay within the relatively small range of, say, $\delta = 0.228$, and maybe up to as high as $\delta = 0.50$. More precisely, the author is of the opinion that the effects of blade aspect ratio (and Reynolds number below 400,000) on the rise in power with thrust can be ignored—at least for practical engineering purposes.

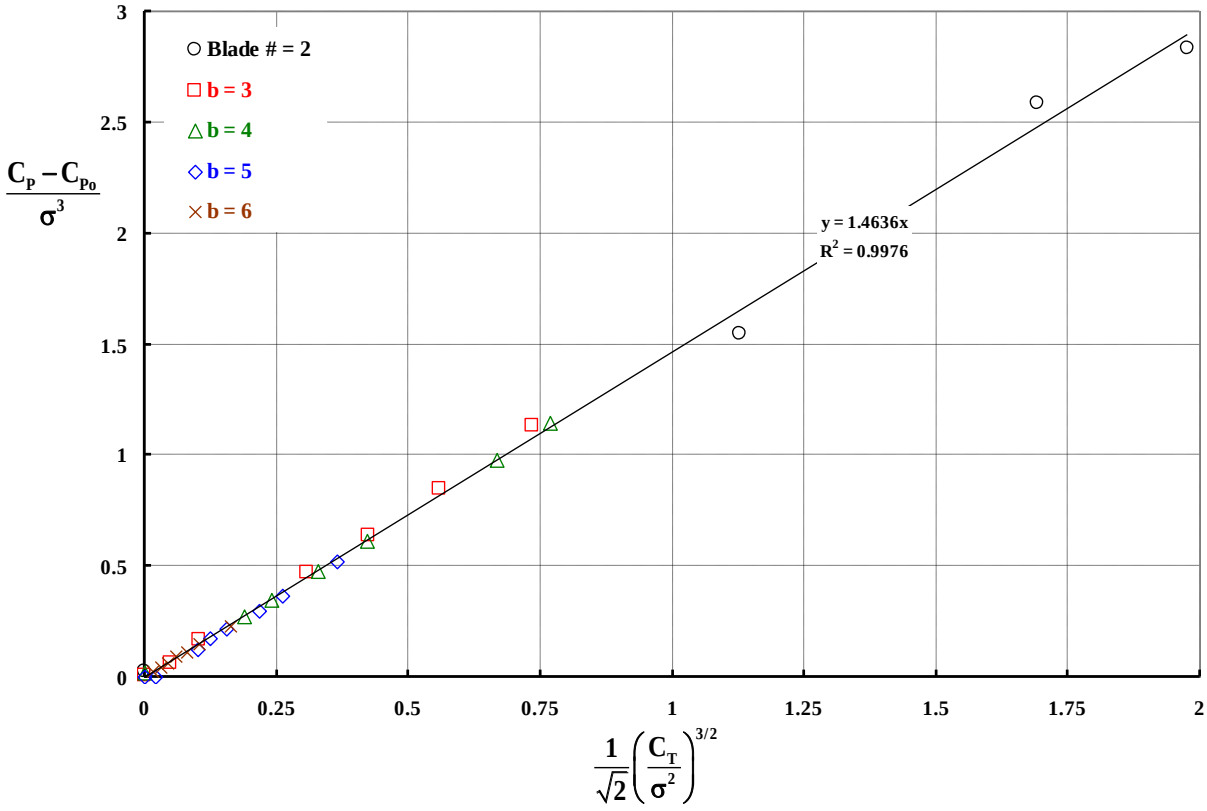

Figure 34. Knight and Hefner's hover performance parameters appear reasonable. (Blade AR = 11.37, Tip RN = 223,244, Ref. 4.)

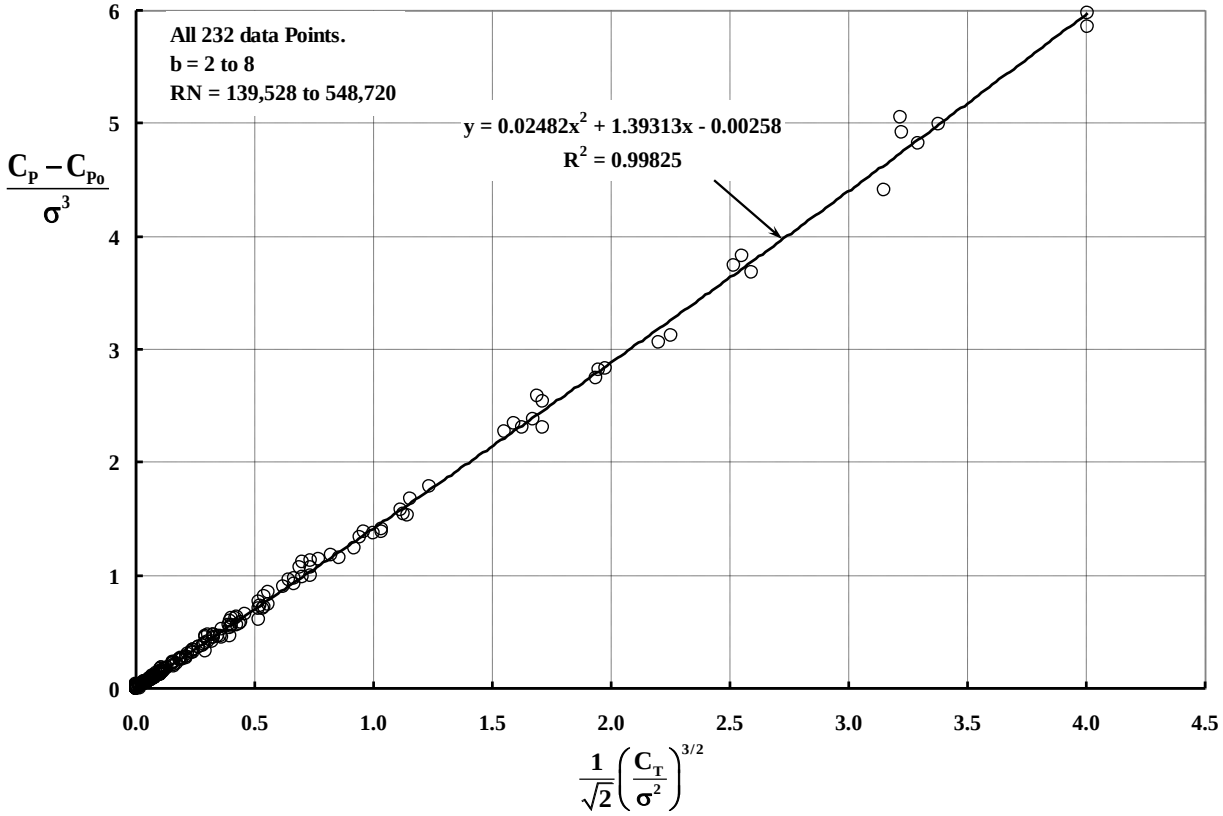

Figure 35. Blade number and tip Reynolds number do not appear as significant variables in the increase of power with thrust—at least for practical engineering purposes.

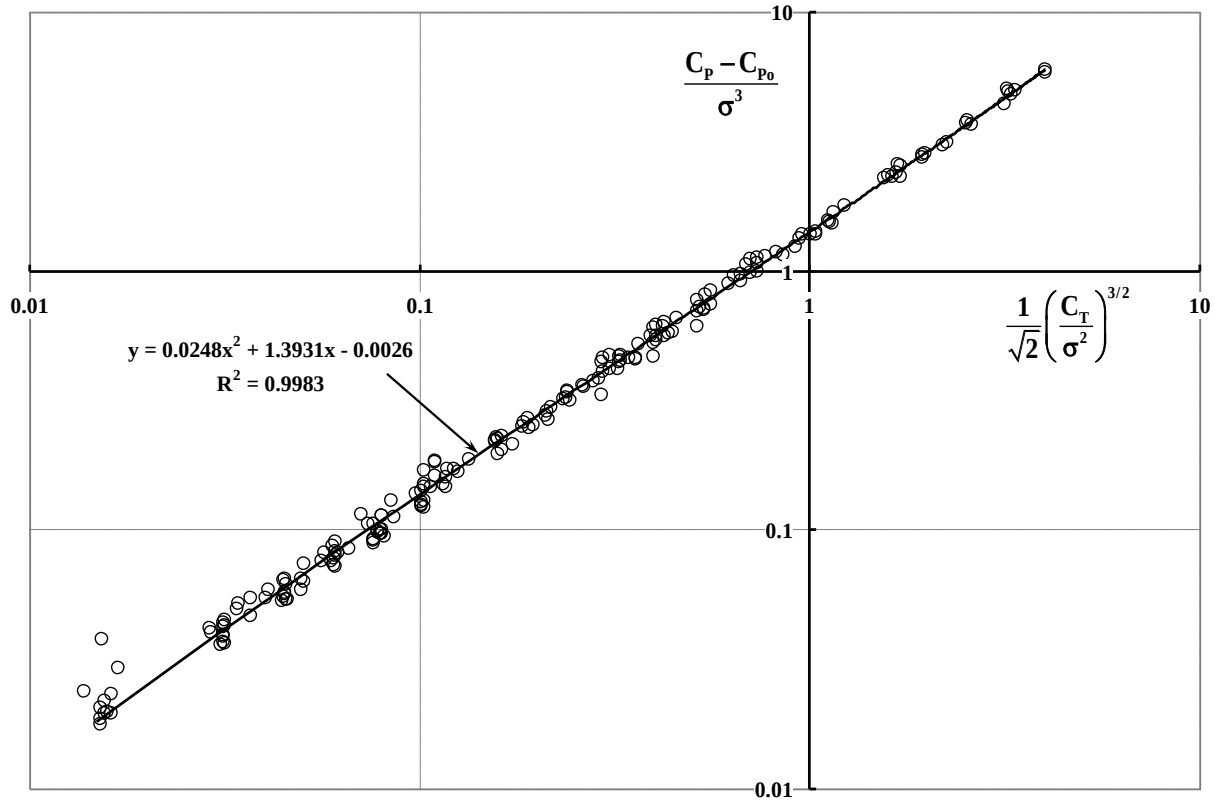

Figure 36. Note the scatter in data points near zero thrust.

Profile Power at Zero Thrust

Based on Figures 35 and 36, the four key references show that hover power increases with thrust as

$$\frac{C_P - C_{Po}}{\sigma^3} = \frac{1.393}{\sqrt{2}}\left(\frac{C_T}{\sigma^2}\right)^{3/2} + 0.0248\left[\frac{1.393}{\sqrt{2}}\left(\frac{C_T}{\sigma^2}\right)^{3/2}\right]^2 \qquad \text{Eq. (22)}$$

and this basic equation applies for all the configurations identified in Tables 1, 2, and 3. The only remaining question has to do with profile power at zero thrust.

Since the geometry of the blades under discussion had no twist, were constant chord, and used a constant airfoil from root to tip, BEMT expects the minimum profile power coefficient (C_{Po}) to be simply $C_{Po} = \sigma C_{do}/8$. Knight and Hefner's NACA 0015 airfoil measurements gave $C_{do} = 0.0113$ at a Reynolds number of 242,000. On this basis, BEMT would say that $C_{Po}/\sigma = C_{do}/8 = 0.00141$. Rotor testing of the several blade number configurations Knight and Hefner experimented with gave

b = 2	3	4	5
$C_{Po}/\sigma = 0.00127$	0.00145	0.00158	0.00141

This gives an average C_{Po}/σ of 0.00143 for a tip Reynolds number of 267,825. One might reasonably ask if the turbulent wake created by blade-to-blade interference leads to an effective Reynolds number considerably different than the airfoil test value of $C_{do} = 0.0113$. Wind tunnels are well known to have a turbulence effect on airfoil tests, which leads to a scattered result in measured C_{do} versus Reynolds number as Jim McCroskey pointed out in 1987 (Ref. 10).

The behavior of the drag coefficient of the NACA 0012 at zero lift in 2D flow has been a subject of many experiments as McCroskey showed with his figure 4 on page 1-5 of his comprehensive report (Ref. 10). His figure is reproduced here as Figure 37. Three additional sources of data have come to the author's attention that extend McCroskey's C_{do} data below a Reynolds number of 1,000,000 down to a Reynolds number of about 40,000 (Refs. 11 and 12). Figure 38 shows this new data added to McCroskey's graph.

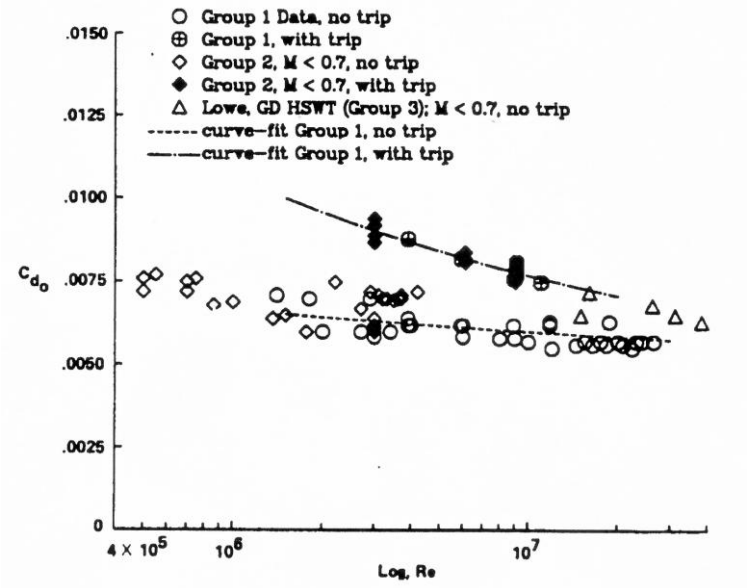

Figure 37. McCroskey's assessment of the NACA 0012 C_{do} as a function of Reynolds number.

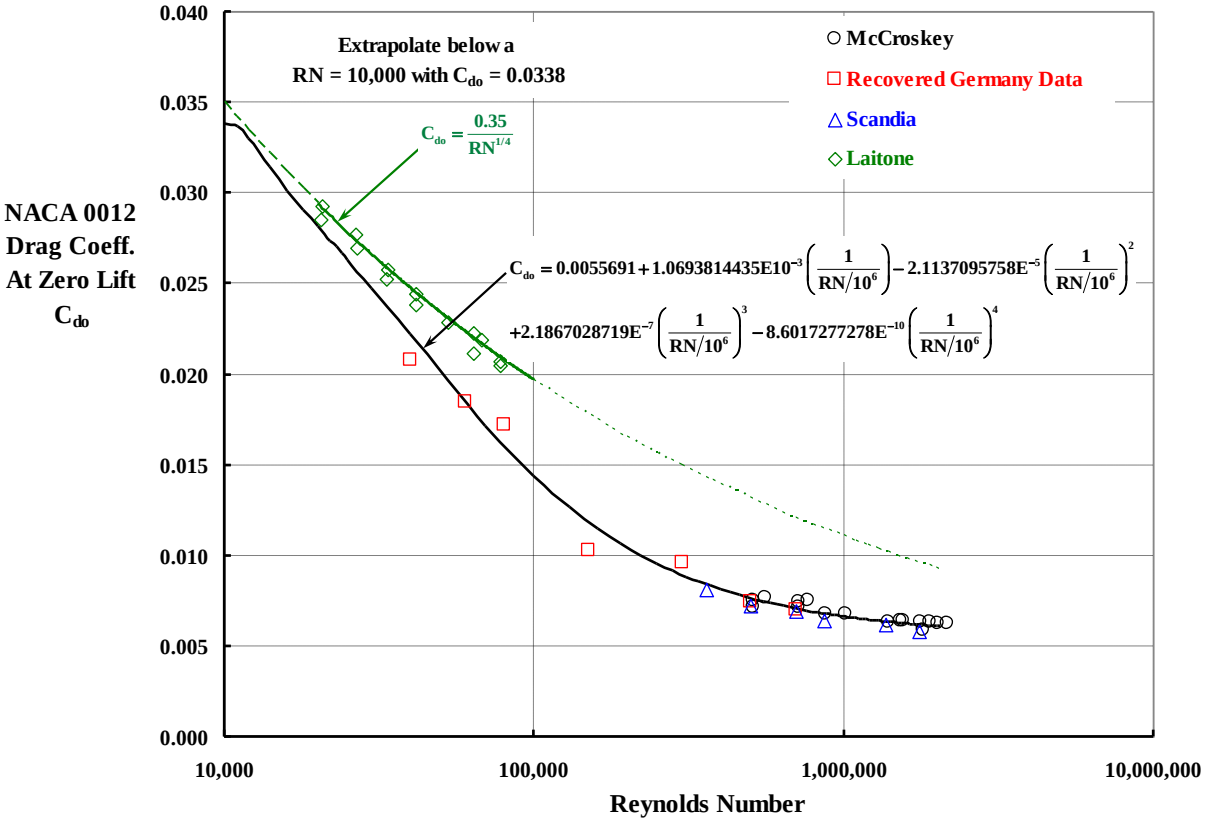

Figure 38. Even today, the NACA 0012 airfoil's C_{do} value below a Reynolds number of 400,000 has not been clearly established by available experiments.

In Knight and Hefner's use of BEMT they subtracted profile power at zero thrust from power at higher thrusts to show the effect of blade number at a constant Reynolds number. This approach leaves the calculation of profile power at zero thrust to the readers of their report. That is, the problem left to the readers was to calculate C_{Po}/s. Simple BEMT states this problem as

$$\frac{C_{Po}}{\sigma} = \tfrac{1}{2}\int_0^1 \left(\text{Airfoil } C_{do}\right) x^3 dx \qquad \text{Eq. (23)}$$

From Figure 38, the author would suggest that the NACA 0012 drag coefficient at zero lift (C_{do}) ***might be*** on the order of

$$C_{do} = 0.035 \quad \text{for RN} \le 10{,}000 \qquad \text{Eq. (24)}$$

For Reynolds numbers greater that 10,000 on up to about 2,000,000, Figure 38 suggests that

$$C_{do} = 0.0055691 + 1.0693814435E10^{-3}\left(\frac{1}{RN/10^6}\right) - 2.1137095758E^{-5}\left(\frac{1}{RN/10^6}\right)^2 + 2.1867028719E^{-7}\left(\frac{1}{RN/10^6}\right)^3 - 8.6017277278E^{-10}\left(\frac{1}{RN/10^6}\right)^4 \qquad \text{Eq. (25)}$$

The integration called for by Eq. (23) allows for the airfoil C_{do} to vary with blade radius station (x = r/R). It is convenient to set the local station Reynolds number in terms of the tip Reynolds number. That is, RN_x = (Tip RN)x when performing the rotor blade integration of Eq. (23).

The integration required by Eq. (23) is easily performed numerically. The author used MathCad 6.0 to make calculations at several tip Reynolds numbers, which yielded the graphical

results shown with the solid black line on Figure 39. Even with the considerable scatter, data from the four key tests differs substantially from what is calculated by Eq. (23) using the 2D airfoil drag coefficient suggested by Eq. (25).

Figure 39 shows that the minimum profile power data gathered from 1937 to 2018 ***might be*** approximated by such simple equations as

$$\frac{C_{Po}}{\sigma} = \frac{0.0035}{(\text{Tip RN}/1{,}000)^{1/8}} \quad \text{or} \quad \frac{0.02125}{(\text{Tip RN})^{1/5}} \qquad \text{Eq. (26)}$$

An upper bound to how C_{Po}/σ ***might*** *vary* with tip Reynolds number can be estimated based on Laitone's (Ref. 13) measurements of NACA 0012 minimum drag coefficient. Laitone gave his finding (as shown in Figure 38) as

$$C_{do} = \frac{0.35}{RN^{1/4}} \quad \text{for } 20{,}000 < RN < 80{,}000 \qquad \text{Eq. (27)}$$

The simple representation of C_{do} with Eq. (27) leads to a simple, closed form solution for C_{Po}/σ. When extrapolated to tip Reynolds numbers well beyond the range Laitone probably intended, the result is

$$\frac{C_{Po}}{\sigma} = \frac{7}{150\left(\text{Tip RN}^{1/4}\right)}\left(1 - xc^{15/4}\right) \qquad \text{Eq. (28)}$$

This estimate of C_{Po}/σ using Laitone's data is shown with the solid brown line on Figure 39.

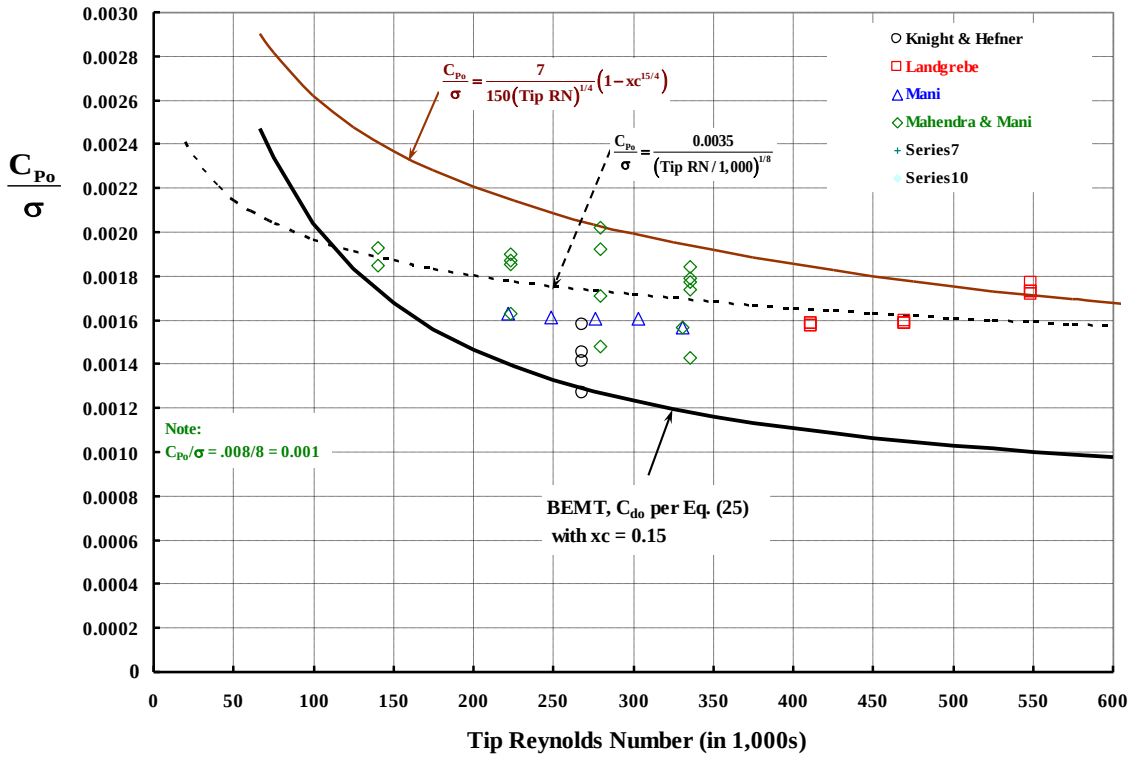

Figure 39. The use of 2D NACA 0012 drag coefficient at zero lift as a function of Reynolds number does not seem to predict minimum profile power of a rotor as a function of tip Reynolds number.

Data Assessment

The preceding pages lead to an equation useable for assessing the adequacy of data from the four references. The thought is that this assessment will be useful for further correlations with more advanced hover performance theories. This equation is based on Eqs. (22) and (26). That is,

$$\frac{C_P - C_{Po}}{\sigma^3} = \frac{1.393}{\sqrt{2}}\left(\frac{C_T}{\sigma^2}\right)^{3/2} + 0.0248\left[\frac{1.393}{\sqrt{2}}\left(\frac{C_T}{\sigma^2}\right)^{3/2}\right]^2 \quad \text{and} \quad \frac{C_{Po}}{\sigma} = \frac{0.0035}{(\text{Tip RN}/1{,}000)^{1/8}} \qquad \text{Eq. (29)}$$

Therefore, Eq. (29) leads immediately to

$$\frac{C_P}{\sigma^3} = \frac{1}{\sigma^2}\left(\frac{C_{Po}}{\sigma}\right) + \frac{1.393}{\sqrt{2}}\left(\frac{C_T}{\sigma^2}\right)^{3/2} + 0.0248\left[\frac{1.393}{\sqrt{2}}\left(\frac{C_T}{\sigma^2}\right)^{3/2}\right]^2 \qquad \text{Eq. (30)}$$

This leads to the assessment equation, which is

$$\frac{C_P}{\sigma^3} = \frac{1}{\sigma^2}\left[\frac{0.0035}{(\text{Tip RN}/1{,}000)^{1/8}}\right] + \frac{1.393}{\sqrt{2}}\left(\frac{C_T}{\sigma^2}\right)^{3/2} + 0.0248\left[\frac{1.393}{\sqrt{2}}\left(\frac{C_T}{\sigma^2}\right)^{3/2}\right]^2 \qquad \text{Eq. (31)}$$

Given the assessment equation, a graph of test C_P/σ^3 versus the results of Eq. (31) allows a linear regression calculation to be made. This calculation leads to an assessment in the form of y = Slope(x) + Intercept using Microsoft Excel's trendline tool. Table 4 compares the linear regression calculation and the R^2 values for each of the four referenced experiments reported over the last eight decades. The assessment is summarized in Table 4, which was constructed from Figures 40 through 44.

Table 4. Summary of Data Assessment

Ref.	Figure Number	Number of Blades	Reynolds Number	Slope	Intercept	R^2
1	40a	3 to 5	267,825	1.0066	– 0.0402	0.9992
1	40b	2	267,825	1.0549	– 0.3436	0.9990
2	41a	2 to 8	411,200	0.9472	– 0.0061	0.9996
2	41b	2 to 8	469,949	0.9441	+ 0.0159	0.9992
2	41c	2 to 8	548,720	1.0077	+ 0.0056	0.9985
3	42a	3	220,596 to 328,984	0.9819	– 0.0474	0.9970
3	42b	6	220,721 to 329,659	0.8961	+ 0.0006	0.9968
4	43a	2 to 6	334,,866	1.0062	+ 0.0022	0.9987
4	43b	2 to 6	279,055	1.0355	– 0.0048	0.9990
4	43c	3 to 6	223,244	1.0410	– 0.0031	0.9983
4	43d	3 & 6	139,528	1.0064	+ 0.0030	0.9996
All	**44**	**All**	**139,528 to 548,720**	**0.9509**	**+ 0.0007**	**0.9976**

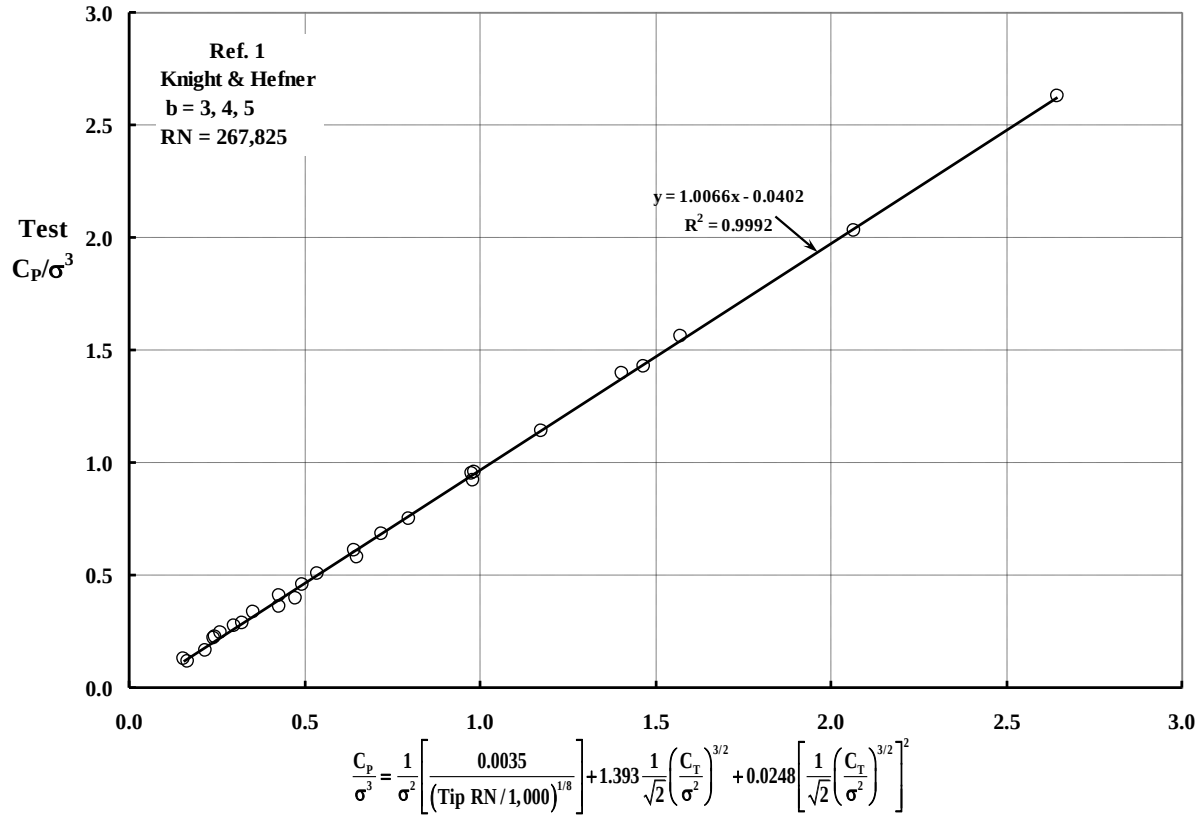

Figure 40a. Knight and Hefner's data reported in 1937.

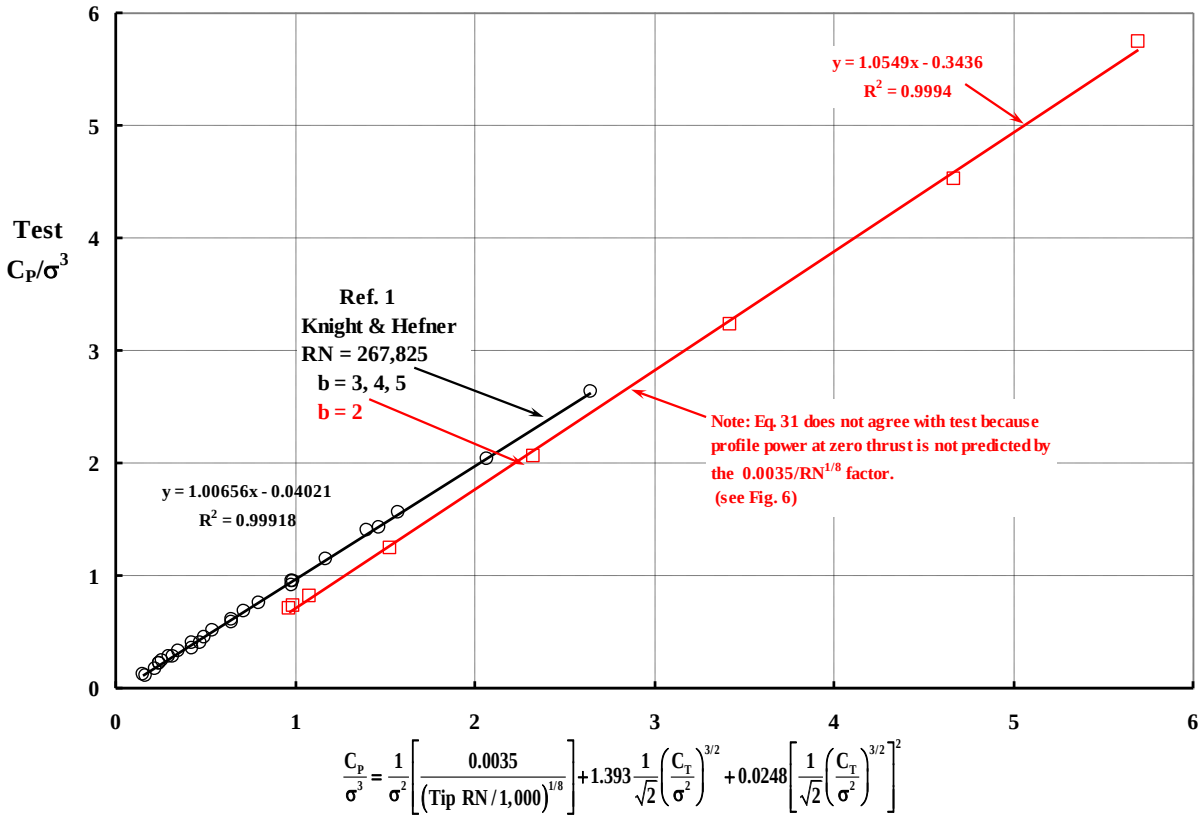

Figure 40b. Knight and Hefner's data reported in 1937.

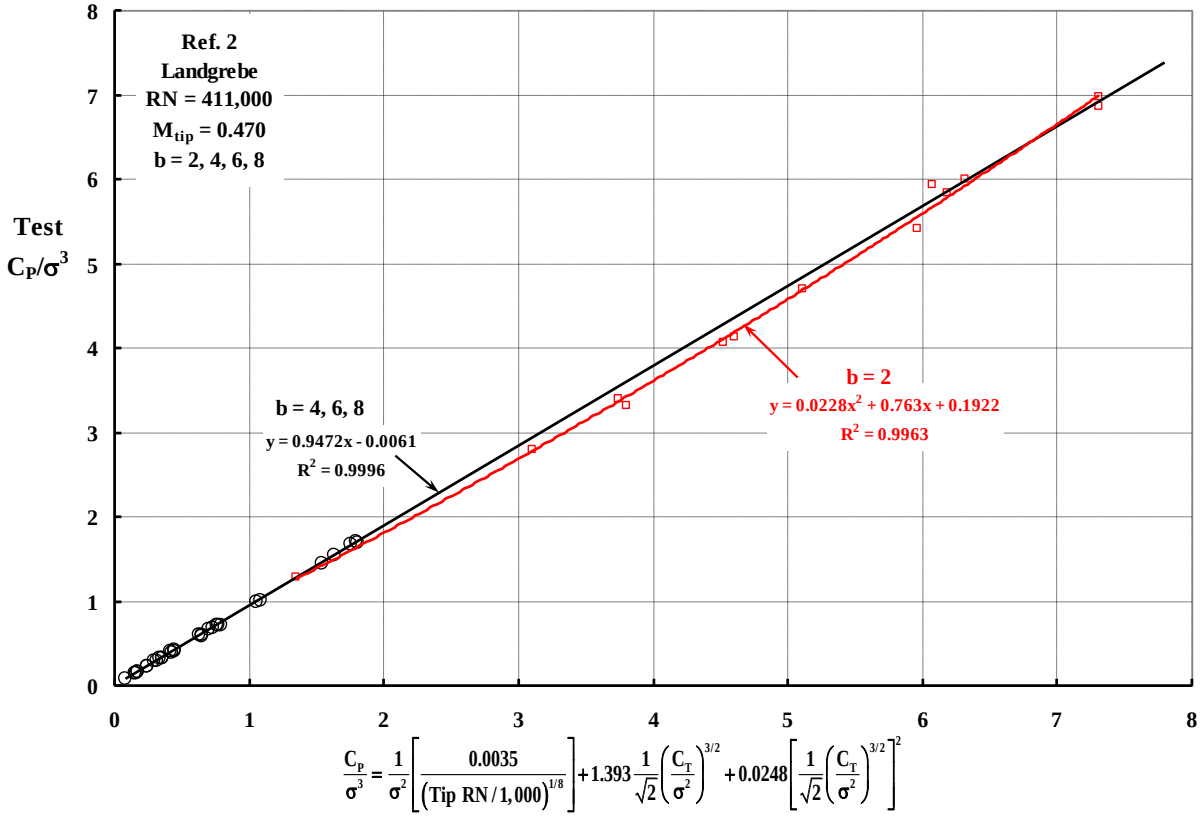

Figure 41a. Landgrebe's data reported in 1971.

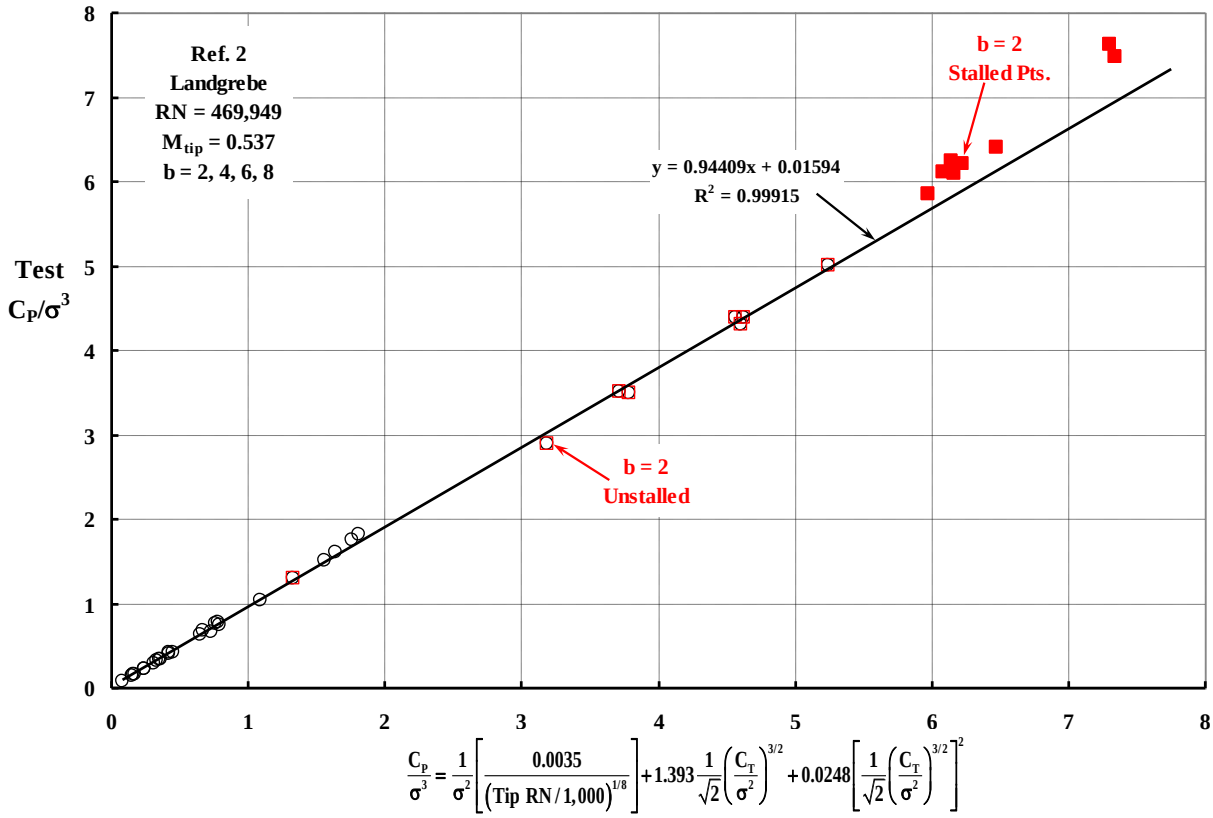

Figure 41b. Landgrebe's data reported in 1971.

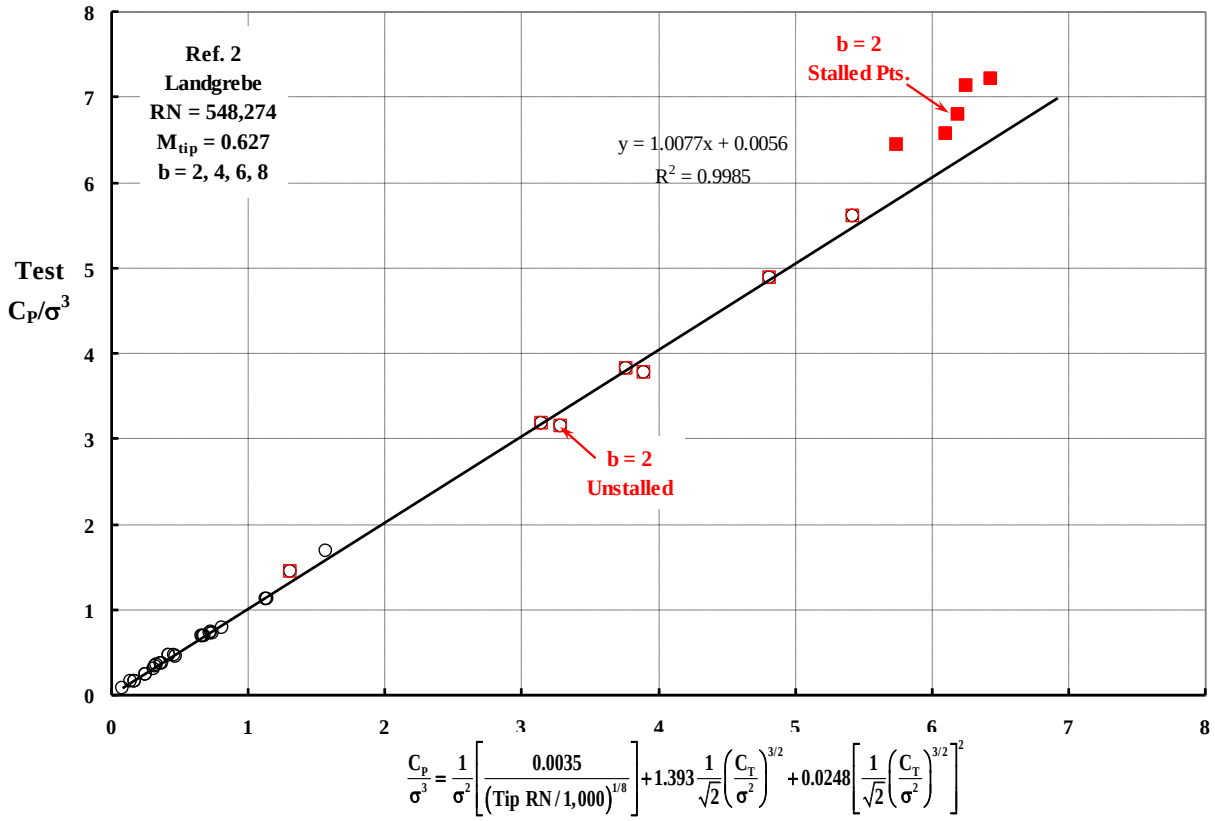

Figure 41c. Landgrebe's data reported in 1971.

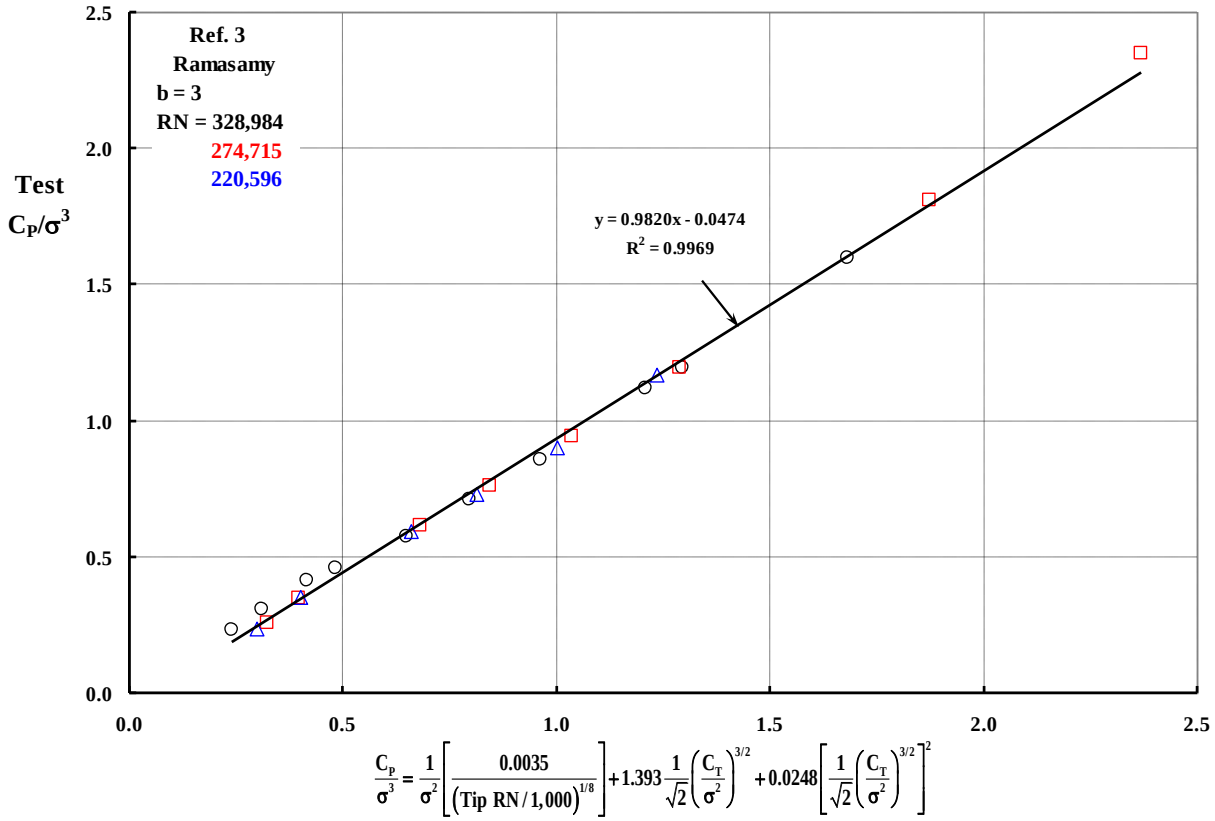

Figure 42a. Ramasamy's data reported in 2015.

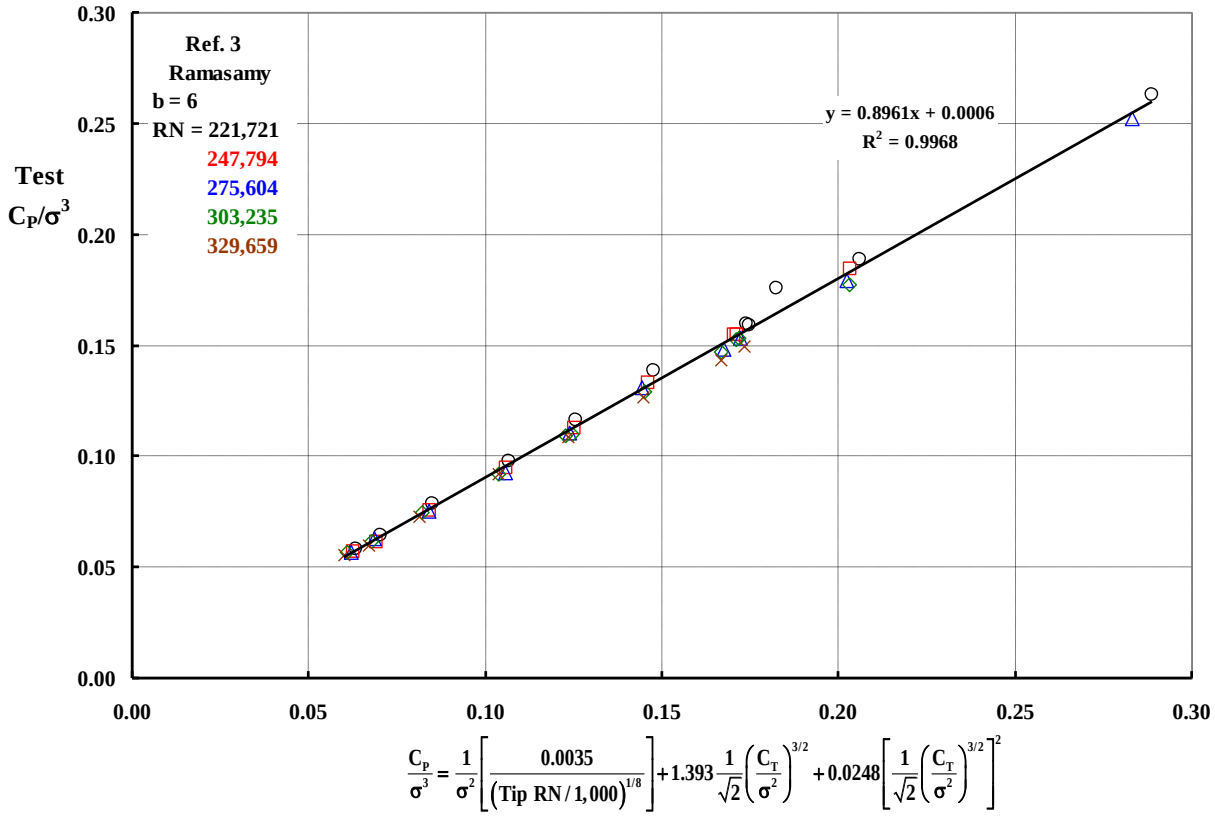

Figure 42b. Ramasamy's data reported in 2015.

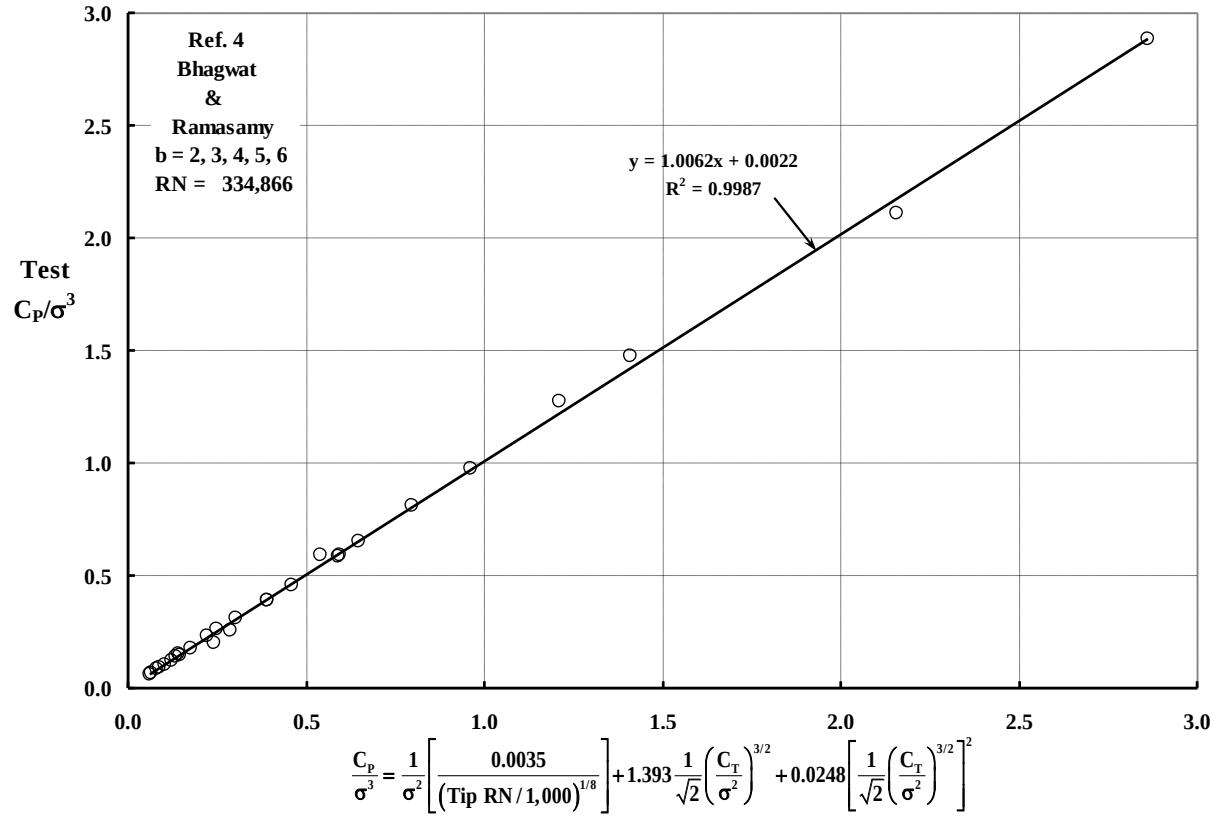

Figure 43a. Bhagwat and Ramasamy's data reported in 2018.

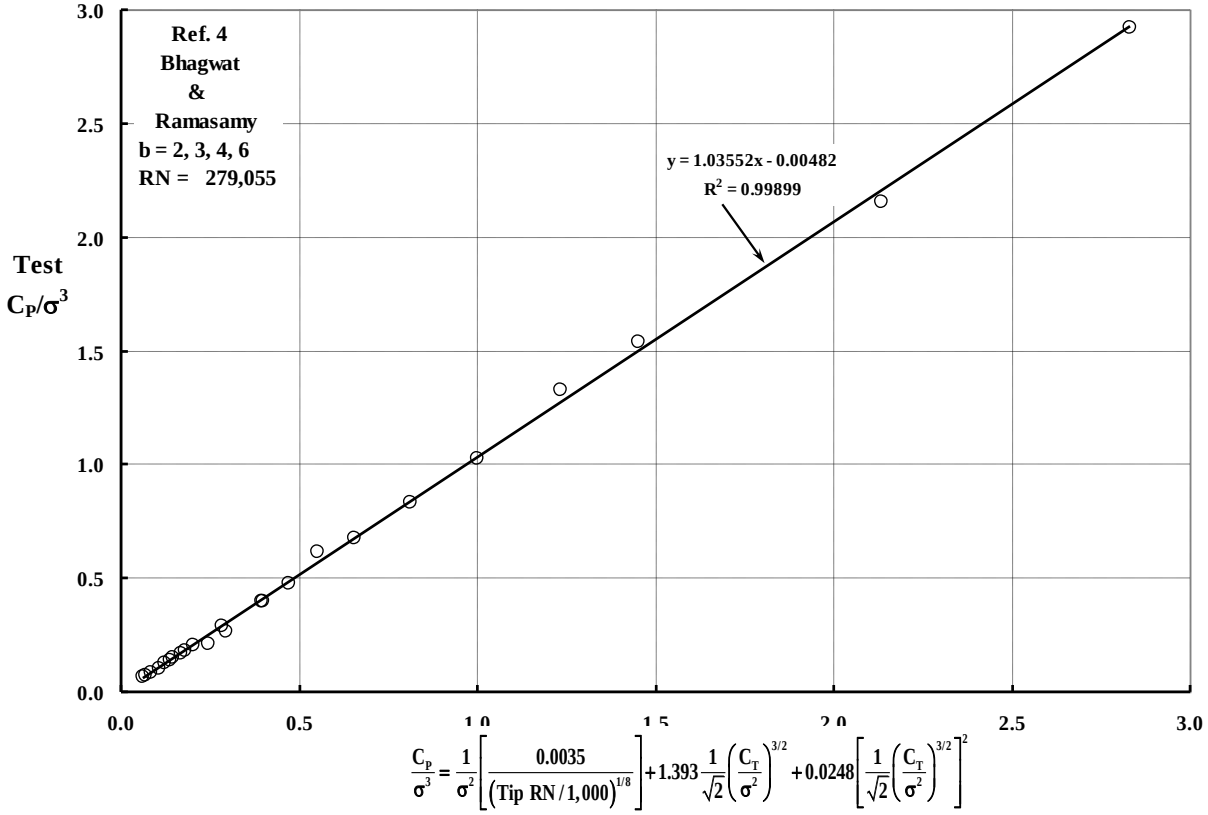

Figure 43b. Bhagwat and Ramasamy's data reported in 2018.

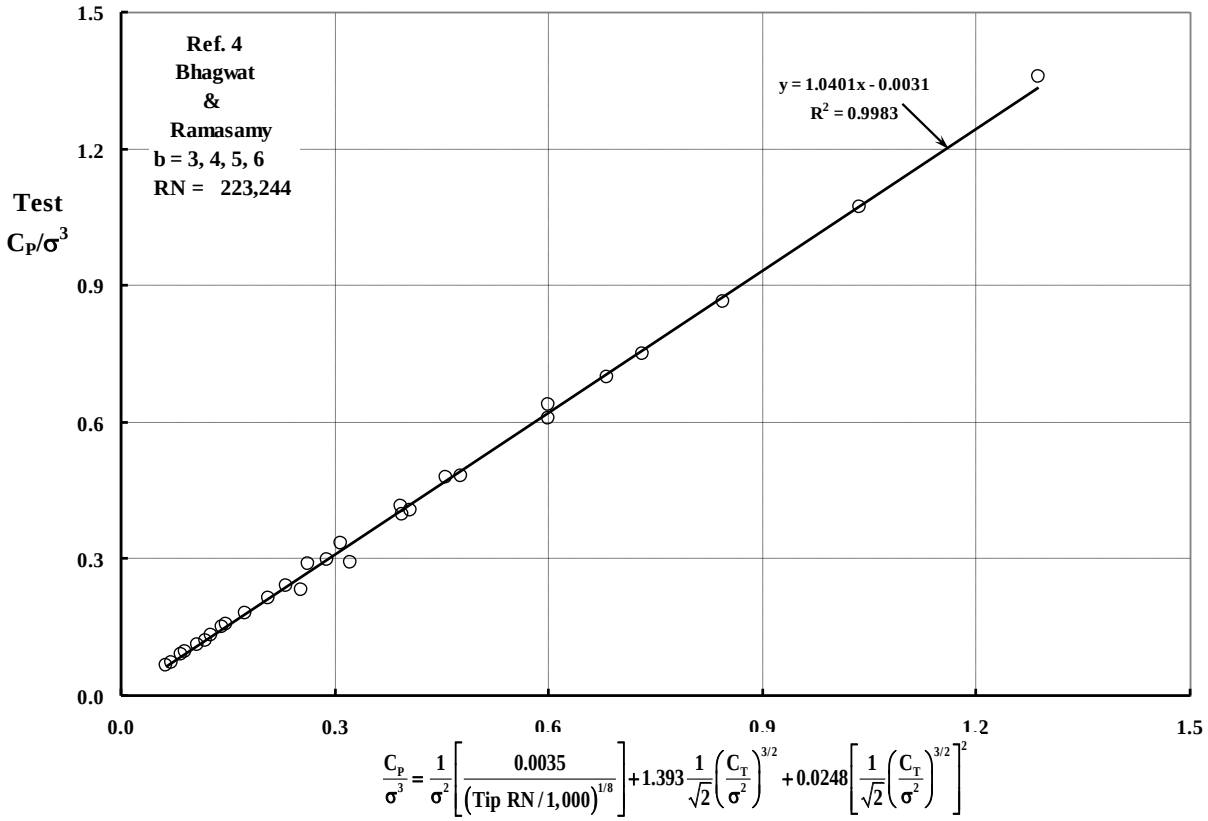

Figure 43c. Bhagwat and Ramasamy's data reported in 2018.

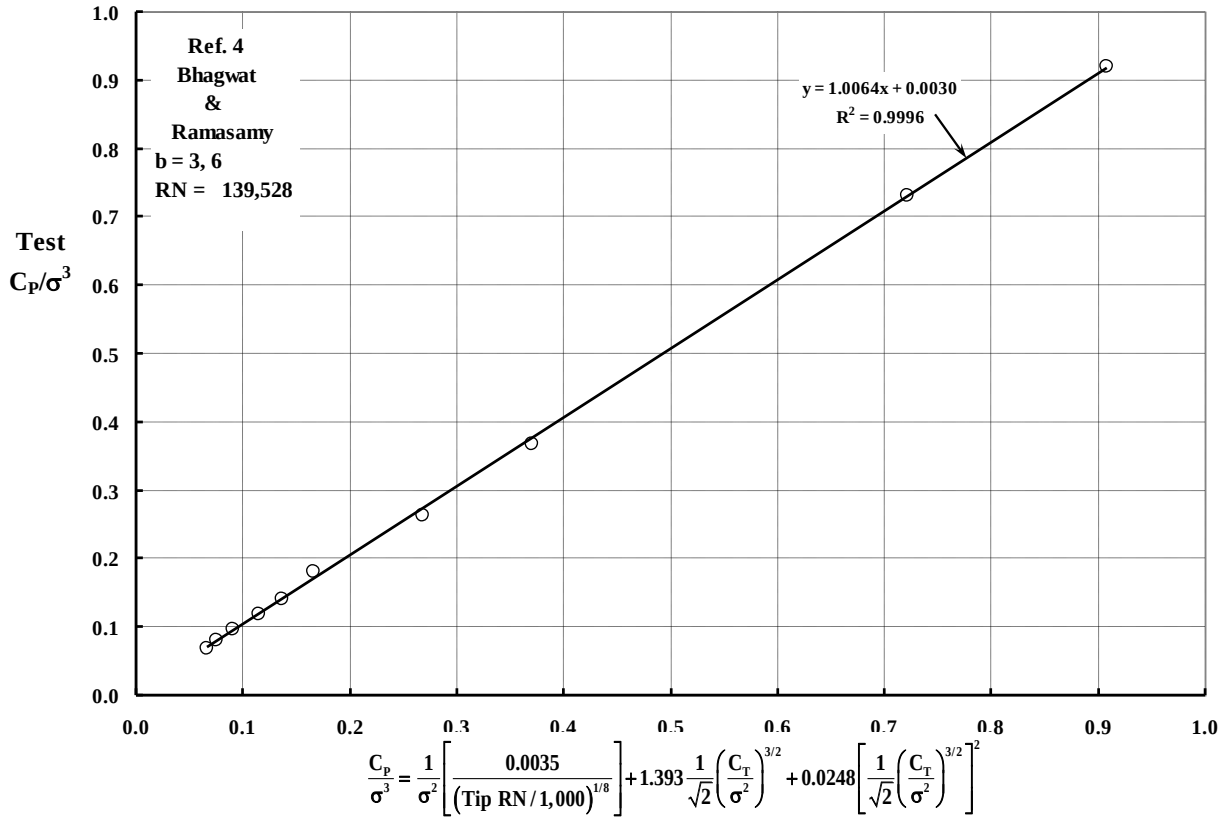

Figure 43d. Bhagwat and Ramasamy's data reported in 2018.

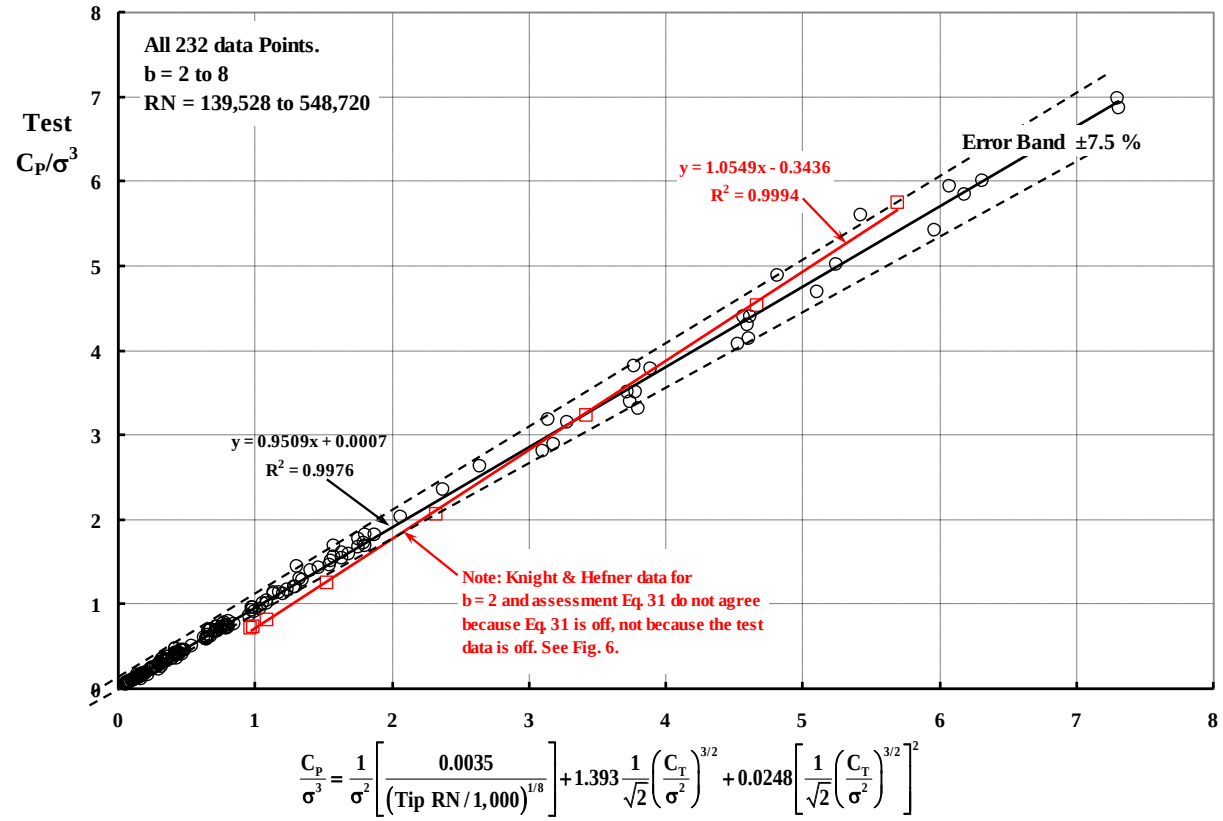

Figure 44. The experimental hover performance data from the four key tests can be semi-empirically approximated to within 7.5% with a simple equation.

CONCLUSIONS

For several decades, many questions about using model rotors to provide estimates of flight-worthy full-scale rotor characteristics have been asked and answered. There are, however, two questions that come up every once in a while that never seem to be definitively answered. This report has addressed those two questions:

1. Does blade aspect ratio influence hover performance or is rotor solidity the fundamental rotor geometry parameter for practical engineering purposes?

2. Is Reynolds number a significant factor in scaling up hover performance to full-scale rotor performance?

Hover performance data from four key experiments has been analyzed in detail to shed some light on these two questions. Each experiment used the simplest blade geometry. The blades were constant chord and untwisted. Three experiments used blades with the NACA 0012 airfoil from root to tip. The NACA 0015 was used in the earliest test. The four experiments provide data spanning a Reynolds number range of 136,500 to 548,700. Based on the analysis of these four experiments, the answers to the two questions are:

1. Rotor solidity is the fundamental rotor geometry parameter for practical engineering purposes. Any effect of blade aspect ratio appears to be such a secondary variable that its effect lies within the range of experimental error.

2. This answer is in two parts. (a) Reynolds number effects on the increase of power with thrust do not appear to be a significant factor for practical engineering purposes. (b) Reynolds number effects on minimum profile power at or very near zero rotor thrust could not be clearly established primarily because the low torque levels could not be accurately measured with the test equipment used.

A number of other observations can be made based on the analysis provided in this report. For instance:

1. The test matrices used in the four key references contained far too few data points. This is especially true when regression analysis is used to curve fit data. A collective pitch variation of four or five data points is quite insufficient to establish experimental accuracy and data repeatability. In fact, the definitive experiments answering the two key questions have yet to be made.

2. A common property of the power-versus-thrust (raised to the 3/2 exponent) graphs was that this curve was linear below the onset of blade stall.

3. The blade-to-blade interference at or near zero thrust may, in fact, be creating a turbulent flow field such that the effective Reynolds number at a blade element is considerably greater than what theories using 2D airfoil properties at a blade element would calculate.

RECOMMENDATIONS

Two recommendations for further study are suggested:

1. Using computational fluid dynamics (CFD), calculate the drag of the NACA 0012 airfoil at zero angle of attack as a function of Reynolds numbers over the range of 10,000 to 500,000. Assume a 2D test. Then repeat the calculation assuming the NACA 0012 is the airfoil on a constant chord, untwisted blade set. Set the blade pitch angle to zero. Vary the tip Reynolds number from 100,000 to 500,000 for blade number sets of 2, 3, 4, 5, 6, 7, and 8.

2. Test for the effect of tip Reynolds number on profile power at virtually zero thrust using the test rig shown in Figure 45.

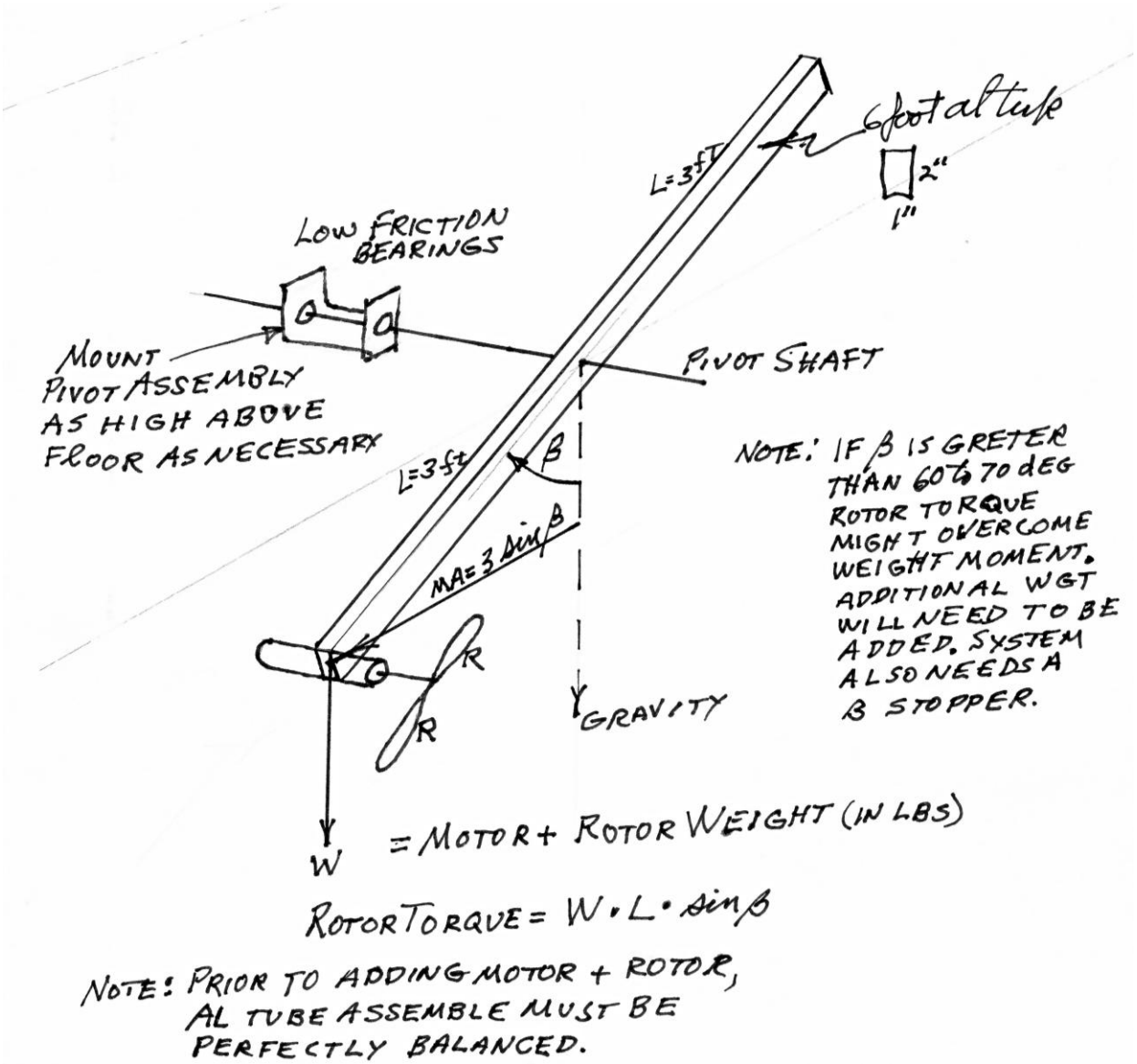

Figure 45. Torque measuring rig for testing rotor blades (and/or) hubs at virtually zero thrust.

REFERENCES

1. Montgomery Knight and Ralph Hefner, *Static Thrust Analysis of the Lifting Airscrew*, NACA TN 626, Dec. 1937.

2. Anton Jack Landgrebe, *An Analytical and Experimental Investigation of Helicopter Rotor Performance and Wake Geometry Characteristics*, USAAMRDLTR 71-24, June 1971.

3. Manikandan Ramasamy, *Hover Performance Measurements Toward Understanding Aerodynamic Interference in Coaxial, Tandem, and Tilt Rotors,* AHS Journal, vol. 60, no. 3, June 2015.

4. Mahendra Bhagwat and Manikandan Ramasamy, *Effect of Blade Number and Solidity on Rotor Hover Performance*, AHS Specialists' Conference on Aeromechanics Design for Transformative Flight, San Francisco, CA, Jan. 16-18, 2018.

5. Ron Gormont, The Boeing Company – Vertol Division, Interoffice Memorandum, *Scale Effects on Model Rotor Performance*, June 24, 1970. See Appendix C herein.

6. Harris, F. D., *Hover Performance of Isolated Proprotors and Propellers—Experimental Data*, NASA/CR–2017-219486, April 2017.

7. Harris, F. D., *Introduction to Autogyros, Helicopters, and Other V/STOL Aircraft, Volume II: Helicopters*, NASA/SP–2012-215959 Vol. II, Oct. 2012.

8. Alfred Gessow and Garry Meyers, *Aerodynamics of the Helicopter*, F. Ungar Publishing Co., Third Printing, 1967.

9. Wayne Johnson, *Helicopter Theory*, Princeton University Press, Princeton, New Jersey, 1980.

10. McCroskey, W. J., *A Critical Assessment of Wind Tunnel Results for the NACA 0012 Airfoil*, NASA TM 100019, USAAVSCOM Technical Report 87-A-5, Oct. 1987.

11. Sheldahl, R.E. and Klimas, P.C., *Aerodynamic Characteristics of Seven Symmetrical Airfoil Sections Through 180-Degree Angle of Attack for Use in Aerodynamic Analysis of Vertical Axis Wind Turbines*, Sand-80-2114, March 1981.

12. Private correspondence from Jim McCroskey to Frank Harris, Nov. 2017.

13. Laitone, E. V., *Aerodynamic Lift at Reynolds Numbers Below 7 × 10^4*, AIAA Journal, vol. 34, no. 9, Sept. 1996.

14. Schmitz, F. W., *Aerodynamics of the Model Airplane. Part I–Airfoil Measurements*, (Awarded the Ludwig Prandtl Prize for 1941), NTRS 19700029685, Nov. 1967.

15. Yamauchi, G. K. and Johnson, W., *Trends of Reynolds Number Effects on Two-Dimensional Airfoil Characteristics for Helicopter Rotor Analyses*, NASA TM-84363, April 1983.

APPENDIX A—TABULATED EXPERIMENTAL DATA

Experimental Data Bank

Knight & Hefner

Number of Blades	Solidity (σ)	Tip Speed (fps)	Tip Reynolds Number	Tip Mach Number	Collective Pitch (deg)	CT	CP	CT/σ	CP/σ	Root Cutout (rc/R)	NOTES About Data Point
2	0.04244	251.3	267,825	0.22511	0.0	0.000000	0.0000540	0.00000	0.001272	0.150	
2	0.04244	251.3	267,825	0.22511	1.0	0.000140	0.0000555	0.00330	0.001308	0.150	
2	0.04244	251.3	267,825	0.22511	2.0	0.000437	0.0000625	0.01028	0.001473	0.150	
2	0.04244	251.3	267,825	0.22511	4.0	0.001240	0.0000955	0.02922	0.002250	0.150	
2	0.04244	251.3	267,825	0.22511	6.0	0.002210	0.0001580	0.05207	0.003723	0.150	
2	0.04244	251.3	267,825	0.22511	8.0	0.003250	0.0002470	0.07658	0.005820	0.150	
2	0.04244	251.3	267,825	0.22511	10.0	0.004235	0.0003455	0.09978	0.008141	0.150	
2	0.04244	251.3	267,825	0.22511	12.0	0.004950	0.0004390	0.11663	0.010344	0.150	
3	0.06366	251.3	267,825	0.22511	0.0	0.000000	0.0000925	0.00000	0.001453	0.150	
3	0.06366	251.3	267,825	0.22511	2.0	0.000510	0.0001030	0.00801	0.001618	0.150	
3	0.06366	251.3	267,825	0.22511	4.0	0.001490	0.0001500	0.02340	0.002356	0.150	
3	0.06366	251.3	267,825	0.22511	6.0	0.002740	0.0002370	0.04304	0.003723	0.150	
3	0.06366	251.3	267,825	0.22511	8.0	0.004165	0.0003675	0.06542	0.005773	0.150	
3	0.06366	251.3	267,825	0.22511	10.0	0.005625	0.0005240	0.08836	0.008231	0.150	
3	0.06366	251.3	267,825	0.22511	12.0	0.006850	0.0006785	0.10760	0.010658	0.150	
4	0.08488	251.3	267,825	0.22511	0.0	0.000000	0.0001340	0.00000	0.001579	0.150	
4	0.08488	251.3	267,825	0.22511	1.0	0.000144	0.0001370	0.00169	0.001614	0.150	
4	0.08488	251.3	267,825	0.22511	2.0	0.000521	0.0001500	0.00614	0.001767	0.150	
4	0.08488	251.3	267,825	0.22511	3.0	0.001070	0.0001690	0.01261	0.001991	0.150	
4	0.08488	251.3	267,825	0.22511	4.0	0.001690	0.0002050	0.01991	0.002415	0.150	
4	0.08488	251.3	267,825	0.22511	5.0	0.002380	0.0002495	0.02804	0.002939	0.150	
4	0.08488	251.3	267,825	0.22511	6.0	0.003225	0.0003100	0.03799	0.003652	0.150	
4	0.08488	251.3	267,825	0.22511	7.0	0.003960	0.0003715	0.04665	0.004377	0.150	
4	0.08488	251.3	267,825	0.22511	8.0	0.004905	0.0004600	0.05779	0.005419	0.150	
4	0.08488	251.3	267,825	0.22511	9.0	0.005910	0.0005810	0.06963	0.006845	0.150	
4	0.08488	251.3	267,825	0.22511	10.0	0.006910	0.0006975	0.08141	0.008217	0.150	

4	0.08488	251.3	267,825	0.22511	11.0	0.007980	0.0008550	0.09401	0.010073	0.150	
4	0.08488	251.3	267,825	0.22511	12.0	0.008725	0.0009550	0.10279	0.011251	0.150	
5	0.10610	251.3	267,825	0.22511	0.0	0.000000	**0.0001500**	0.00000	0.001414	0.150	**Questionable**
5	0.10610	251.3	267,825	0.22511	2.0	0.000591	0.0001350	0.00557	0.001272	0.150	
5	0.10610	251.3	267,825	0.22511	4.0	0.001810	0.0001980	0.01706	0.001866	0.150	
5	0.10610	251.3	267,825	0.22511	6.0	0.003470	0.0003400	0.03270	0.003204	0.150	
5	0.10610	251.3	267,825	0.22511	8.0	0.005515	0.0005430	0.05198	0.005118	0.150	
5	0.10610	251.3	267,825	0.22511	10.0	0.007740	0.0008175	0.07295	0.007705	0.150	
5	0.10610	251.3	267,825	0.22511	12.0	0.010000	0.0011400	0.09425	0.010744	0.150	

Landgrebe

Number of Blades	Solidity (σ)	Tip Speed (fps)	Tip Reynolds Number	Tip Mach Number	Collective Pitch (deg)	CT	CP	CT/σ	CP/ σ	Root Cutout (rc/R)	NOTES About Data Point
2	0.03498	700.0	548,274	0.62699	0.0	-0.000052	0.0000619	-0.00150	0.001770	0.148	
2	0.03498	700.0	548,274	0.62699	6.0	0.001837	0.0001361	0.05250	0.003890	0.148	
2	0.03498	700.0	548,274	0.62699	6.0	0.001924	0.0001350	0.05500	0.003860	0.148	
2	0.03498	700.0	548,274	0.62699	7.0	0.002218	0.0001634	0.06340	0.004670	0.148	
2	0.03498	700.0	548,274	0.62699	7.0	0.002288	0.0001616	0.06540	0.004620	0.148	
2	0.03498	700.0	548,274	0.62699	8.0	0.002785	0.0002089	0.07960	0.005970	0.148	
2	0.03498	700.0	548,274	0.62699	9.0	0.003082	0.0002400	0.08810	0.006860	0.148	
2	0.03498	700.0	548,274	0.62699	10.0	0.003233	0.0002760	0.09240	0.007890	0.148	**STALL**
2	0.03498	700.0	548,274	0.62699	10.0	0.003397	0.0002813	0.09710	0.008040	0.148	**STALL**
2	0.03498	700.0	548,274	0.62699	10.0	0.003435	0.0002911	0.09820	0.008320	0.148	**STALL**
2	0.03498	700.0	548,274	0.62699	10.0	0.003463	0.0003051	0.09900	0.008720	0.148	**STALL**
2	0.03498	700.0	548,274	0.62699	10.5	0.003540	0.0003086	0.10120	0.008820	0.148	**STALL**
4	0.06997	700.0	548,274	0.62699	0.0	-0.000014	0.0001203	-0.00020	0.001720	0.148	
4	0.06997	700.0	548,274	0.62699	6.0	0.002645	0.0002477	0.03780	0.003540	0.148	
4	0.06997	700.0	548,274	0.62699	6.0	0.002680	0.0002512	0.03830	0.003590	0.148	
4	0.06997	700.0	548,274	0.62699	6.0	0.002764	0.0002456	0.03950	0.003510	0.148	
4	0.06997	700.0	548,274	0.62699	6.0	0.003047	0.0002704	0.04355	0.003865	0.148	
4	0.06997	700.0	548,274	0.62699	8.0	0.004275	0.0003869	0.06110	0.005530	0.148	
4	0.06997	700.0	548,274	0.62699	8.0	0.004268	0.0003855	0.06100	0.005510	0.148	
4	0.06997	700.0	548,274	0.62699	10.0	0.005681	0.0005786	0.08120	0.008270	0.148	
4	0.06997	700.0	548,274	0.62699	10.0	0.005660	0.0005786	0.08090	0.008270	0.148	**STALL**

4	0.06997	700.0	548,274	0.62699	10.5	0.005772	0.0006353	0.08250	0.009080	0.148	**STALL**
4	0.06997	700.0	548,274	0.62699	11.0	0.006129	0.0007242	0.08760	0.010350	0.148	**STALL**
4	0.06997	700.0	548,274	0.62699	11.0	0.006178	0.0007606	0.08830	0.010870	0.148	**STALL**
4	0.06997	700.0	548,274	0.62699	11.0	0.006003	0.0007060	0.08580	0.010090	0.148	**STALL**
6	0.10495	700.0	548,274	0.62699	0.0	0.000000	0.0001816	0.00000	0.001730	0.148	
6	0.10495	700.0	548,274	0.62699	6.0	0.003338	0.0003484	0.03180	0.003320	0.148	
6	0.10495	700.0	548,274	0.62699	6.0	0.003463	0.0003946	0.03300	0.003760	0.148	
6	0.10495	700.0	548,274	0.62699	8.0	0.005185	0.0005300	0.04940	0.005050	0.148	
6	0.10495	700.0	548,274	0.62699	8.0	0.005216	0.0005279	0.04970	0.005030	0.148	
6	0.10495	700.0	548,274	0.62699	10.0	0.007137	0.0007934	0.06800	0.007560	0.148	
6	0.10495	700.0	548,274	0.62699	10.0	0.007263	0.0008018	0.06920	0.007640	0.148	
6	0.10495	700.0	548,274	0.62699	10.0	0.007273	0.0007997	0.06930	0.007620	0.148	
6	0.10495	700.0	548,274	0.62699	11.0	0.007934	0.0010149	0.07560	0.009670	0.148	**STALL**
6	0.10495	700.0	548,274	0.62699	11.0	0.007955	0.0010128	0.07580	0.009650	0.148	**STALL**
8	0.13994	700.0	548,274	0.62699	0.0	-0.000028	0.0002421	-0.00020	0.001730	0.148	
8	0.13994	700.0	548,274	0.62699	6.0	0.003932	0.0004534	0.02810	0.003240	0.148	
8	0.13994	700.0	548,274	0.62699	6.0	0.003946	0.0004520	0.02820	0.003230	0.148	
8	0.13994	700.0	548,274	0.62699	8.0	0.006045	0.0006745	0.04320	0.004820	0.148	
8	0.13994	700.0	548,274	0.62699	8.0	0.006059	0.0006717	0.04330	0.004800	0.148	
8	0.13994	700.0	548,274	0.62699	10.0	0.008452	0.0010089	0.06040	0.007210	0.148	
8	0.13994	700.0	548,274	0.62699	10.0	0.008564	0.0010285	0.06120	0.007350	0.148	
8	0.13994	700.0	548,274	0.62699	11.0	0.009628	0.0012692	0.06880	0.009070	0.148	
8	0.13994	700.0	548,274	0.62699	11.0	0.009670	0.0012720	0.06910	0.009090	0.148	
2	0.03498	600.0	469,949	0.53742	0.0	-0.000038	0.0000554	-0.00109	0.001584	0.148	Average
2	0.03498	600.0	469,949	0.53742	6.0	0.001846	0.0001240	0.05276	0.003544	0.148	
2	0.03498	600.0	469,949	0.53742	7.0	0.002211	0.0001498	0.06319	0.004283	0.148	
2	0.03498	600.0	469,949	0.53742	7.0	0.002174	0.0001503	0.06215	0.004296	0.148	
2	0.03498	600.0	469,949	0.53742	8.0	0.002661	0.0001844	0.07605	0.005272	0.148	
2	0.03498	600.0	469,949	0.53742	8.0	0.002671	0.0001880	0.07636	0.005373	0.148	
2	0.03498	600.0	469,949	0.53742	8.0	0.002643	0.0001883	0.07555	0.005381	0.148	
2	0.03498	600.0	469,949	0.53742	9.0	0.002986	0.0002145	0.08536	0.006133	0.148	
2	0.03498	600.0	469,949	0.53742	10.0	0.003326	0.0002503	0.09507	0.007154	0.148	STALL
2	0.03498	600.0	469,949	0.53742	10.0	0.003377	0.0002617	0.09654	0.007481	0.148	STALL
2	0.03498	600.0	469,949	0.53742	10.0	0.003400	0.0002675	0.09720	0.007646	0.148	STALL

2	0.03498	600.0	469,949	0.53742	10.0	0.003439	0.0002656	0.09831	0.007593	0.148	STALL
2	0.03498	600.0	469,949	0.53742	10.0	0.003411	0.0002614	0.09750	0.007472	0.148	STALL
2	0.03498	600.0	469,949	0.53742	10.0	0.003546	0.0002746	0.10137	0.007850	0.148	STALL
2	0.03498	600.0	469,949	0.53742	11.0	0.003911	0.0003204	0.11181	0.009158	0.148	STALL
2	0.03498	600.0	469,949	0.53742	11.0	0.003897	0.0003265	0.11139	0.009332	0.148	STALL
4	0.06997	600.0	469,949	0.53742	0.0	-0.000089	0.0001109	-0.00127	0.001586	0.148	Average
4	0.06997	600.0	469,949	0.53742	6.0	0.002655	0.0002307	0.03794	0.003297	0.148	
4	0.06997	600.0	469,949	0.53742	6.0	0.002939	0.0002535	0.04200	0.003623	0.148	
4	0.06997	600.0	469,949	0.53742	8.0	0.004096	0.0003548	0.05854	0.005070	0.148	
4	0.06997	600.0	469,949	0.53742	10.0	0.005610	0.0005160	0.08018	0.007375	0.148	
4	0.06997	600.0	469,949	0.53742	10.5	0.005859	0.0005526	0.08374	0.007899	0.148	
4	0.06997	600.0	469,949	0.53742	11.0	0.006208	0.0006039	0.08873	0.008631	0.148	
4	0.06997	600.0	469,949	0.53742	11.0	0.006341	0.0006219	0.09062	0.008889	0.148	
6	0.10495	600.0	469,949	0.53742	0.0	-0.000140	0.0001668	- 0.00133	0.001589	0.148	Average
6	0.10495	600.0	469,949	0.53742	6.0	0.003302	0.0003403	0.03146	0.003242	0.148	
6	0.10495	600.0	469,949	0.53742	8.0	0.004993	0.0004947	0.04757	0.004714	0.148	
6	0.10495	600.0	469,949	0.53742	10.0	0.007054	0.0007265	0.06721	0.006923	0.148	
6	0.10495	600.0	469,949	0.53742	10.5	0.007197	0.0007883	0.06857	0.007511	0.148	
6	0.10495	600.0	469,949	0.53742	11.0	0.008033	0.0008854	0.07654	0.008436	0.148	
6	0.10495	600.0	469,949	0.53742	11.0	0.008154	0.0008981	0.07770	0.008557	0.148	
8	0.13994	600.0	469,949	0.53742	0.0	-0.000193	0.0002233	-0.00138	0.001596	0.148	
8	0.13994	600.0	469,949	0.53742	6.0	0.003895	0.0004250	0.02783	0.003037	0.148	
8	0.13994	600.0	469,949	0.53742	6.0	0.003733	0.0004375	0.02668	0.003126	0.148	
8	0.13994	600.0	469,949	0.53742	8.0	0.005836	0.0006232	0.04171	0.004453	0.148	
8	0.13994	600.0	469,949	0.53742	8.0	0.005869	0.0006350	0.04194	0.004538	0.148	
8	0.13994	600.0	469,949	0.53742	10.0	0.008179	0.0009171	0.05845	0.006554	0.148	
8	0.13994	600.0	469,949	0.53742	10.0	0.008309	0.0009340	0.05938	0.006674	0.148	
8	0.13994	600.0	469,949	0.53742	11.0	0.009587	0.0011244	0.06851	0.008035	0.148	
8	0.13994	600.0	469,949	0.53742	11.0	0.009554	0.0011396	0.06828	0.008144	0.148	
2	0.03498	525.0	411,205	0.47024	0.0	-0.000003	0.0000551	-0.00007	0.001576	0.148	
2	0.03498	525.0	411,205	0.47024	6.0	0.001774	0.0001199	0.05071	0.003427	0.148	
2	0.03498	525.0	411,205	0.47024	7.0	0.002207	0.0001419	0.06308	0.004055	0.148	

2	0.03498	525.0	411,205	0.47024	7.0	0.002173	0.0001454	0.06211	0.004155	0.148
2	0.03498	525.0	411,205	0.47024	8.0	0.002611	0.0001743	0.07463	0.004983	0.148
2	0.03498	525.0	411,205	0.47024	8.0	0.002651	0.0001772	0.07577	0.005064	0.148
2	0.03498	525.0	411,205	0.47024	9.0	0.002909	0.0002009	0.08315	0.005742	0.148
2	0.03498	525.0	411,205	0.47024	9.5	0.003310	0.0002319	0.09463	0.006630	0.148
2	0.03498	525.0	411,205	0.47024	10.0	0.003363	0.0002540	0.09613	0.007261	0.148
2	0.03498	525.0	411,205	0.47024	10.0	0.003410	0.0002498	0.09748	0.007141	0.148
2	0.03498	525.0	411,205	0.47024	10.0	0.003470	0.0002569	0.09920	0.007342	0.148
2	0.03498	525.0	411,205	0.47024	11.0	0.003889	0.0002940	0.11117	0.008403	0.148
2	0.03498	525.0	411,205	0.47024	11.0	0.003889	0.0002989	0.11116	0.008544	0.148
4	0.06997	525.0	411,205	0.47024	0.0	0.000000	0.0001109	0.00000	0.001584	0.148
4	0.06997	525.0	411,205	0.47024	6.0	0.002536	0.0002258	0.03624	0.003227	0.148
4	0.06997	525.0	411,205	0.47024	6.0	0.002635	0.0002315	0.03766	0.003308	0.148
4	0.06997	525.0	411,205	0.47024	6.0	0.002898	0.0002465	0.04141	0.003523	0.148
4	0.06997	525.0	411,205	0.47024	8.0	0.003959	0.0003424	0.05659	0.004894	0.148
4	0.06997	525.0	411,205	0.47024	8.0	0.004075	0.0003439	0.05824	0.004915	0.148
4	0.06997	525.0	411,205	0.47024	10.0	0.005558	0.0004976	0.07944	0.007112	0.148
4	0.06997	525.0	411,205	0.47024	10.5	0.005834	0.0005281	0.08338	0.007547	0.148
4	0.06997	525.0	411,205	0.47024	11.0	0.006173	0.0005745	0.08822	0.008211	0.148
4	0.06997	525.0	411,205	0.47024	11.0	0.006306	0.0005872	0.09013	0.008393	0.148
4	0.06997	525.0	411,205	0.47024	11.0	0.006315	0.0005788	0.09025	0.008272	0.148
6	0.10495	525.0	411,205	0.47024	0.0	-0.000020	0.0001663	0.00019	0.001584	0.148
6	0.10495	525.0	411,205	0.47024	6.0	0.003317	0.0003300	0.03160	0.003145	0.148
6	0.10495	525.0	411,205	0.47024	6.0	0.003127	0.0003299	0.02980	0.003144	0.148
6	0.10495	525.0	411,205	0.47024	8.0	0.004974	0.0004698	0.04739	0.004476	0.148
6	0.10495	525.0	411,205	0.47024	8.0	0.004905	0.0004816	0.04674	0.004588	0.148
6	0.10495	525.0	411,205	0.47024	10.0	0.007011	0.0006860	0.06680	0.006536	0.148
6	0.10495	525.0	411,205	0.47024	10.0	0.007010	0.0006965	0.06680	0.006636	0.148
6	0.10495	525.0	411,205	0.47024	10.0	0.006829	0.0006922	0.06507	0.006595	0.148
6	0.10495	525.0	411,205	0.47024	11.0	0.007959	0.0008262	0.07584	0.007872	0.148
6	0.10495	525.0	411,205	0.47024	11.0	0.008072	0.0008359	0.07691	0.007965	0.148
8	0.13994	525.0	411,205	0.47024	0.0	-0.000037	0.0002206	-0.00026	0.001576	0.148
8	0.13994	525.0	411,205	0.47024	6.0	0.003618	0.0004161	0.02585	0.002973	0.148

8	0.13994	525.0	411,205	0.47024	6.0	0.003848	0.0004302	0.02750	0.003074	0.148
8	0.13994	525.0	411,205	0.47024	6.0	0.004036	0.0004399	0.02884	0.003143	0.148
8	0.13994	525.0	411,205	0.47024	8.0	0.005843	0.0006176	0.04175	0.004413	0.148
8	0.13994	525.0	411,205	0.47024	8.0	0.005896	0.0006429	0.04213	0.004594	0.148
8	0.13994	525.0	411,205	0.47024	10.0	0.008194	0.0008899	0.05856	0.006359	0.148
8	0.13994	525.0	411,205	0.47024	10.0	0.008311	0.0009068	0.05939	0.006480	0.148
8	0.13994	525.0	411,205	0.47024	11.0	0.009620	0.0010719	0.06875	0.007660	0.148
8	0.13994	525.0	411,205	0.47024	11.0	0.009485	0.0010954	0.06778	0.007828	0.148

Mani's Test Data, θt = 0

Number of Blades	Solidity (σ)	Tip Speed (fps)	Tip Reynolds Number	Tip Mach Number	Collective Pitch (deg)	CT	CP	CT/σ	CP/σ	Root Cutout (rc/R)	NOTES About Data Point
6	0.16796	182.5	221,561	0.16351	0	0.000057	0.0002746	0.00034	0.001635	0.1910	
6	0.16796	182.2	221,142	0.16320	3.25	0.001069	0.0003062	0.00636	0.001823	0.1910	
6	0.16796	180.9	219,595	0.16206	3.85	0.002218	0.0003722	0.01321	0.002216	0.1910	
6	0.16796	180.9	219,512	0.16200	5.95	0.003535	0.0004629	0.02105	0.002756	0.1910	
6	0.16796	182.1	220,974	0.16307	6.57	0.004498	0.0005500	0.02678	0.003275	0.1910	
6	0.16796	182.2	221,164	0.16321	7.36	0.005491	0.0006556	0.03269	0.003903	0.1910	
6	0.16796	183.5	222,756	0.16439	7.59	0.006610	0.0007533	0.03936	0.004485	0.1910	
6	0.16796	180.8	219,410	0.16192	8.16	0.006582	0.0007568	0.03919	0.004506	0.1910	
6	0.16796	182.0	220,847	0.16298	9.08	0.006918	0.0008334	0.04119	0.004962	0.1910	
6	0.16796	181.4	220,213	0.16251	9.17	0.007799	0.0008941	0.04643	0.005323	0.1910	
6	0.16796	181.9	220,759	0.16292	10.7	0.010566	0.0012461	0.06291	0.007419	0.1910	
		181.9	**220,721**	**0.16289**							
	0.00000										
6	0.16796	204.7	248,403	0.18332	0	0.000112	0.0002710	0.00067	0.001614	0.1910	
6	0.16796	204.1	247,725	0.18282	3.25	0.001043	0.0002904	0.00621	0.001729	0.1910	
6	0.16796	203.8	247,374	0.18256	3.85	0.002236	0.0003582	0.01331	0.002132	0.1910	
6	0.16796	204.2	247,887	0.18294	5.95	0.003533	0.0004497	0.02104	0.002677	0.1910	
6	0.16796	203.7	247,201	0.18243	6.57	0.004514	0.0005324	0.02688	0.003170	0.1910	
6	0.16796	204.6	248,323	0.18326	7.36	0.005474	0.0006310	0.03259	0.003757	0.1910	
6	0.16796	203.6	247,065	0.18233	8.16	0.006478	0.0007313	0.03857	0.004354	0.1910	
6	0.16796	205.5	249,451	0.18409	8.16	0.006507	0.0007322	0.03874	0.004359	0.1910	
6	0.16796	203.3	246,715	0.18207	9.17	0.007723	0.0008721	0.04598	0.005192	0.1910	
		204.2	**247,794**	**0.18287**							
6	0.16796	227.3	275,890	0.20360	0	0.000107	0.0002702	0.00064	0.001609	0.1910	

6	0.16796	226.8	275,258	0.20313	3.25	0.001038	0.0002992	0.00618	0.001781	0.1910
6	0.16796	227.4	276,000	0.20368	3.85	0.002272	0.0003573	0.01353	0.002127	0.1910
6	0.16796	226.8	275,236	0.20312	5.95	0.003559	0.0004382	0.02119	0.002609	0.1910
6	0.16796	228.1	276,883	0.20433	6.57	0.004486	0.0005254	0.02671	0.003128	0.1910
6	0.16796	227.4	276,055	0.20372	7.36	0.005423	0.0006222	0.03229	0.003704	0.1910
6	0.16796	225.4	273,568	0.20189	7.59	0.006568	0.0007260	0.03911	0.004323	0.1910
6	0.16796	227.0	275,559	0.20336	8.16	0.006382	0.0007022	0.03800	0.004181	0.1910
6	0.16796	227.1	275,589	0.20338	9.17	0.007717	0.0008510	0.04595	0.005067	0.1910
6	0.16796	227.4	276,000	0.20368	10.7	0.010436	0.0011968	0.06214	0.007126	0.1910
		227.1	**275,604**	**0.20339**						
6	0.16796	249.8	303,140	0.22371	0	0.000021	0.0002702	0.00013	0.001609	0.1910
6	0.16796	249.4	302,643	0.22334	3.25	0.001033	0.0002922	0.00615	0.001740	0.1910
6	0.16796	249.3	302,561	0.22328	3.85	0.002185	0.0003538	0.01301	0.002106	0.1910
6	0.16796	250.5	304,022	0.22436	5.95	0.003501	0.0004374	0.02084	0.002604	0.1910
6	0.16796	250.2	303,636	0.22408	6.57	0.004464	0.0005183	0.02658	0.003086	0.1910
6	0.16796	249.7	303,112	0.22369	7.36	0.004560	0.0005218	0.02715	0.003107	0.1910
6	0.16796	250.0	303,471	0.22395	7.36	0.005481	0.0006134	0.03263	0.003652	0.1910
6	0.16796	249.9	303,360	0.22387	7.59	0.006553	0.0007242	0.03902	0.004312	0.1910
6	0.16796	249.7	303,112	0.22369	7.59	0.006589	0.0007269	0.03923	0.004328	0.1910
6	0.16796	249.0	302,230	0.22304	8.16	0.006392	0.0006987	0.03806	0.004160	0.1910
6	0.16796	250.7	304,298	0.22457	9.17	0.007778	0.0008422	0.04631	0.005014	0.1910
		249.8	**303,235**	**0.22378**						
6	0.16796	272.5	330,776	0.24411	0	0.000001	0.0002631	0.00001	0.001567	0.1910
6	0.16796	271.5	329,534	0.24319	3.25	0.001008	0.0002834	0.00600	0.001687	0.1910
6	0.16796	272.3	330,445	0.24386	3.85	0.002183	0.0003450	0.01300	0.002054	0.1910
6	0.16796	271.3	329,231	0.24297	5.95	0.003533	0.0004356	0.02104	0.002594	0.1910
6	0.16796	272.4	330,665	0.24402	6.57	0.004536	0.0005166	0.02701	0.003076	0.1910
6	0.16796	271.1	329,066	0.24284	7.36	0.005497	0.0006019	0.03273	0.003584	0.1910
6	0.16796	270.2	327,907	0.24199	7.59	0.006664	0.0007093	0.03968	0.004223	0.1910
6	0.16796	271.6	329,645	0.24327	10.7	0.006405	0.0006811	0.03813	0.004055	0.1910
		271.6	**329,659**	**0.2433**						
	0.00000									
3	0.08398	272.7	330,941	0.24423	0.00	0.000000	0.0001364	0.00000	0.001624	0.1910
3	0.08398	272.7	330,941	0.24423	3.61	0.001214	0.0001828	0.01446	0.002177	0.1910
3	0.08398	272.4	330,583	0.24396	4.60	0.002230	0.0002446	0.02655	0.002913	0.1910

3	0.08398	272.4	330,583	0.24396	6.00	0.002769	0.0002719	0.03297	0.003238	0.1910
3	0.08398	270.9	328,817	0.24266	8.34	0.003914	0.0003414	0.04661	0.004066	0.1910
3	0.08398	272.3	330,445	0.24386	9.30	0.004807	0.0004215	0.05724	0.005019	0.1910
3	0.08398	272.5	330,748	0.24408	10.40	0.005707	0.0005086	0.06796	0.006057	0.1910
3	0.08398	271.0	328,928	0.24274	11.72	0.006935	0.0006626	0.08258	0.007891	0.1910
3	0.08398	271.0	328,928	0.24274	12.27	0.007323	0.0007084	0.08720	0.008436	0.1910
3	0.08398	271.0	328,928	0.24274	14.30	0.009004	0.0009460	0.10722	0.011265	0.1910
		271.9	**329,984**	**0.24352**						
3	0.08398	181.4	220,155	0.16247	4.68	0.001203	0.0001522	0.01433	0.001813	0.1910
3	0.08398	181.6	220,356	0.16262	3.61	0.001948	0.0002068	0.02320	0.002463	0.1910
3	0.08398	181.2	219,931	0.16230	8.34	0.004044	0.0003643	0.04816	0.004338	0.1910
3	0.08398	182.0	220,836	0.16297	9.30	0.005007	0.0004506	0.05962	0.005365	0.1910
3	0.08398	182.4	221,360	0.16336	10.40	0.006030	0.0005588	0.07180	0.006654	0.1910
3	0.08398	180.6	219,184	0.16175	11.72	0.007236	0.0007075	0.08617	0.008425	0.1910
3	0.08398	183.7	223,015	0.16458	16.21	0.009720	0.0010727	0.11574	0.012774	0.1910
3	0.08398	181.2	219,929	0.16230	17.07	0.011566	0.0013913	0.13773	0.016567	0.1910
		234.8	**220,596**	**0.16279**						
3	0.08398	225.6	273,863	0.20210	4.68	0.000986	0.0001390	0.01174	0.001656	0.1910
3	0.08398	225.9	274,185	0.20234	3.61	0.002035	0.0002077	0.02423	0.002473	0.1910
3	0.08398	226.2	274,503	0.20258	8.34	0.003933	0.0003520	0.04683	0.004192	0.1910
3	0.08398	227.8	276,442	0.20401	9.30	0.004861	0.0004330	0.05788	0.005156	0.1910
3	0.08398	224.7	272,773	0.20130	10.40	0.005879	0.0005342	0.07001	0.006361	0.1910
3	0.08398	227.8	276,524	0.20407	11.72	0.007025	0.0006917	0.08365	0.008236	0.1910
		243.2	**274,715**	**0.20273**						

Mahendra & Mani

Number of Blades	Solidity (σ)	Tip Speed (fps)	Tip Reynolds Number	Tip Mach Number	Collective Pitch (deg)	CT	CP	CT/σ	CP/σ	Root Cutout (rc/R)	NOTES About Data Point
6	0.16794	273.6	334,866	0.24504	0.0	0.000001	0.0002987	0.00000	0.001778	0.1910	
6	0.16794	273.6	334,866	0.24504	3.3	0.001008	0.0003220	0.00600	0.001917	0.1910	
6	0.16794	273.6	334,866	0.24504	3.9	0.002183	0.0003918	0.01300	0.002333	0.1910	
6	0.16794	273.6	334,866	0.24504	6.0	0.003533	0.0004952	0.02104	0.002949	0.1910	

6	0.16794	273.6	334,866	0.24504	6.6	0.004536	0.0005865	0.02701	0.003493	0.1910	
6	0.16794	273.6	334,866	0.24504	7.4	0.005497	0.0006845	0.03273	0.004076	0.1910	
5	0.13995	273.6	334,866	0.24504	0.0	0.000000	0.0002510	0.00000	0.001793	0.1910	Extrapolated
5	0.13995	273.6	334,866	0.24504	6.0	0.002928	0.0004110	0.02092	0.002936	0.1910	
5	0.13995	273.6	334,866	0.24504	7.2	0.005252	0.0006290	0.03753	0.004494	0.1910	
5	0.13995	273.6	334,866	0.24504	7.7	0.005938	0.0007237	0.04243	0.005171	0.1910	
5	0.13995	273.6	334,866	0.24504	8.2	0.007156	0.0008591	0.05114	0.006138	0.1910	
4	0.11196	273.6	334,866	0.24504	0.0	0.000000	0.0001950	0.00000	0.001742	0.1910	Extrapolated
4	0.11196	273.6	334,866	0.24504	3.0	0.001499	0.0002514	0.01339	0.002245	0.1910	
4	0.11196	273.6	334,866	0.24504	7.4	0.005103	0.0005454	0.04557	0.004871	0.1910	
4	0.11196	273.6	334,866	0.24504	8.2	0.005980	0.0006444	0.05341	0.005756	0.1910	
4	0.11196	273.6	334,866	0.24504	11.8	0.007529	0.0008272	0.06724	0.007388	0.1910	
4	0.11196	273.6	334,866	0.24504	11.8	0.007475	0.0008190	0.06677	0.007315	0.1910	
3	0.08397	273.6	334,866	0.24504	0.0	0.000000	0.0001201	0.00000	0.001430	0.1910	Extrapolated
3	0.08397	273.6	334,866	0.24504	3.6	0.002035	0.0002323	0.02424	0.002767	0.1910	Questionable
3	0.08397	273.6	334,866	0.24504	4.7	0.000935	0.0001530	0.01114	0.001822	0.1910	
3	0.08397	273.6	334,866	0.24504	8.3	0.003914	0.0003880	0.04661	0.004621	0.1910	
3	0.08397	273.6	334,866	0.24504	9.3	0.004807	0.0004792	0.05724	0.005706	0.1910	
3	0.08397	273.6	334,866	0.24504	10.4	0.005707	0.0005783	0.06797	0.006887	0.1910	
3	0.08397	273.6	334,866	0.24504	11.7	0.006935	0.0007531	0.08259	0.008969	0.1910	
2	0.05598	273.6	334,866	0.24504	0.0	0.000026	0.0001033	0.00047	0.001846	0.1910	
2	0.05598	273.6	334,866	0.24504	6.0	0.002867	0.0002583	0.05122	0.004615	0.1910	
2	0.05598	273.6	334,866	0.24504	8.1	0.004314	0.0003698	0.07707	0.006606	0.1910	
2	0.05598	273.6	334,866	0.24504	10.3	0.005460	0.0005061	0.09754	0.009042	0.1910	STALL
6	0.16794	228.0	279,055	0.20420	0.0	0.000107	0.0003073	0.00063	0.001830	0.1910	
6	0.16794	228.0	279,055	0.20420	3.3	0.001038	0.0003395	0.00618	0.002022	0.1910	
6	0.16794	228.0	279,055	0.20420	3.9	0.002272	0.0004060	0.01353	0.002417	0.1910	
6	0.16794	228.0	279,055	0.20420	6.0	0.003559	0.0004981	0.02119	0.002966	0.1910	
6	0.16794	228.0	279,055	0.20420	6.6	0.004486	0.0005966	0.02671	0.003553	0.1910	

6	0.16794	228.0	279,055	0.20420	7.4	0.005423	0.0007067	0.03229	0.004208	0.1910	
6	0.16794	228.0	279,055	0.20420	8.2	0.006382	0.0007976	0.03800	0.004749	0.1910	
6	0.16794	228.0	279,055	0.20420	9.2	0.007717	0.0009666	0.04595	0.005756	0.1910	
6	0.16794	228.0	279,055	0.20420	10.7	0.010436	0.0013600	0.06214	0.008098	0.1910	
4	0.11196	228.0	279,055	0.20420	0.0	0.000000	0.0001919	0.00000	0.001714	0.1910	Extrapolated
4	0.11196	228.0	279,055	0.20420	8.2	0.006092	0.0006709	0.05441	0.005993	0.1910	
4	0.11196	228.0	279,055	0.20420	7.4	0.005122	0.0005554	0.04574	0.004961	0.1910	
4	0.11196	228.0	279,055	0.20420	3.0	0.001488	0.0002504	0.01329	0.002236	0.1910	
3	0.08397	228.0	279,055	0.20420	0.0	0.000000	0.0001244	0.00000	0.001482	0.1910	Extrapolated
3	0.08397	228.0	279,055	0.20420	3.6	0.002035	0.0002360	0.02423	0.002811	0.1910	
3	0.08397	228.0	279,055	0.20420	4.7	0.000986	0.0001584	0.01174	0.001886	0.1910	
3	0.08397	228.0	279,055	0.20420	8.3	0.003933	0.0004001	0.04683	0.004764	0.1910	
3	0.08397	228.0	279,055	0.20420	9.3	0.004861	0.0004919	0.05789	0.005858	0.1910	
3	0.08397	228.0	279,055	0.20420	10.4	0.005879	0.0006075	0.07001	0.007234	0.1910	
3	0.08397	228.0	279,055	0.20420	11.7	0.007025	0.0007859	0.08366	0.009360	0.1910	
2	0.05598	228.0	279,055	0.20420	0.0	0.000033	0.0001078	0.00059	0.001926	0.1910	
2	0.05598	228.0	279,055	0.20420	6.0	0.002936	0.0002700	0.05244	0.004824	0.1910	
2	0.05598	228.0	279,055	0.20420	8.1	0.004252	0.0003783	0.07595	0.006758	0.1910	
2	0.05598	228.0	279,055	0.20420	10.3	0.005389	0.0005128	0.09627	0.009160	0.1910	STALL
6	0.16794	182.4	223,244	0.16336	0.0	0.000057	0.0003121	0.00034	0.001858	0.1910	
6	0.16794	182.4	223,244	0.16336	3.3	0.001069	0.0003477	0.00636	0.002070	0.1910	
6	0.16794	182.4	223,244	0.16336	3.9	0.002218	0.0004227	0.01321	0.002517	0.1910	
6	0.16794	182.4	223,244	0.16336	6.0	0.003535	0.0005261	0.02105	0.003133	0.1910	
6	0.16794	182.4	223,244	0.16336	6.6	0.004498	0.0006245	0.02679	0.003719	0.1910	
6	0.16794	182.4	223,244	0.16336	7.4	0.005491	0.0007450	0.03270	0.004436	0.1910	
6	0.16794	182.4	223,244	0.16336	8.2	0.006582	0.0008601	0.03919	0.005122	0.1910	
6	0.16794	182.4	223,244	0.16336	9.2	0.007799	0.0010163	0.04644	0.006051	0.1910	
6	0.16794	182.4	223,244	0.16336	10.7	0.010566	0.0014163	0.06291	0.008433	0.1910	

5	0.13995	182.4	223,244	0.16336	0.0	0.000000	0.0002624	0.00000	0.001875	0.1910	Extrapolated
5	0.13995	182.4	223,244	0.16336	3.8	0.001797	0.0003280	0.01284	0.002343	0.1910	
5	0.13995	182.4	223,244	0.16336	7.2	0.005367	0.0006631	0.03835	0.004738	0.1910	
5	0.13995	182.4	223,244	0.16336	7.7	0.006102	0.0007890	0.04360	0.005638	0.1910	
5	0.13995	182.4	223,244	0.16336	8.2	0.007139	0.0009191	0.05101	0.006568	0.1910	
5	0.13995	182.4	223,244	0.16336	9.5	0.008906	0.0011354	0.06364	0.008113	0.1910	
5	0.13995	182.4	223,244	0.16336	10.6	0.010093	0.0013160	0.07212	0.009403	0.1910	
5	0.13995	182.4	223,244	0.16336	12.8	0.012594	0.0017479	0.08999	0.012490	0.1910	
4	0.11196	182.4	223,244	0.16336	0.0	0.000058	0.0002129	0.00052	0.001902	0.1910	
4	0.11196	182.4	223,244	0.16336	11.8	0.007507	0.0008547	0.06705	0.007634	0.1910	
4	0.11196	182.4	223,244	0.16336	8.2	0.006098	0.0006750	0.05447	0.006029	0.1910	
4	0.11196	182.4	223,244	0.16336	7.4	0.005218	0.0005703	0.04661	0.005094	0.1910	
4	0.11196	182.4	223,244	0.16336	10.8	0.008881	0.0010524	0.07933	0.009400	0.1910	
3	0.08397	182.4	223,244	0.16336	0.0	0.000000	0.0001370	0.00000	0.001632	0.1910	Extrapolated
3	0.08397	182.4	223,244	0.16336	3.6	0.001948	0.0002355	0.02320	0.002804	0.1910	
3	0.08397	182.4	223,244	0.16336	4.7	0.001203	0.0001734	0.01433	0.002065	0.1910	
3	0.08397	182.4	223,244	0.16336	8.3	0.004044	0.0004138	0.04816	0.004929	0.1910	
3	0.08397	182.4	223,244	0.16336	9.3	0.005007	0.0005119	0.05963	0.006097	0.1910	
3	0.08397	182.4	223,244	0.16336	10.4	0.006030	0.0006351	0.07181	0.007563	0.1910	
3	0.08397	182.4	223,244	0.16336	11.7	0.007236	0.0008042	0.08618	0.009577	0.1910	
6	0.16794	114.0	139,528	0.10210	0.0	0.000021	0.0003245	0.00012	0.001932	0.1910	
6	0.16794	114.0	139,528	0.10210	3.3	0.001187	0.0003816	0.00707	0.002272	0.1910	
6	0.16794	114.0	139,528	0.10210	3.9	0.002345	0.0004545	0.01396	0.002707	0.1910	
6	0.16794	114.0	139,528	0.10210	6.0	0.003762	0.0005634	0.02240	0.003355	0.1910	
6	0.16794	114.0	139,528	0.10210	6.6	0.004845	0.0006668	0.02885	0.003970	0.1910	
6	0.16794	114.0	139,528	0.10210	7.4	0.006102	0.0008572	0.03634	0.005104	0.1910	
3	0.08397	114.0	139,528	0.10210	0.0	0.000000	0.0001555	0.00000	0.001852	0.1910	Extrapolated
3	0.08397	114.0	139,528	0.10210	3.6	0.001565	0.0002180	0.01864	0.000005	0.1910	
3	0.08397	114.0	139,528	0.10210	8.3	0.004198	0.0004330	0.04999	0.000005	0.1910	
3	0.08397	114.0	139,528	0.10210	9.3	0.005277	0.0005443	0.06284	0.000005	0.1910	

APPENDIX B—KNIGHT AND HEFNER'S BEMT EQUATIONS

KNIGHT AND HEFNER'S BEMT EQUATIONS

Blade element momentum theory's classical assumption is that a blade element has an angle of attack (α) calculated as the difference between a geometric blade angle (θ) and an inflow (ϕ) angle. Knight and Hefner clearly stated that all angles would be assumed to be small.

$$\alpha = \theta - \phi \qquad \text{Eq. (1)}$$

Application of BEMT yields the result for the inflow angle, which is

$$\phi = \frac{\sigma a}{16 x}\left(\sqrt{1+\frac{32\theta x}{\sigma a}}-1\right) \qquad \text{Eq. (2)}$$

where (a) is the lift curve slope of the airfoil being on the order of 5.73 per radian and (x) is the nondimensional blade radius station, calculated as x = r/R. Knight and Hefner saw that the blade element angle of attack would then appear as

$$\alpha = \theta - \frac{\sigma a}{16 x}\left(\sqrt{1+\frac{32\theta x}{\sigma a}}-1\right) \qquad \text{Eq. (3)}$$

To Knight and Hefner, it was a simple step to factor ($\sigma a/16$) out in Eq. (3) to show that the blade element of attack could be written as

$$\alpha = \frac{\sigma a}{16}\left[\frac{16\theta}{\sigma a}-\frac{1}{x}\left(\sqrt{1+\frac{32\theta x}{\sigma a}}-1\right)\right] = \frac{\sigma a}{16}\left[\Theta-\frac{1}{x}\left(\sqrt{1+2\Theta x}-1\right)\right] \qquad \text{Eq. (4)}$$

and that the blade geometric angle (θ) could be redefined as ($\Theta = 16\,\theta/\sigma\, a$). They used Eq. (4) as the basis for their view of how BEMT should be used. Then they used their form of blade element angle of attack in calculating the primary blade element force coefficients of lift and drag by

$$C_\ell = a\alpha \quad C_d = C_{do} + \delta\alpha^2 \qquad \text{Eq. (5)}$$

when a symmetrical airfoil such as the NACA 0012 or 0015 was under consideration. The calculation of a thrust coefficient (C_T), induced power coefficient ($C_{P\text{-}ind}$), minimum profile coefficient (C_{Po}), and delta profile power due to lift (ΔC_{Po}) was a relatively simple matter of radial integration. These hover performance parameters are calculated as follows.

Thrust Coefficient (C_T)

$$C_T = \frac{\sigma a}{2}\int_{xc}^{1}\alpha x^2 dx = \frac{\sigma a}{2}\int_{xc}^{1}\frac{\sigma a}{16}\left[\Theta-\frac{1}{x}\left(\sqrt{1+2\Theta x}-1\right)\right]x^2 dx = \frac{\sigma^2 a^2}{32}F_T \qquad \text{Eq. (6)}$$

$$F_T = \frac{1}{2}\left(1-xc^2\right)+\frac{1}{3}\left(1-xc^3\right)\Theta+\left[\frac{(1+2\Theta)^{\frac{3}{2}}-(1+2\Theta xc)^{\frac{3}{2}}}{6\Theta^2}\right]-\left[\frac{(1+2\Theta)^{\frac{5}{2}}-(1+2\Theta xc)^{\frac{5}{2}}}{10\,\Theta^2}\right] \qquad \text{Eq. (7)}$$

$$F_T \to \frac{1}{8}\left(1-xc^4\right)\Theta^2-\frac{1}{10}\left(1-xc^5\right)\Theta^3 \text{ for } \Theta << 0.1 \text{ and } F_T = \frac{15\Theta^2+10\Theta^3+2\left(1-\Theta-6\Theta^2\right)\sqrt{1+2\Theta}-2}{30\Theta^2} \quad \text{if} \quad xc = 0$$

Induced Power Coefficient ($C_{P\text{-}ind}$)

$$C_{P-ind} = \frac{\sigma a}{2}\int_{xc}^{1} \alpha\,\phi\, x^3 dx = \frac{\sigma a}{2}\int_{xc}^{1} \frac{\sigma a}{16}\left[\Theta - \frac{1}{x}\left(\sqrt{1+2\Theta x}-1\right)\right]\left[\frac{\sigma a}{16x}\sqrt{1+\frac{32\theta x}{\sigma a}}-1\right] x^3 dx = \frac{\sigma^3 a^3}{512} F_{P-ind} \quad \text{Eq. (8)}$$

$$F_{P-ind} = \left[\frac{(1+2\Theta)^{\frac{7}{2}} - (1+2\Theta xc)^{\frac{7}{2}}}{28\Theta^2}\right] + \left[\frac{(1+2\Theta)^{\frac{5}{2}} - (1+2\Theta xc)^{\frac{5}{2}}}{10\Theta^2}\right] - \left[\frac{(1+2\Theta)^{\frac{3}{2}} - (1+2\Theta xc)^{\frac{3}{2}}}{4\Theta^2}\right] - \left(1-xc^2\right) - \left(1-xc^3\right)\Theta$$

$$F_{P-ind} \to \frac{1}{10}\left(1-xc^5\right)\Theta^3 - \frac{1}{8}\left(1-xc^6\right)\Theta^4 \qquad \text{for } \Theta << 0.1 \qquad \text{Eq. (9)}$$

$$F_{P-ind} = \frac{4 - 35\Theta^2 - 35\Theta^3 + \left(5\Theta^2 + 12\Theta^2 - 4\right)(1+2\Theta)^{\frac{3}{2}}}{35\Theta^2} \quad \text{if} \quad xc = 0$$

Minimum Profile Coefficient (C_{Po})

$$C_{Po} = \frac{\sigma C_{do}}{2}\int_{xc}^{1} x^3 dx = \frac{\sigma C_{do}}{8}\left(1-xc^4\right) \quad \text{Eq. (10)}$$

Delta Profile Power due to Thrust (ΔC_{Po})

$$\Delta C_{Po} = \delta\frac{\sigma}{2}\int_{xc}^{1} \alpha^2 x^3 dx = \delta\frac{\sigma}{2}\int_{xc}^{1} \left(\frac{\sigma a}{16}\right)^2\left[\Theta - \frac{1}{x}\left(\sqrt{1+2\Theta x}-1\right)\right]^2 x^3 dx = \delta\frac{\sigma^3 a^2}{512} F_{\Delta Po} \quad \text{Eq. (11)}$$

$$F_{\Delta Po} = \left(1-xc^2\right) + \frac{4\left(1-xc^3\right)}{3}\Theta + \frac{\left(1-xc^4\right)}{4}\Theta^2 + \left[\frac{(1+2\Theta)^{\frac{3}{2}} - (1+2\Theta xc)^{\frac{3}{2}}}{6\Theta^2}\right] - \left[\frac{(1+2\Theta)^{\frac{7}{2}} - (1+2\Theta xc)^{\frac{7}{2}}}{14\Theta^2}\right]$$

$$F_{\Delta Po} \to \frac{1}{24}\left(1-xc^6\right)\Theta^4 - \frac{1}{14}\left(1-xc^7\right)\Theta^5 \qquad \text{for } \Theta << 0.1 \qquad \text{Eq. (12)}$$

$$F_{\Delta Po} = \frac{84\Theta^2 + 112\Theta^3 + 21\Theta^4 + 8\left(1-\Theta-9\Theta^2-6\Theta^3\right) - 8}{84\Theta^2} \quad \text{if} \quad xc = 0$$

Total Power due to Thrust (ΔC_{Po})

$$C_P = C_{P0} + \Delta C_{Po} + C_{P-ind} \quad \text{Eq. (13)}$$

The last step Knight and Hefner took was to state that if the minimum profile power coefficient is subtracted from the total power coefficient (i.e. Test C_P–C_{Po} = Theory $C_{P\text{-}ind}$ + ΔC_{PO}) then the correct way to begin studying hover performance *with rectangular blades having zero twist using the same airfoil from blade root to tip* would be

$$\frac{C_P - C_{Po}}{\sigma^3} \text{ versus } \frac{C_T}{\sigma^2} \quad \text{and} \quad \frac{C_T}{\sigma^2} \text{ versus } \frac{\theta}{\sigma} \quad \text{Eq. (14)}$$

APPENDIX C—BOEING–VERTOL INTEROFFICE MEMO (REF. 5)

memorandum

THE BOEING COMPANY – VERTOL DIVISION | INTEROFFICE

TO:	C. Ellis	P32-79	DATE: June 24, 1970
	C. Fay	P32-75	
	F. Harris	P38-07	REF.: 8-7441-1-410
	G. Schairer	10-47 Org. 1-8001	
	W. Walls	P32-74	FROM: Aerodynamics Research
	W. Wiesner	10-47 Org. 1-8003	M/S: P32-56
cc:	E. Austin	P32-56	
	B. Blake	P32-74	
	R. Burnstead	P39-79	
	T. Garnett	P32-74	
	R. Haris	P32-48	
	M. Maisel	P39-31	
	F. McHugh	P32-74	
	R. Wiesner	P32-74	

SUBJECT: Scale Effects on Model Rotor Performance

REFERENCE: Appendix B

ENCLOSURES: (1)-(6): Reynolds Number Correlations
Appendix A: Reynolds Number Discussion

Introduction:

This memorandum contains a summary of efforts conducted by the Aero Research Unit to identify the effects of Reynolds Number on scale model rotor performance characteristics. The procedures outlined herein provide a method of adjusting model performance data obtained at low M_{TIP}'s and R_e's to representative full scale conditions. The data correction procedure described in this memorandum will enable continued use of the well established low tip speed wind tunnel test techniques (such as the UHM) for design studies of high speed helicopters.

Reynolds Number Effect on Drag Coefficient:

Enclosure (1) is a compendium of drag data for numerous airfoil sections. It is evident from the figure that there is a considerable variation in the drag levels over the range of Reynolds Numbers experienced by the Boeing-Vertol Universal Helicopter Model (UHM) up to and including proposed Heavy Lift Helicopter (HLH) configurations. Enclosure (2) includes the section data previously shown and adds rotor $\bar{C}_{d_o}$ data obtained for rotors at zero thrust in hover (where $\bar{C}_{d_o} = 8\, C_{p_o}/\sigma)_o$. It can be concluded from the enclosure that the rotor average drag coefficients are in substantial agreement with the airfoil section data.

FORM 52982 (10/66) (MASTER)

Correlation - Hover Performance:

The fairings shown in Enclosures (1) and (2) have been utilized to make first approximation Reynolds Number corrections to some available rotor data. Enclosure (3) illustrates the variation in measured hover performance for both model and full scale rotors. Enclosure (4) contains the same data but with the model data corrected to full scale Reynolds Number. The corrections move the model data into substantial agreement with full scale data.

Correlation - Forward Flight Performance:

Enclosure (5) and (6) compare full scale CH-47C test data with Dynamic Rotor Test Stand (DRTS) and UHM model test data. The first approximation Reynolds Number correction in conjunction with a compressibility correction brings the model data within a reasonable degree of correlation with the full scale data both in level and trend.

Conclusions:

° It can be concluded from the studies performed to date that model scale tests can result in performance characteristics which are not completely representative of full scale capabilities due to Reynolds Number Effects.

° Model performance test results tend to be conservative compared to full scale test data.

° The "first approximation" Reynolds Number correction described in this memorandum appears to bring model test results into good agreement with existing full scale data.

° Model scale such as currently used on the UHM (1/11th scale) can be used to obtain estimated full scale performance if proper Reynolds Number corrections are applied.

Recommendations:

° It is recommended that scale model performance test data, which is to be utilized to predict full scale performance capabilities, be modified using the drag corrections vs Reynolds Number outlined in Appendix A of this memorandum.

° Correlation of methodologies with model test data should be conducted utilizing airfoil tables which have been adjusted to be representative of the model scale being correlated.

- Pre-test predictions for future model tests should be performed using airfoil tables which have been adjusted to be representative of the anticipated model Reynolds Number.

Prepared By: R. Gormont
R. Gormont

Approved By: R. F. Child
R. Child

RG/mck

Enclosures

ENCLOSURE 1

8-7441-1-410

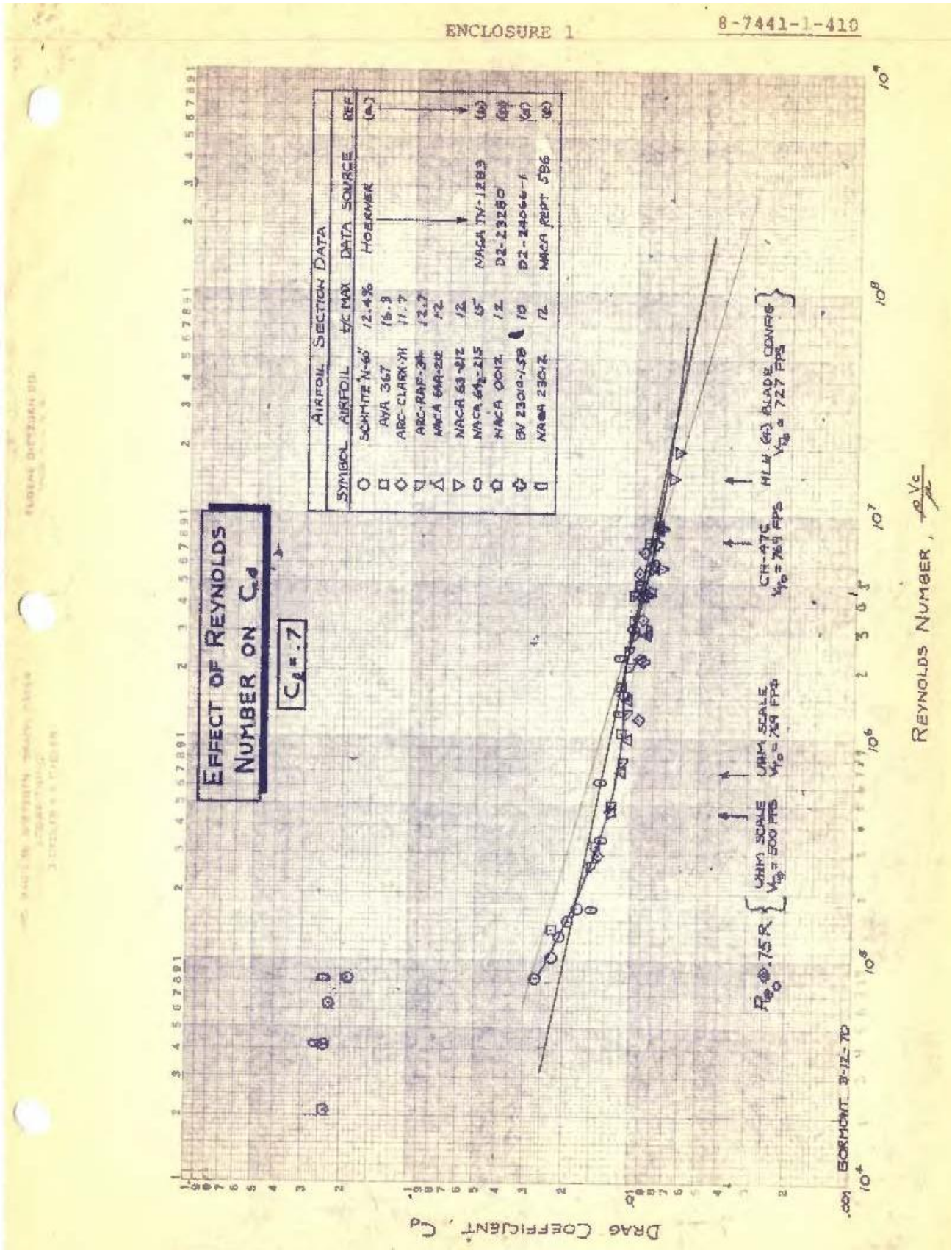

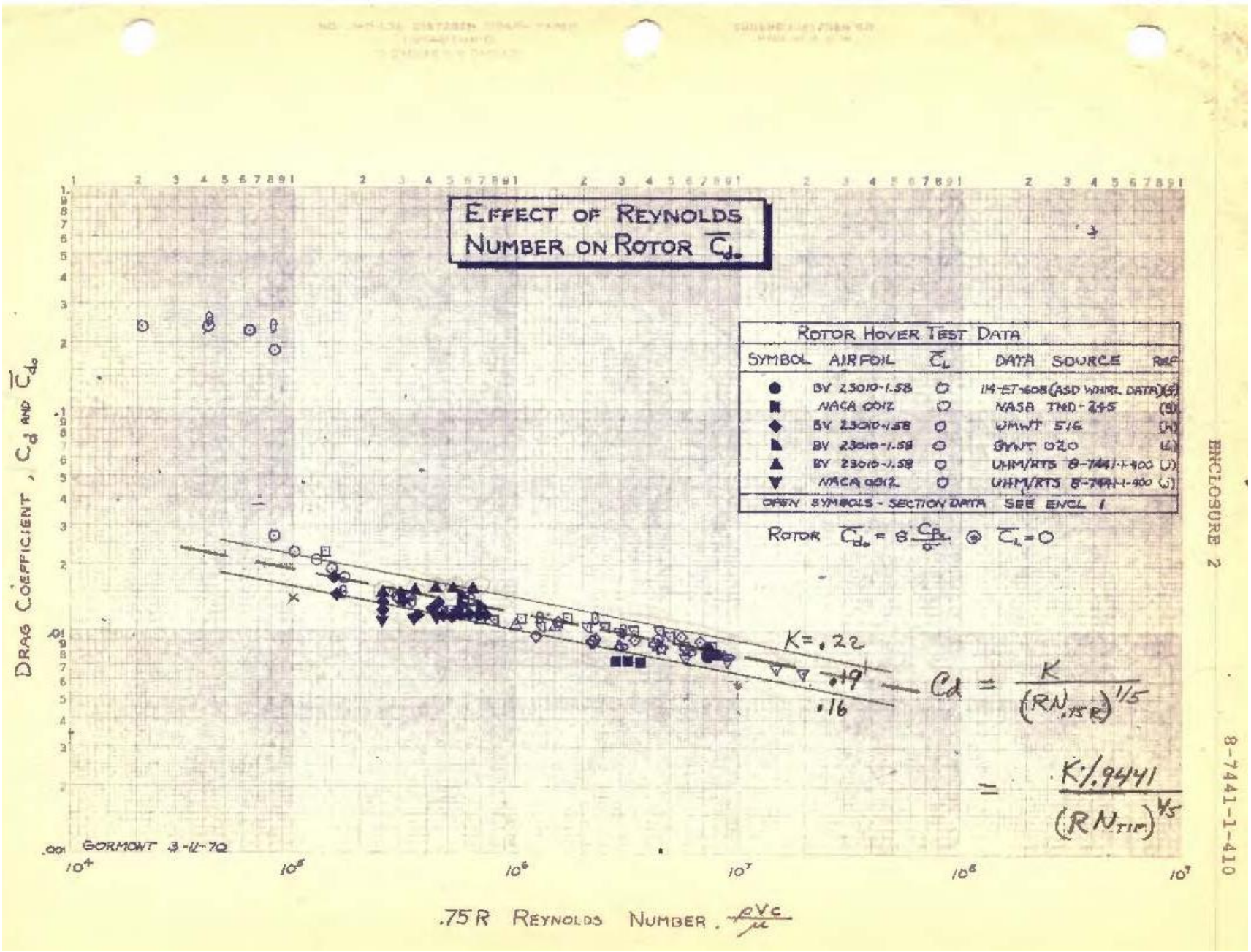

ENCLOSURE 2

8-7441-1-410

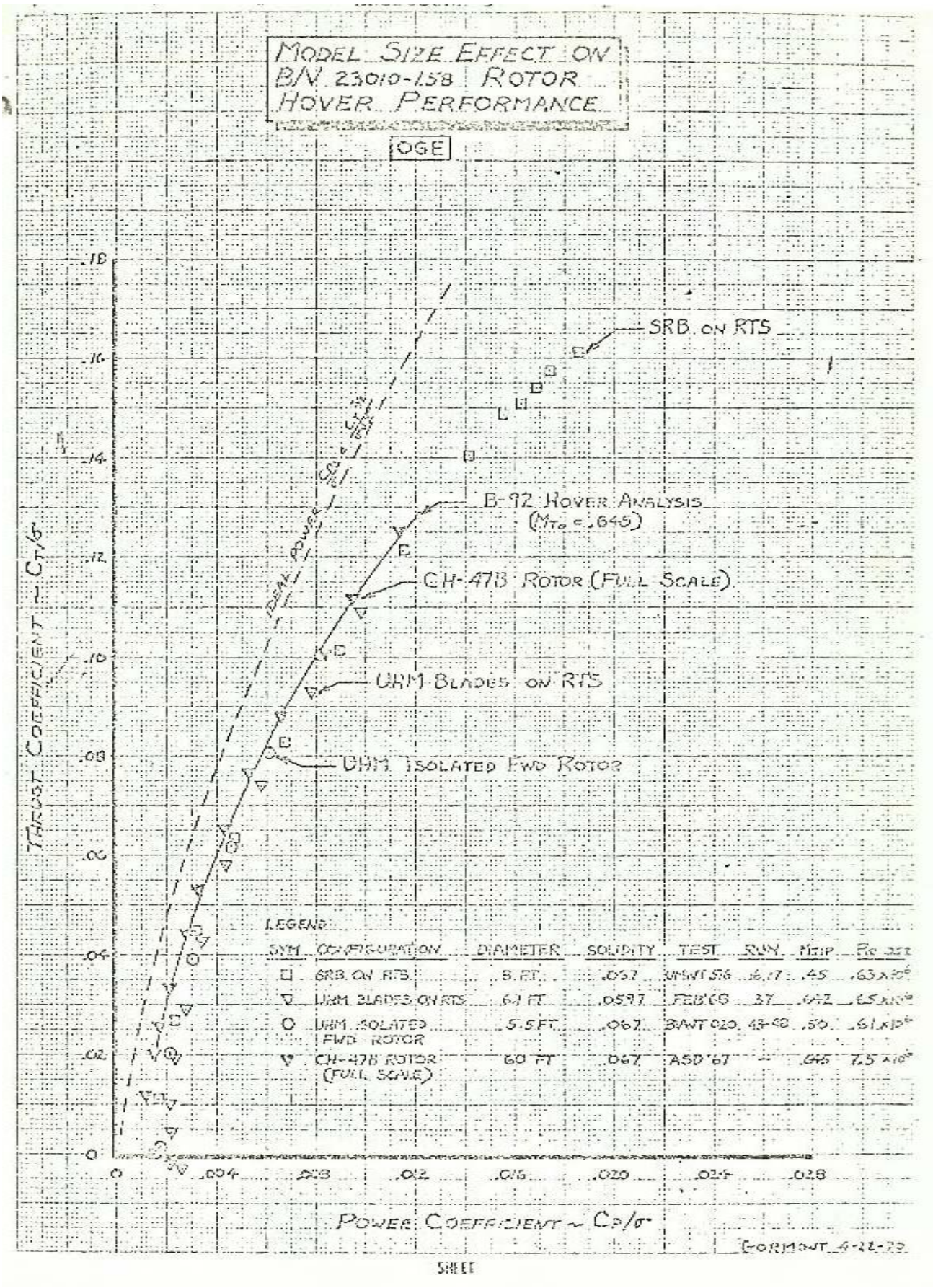
MODEL SIZE EFFECT ON B/N 23010-1.58 ROTOR HOVER PERFORMANCE
OGE
SRB ON RTS
B-92 HOVER ANALYSIS (M_{TO} = .645)
CH-47B ROTOR (FULL SCALE)
UHM BLADES ON RTS
UHM ISOLATED FWD ROTOR
THRUST COEFFICIENT ~ C_T/σ
POWER COEFFICIENT ~ C_P/σ
.18
.16
.14
.12
.10
.08
.06
.04
.02
0
.004
.008
.012
.016
.020
.024
.028
LEGEND
SYM CONFIGURATION DIAMETER SOLIDITY TEST RUN M_{TIP} Re_{TIP}
□ SRB ON RTS 8 FT .057 UHMT 536 16,17 .45 .63 x 10^6
▽ UHM BLADES ON RTS 6.4 FT .0597 FEB '69 37 .642 .65 x 10^6
○ UHM ISOLATED FWD ROTOR 5.5 FT .067 BHMT 020 48-50 .50 .61 x 10^6
▽ CH-47B ROTOR (FULL SCALE) 60 FT .067 ASD '67 — .645 7.5 x 10^6
GORMONT 4-22-70
SHEET

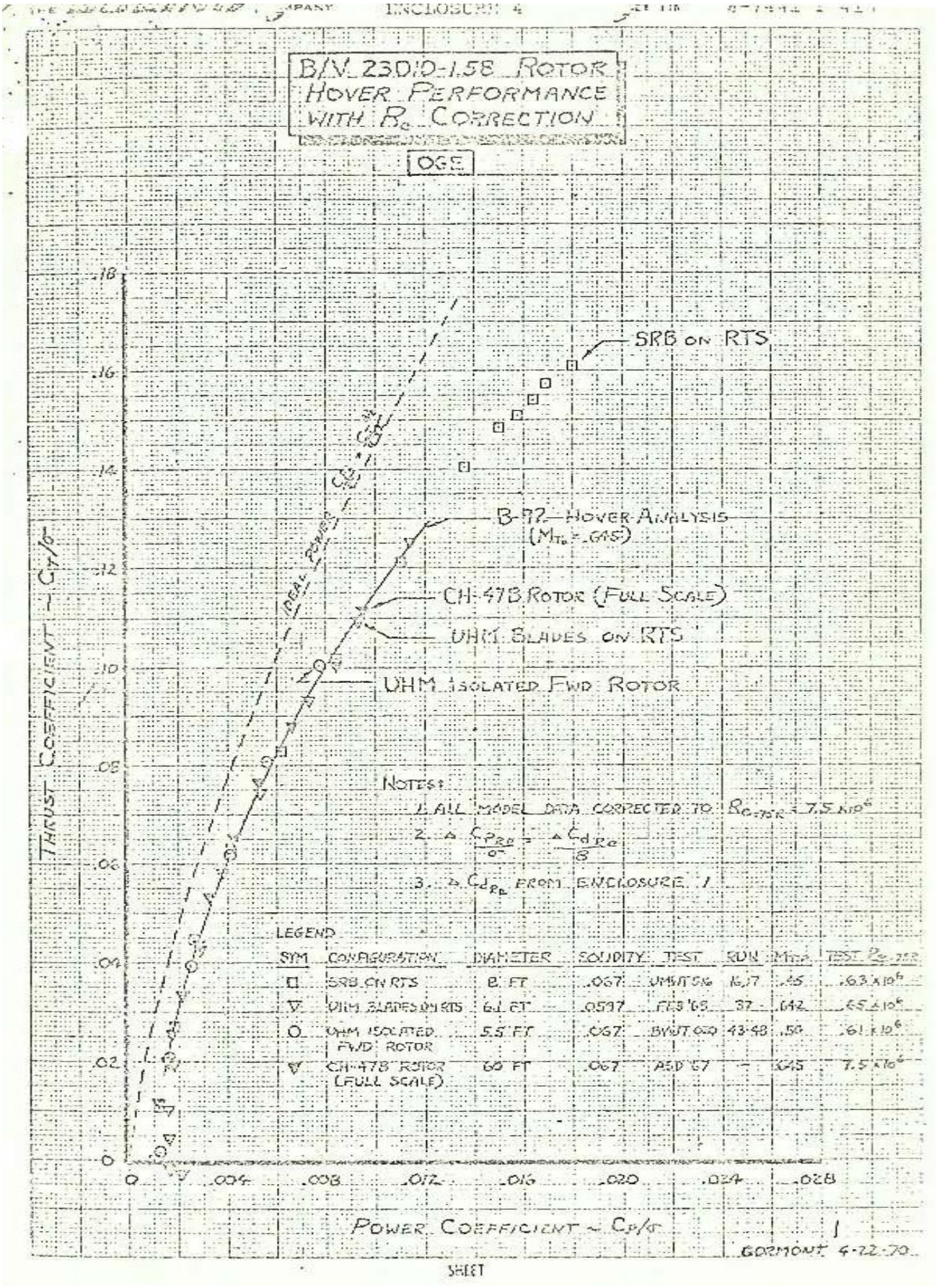
ENCLOSURE 4
B/V 23010-1.58 ROTOR
HOVER PERFORMANCE
WITH R_e CORRECTION
OGE
SRB ON RTS
B-97 HOVER ANALYSIS (M_{TIP} = .648)
CH-47B ROTOR (FULL SCALE)
UHM BLADES ON RTS
UHM ISOLATED FWD ROTOR
IDEAL POWER
THRUST COEFFICIENT - C_T/σ
POWER COEFFICIENT - C_P/σ
.18
.16
.14
.12
.10
.08
.06
.04
.02
0
.004
.008
.012
.016
.020
.024
.028
NOTES:
1. ALL MODEL DATA CORRECTED TO $R_{e_{TIP}} = 7.5 \times 10^6$
2. $\Delta \frac{C_{P_{RE}}}{\sigma} = \frac{\Delta C_{d_{RE}}}{8}$
3. $\Delta C_{d_{RE}}$ FROM ENCLOSURE 1
LEGEND
SYM | CONFIGURATION | DIAMETER | SOLIDITY | TEST | RUN | M_{TIP} | TEST $R_{e_{TIP}}$
□ | SRB ON RTS | 8. FT | .067 | UMAT 596 | 16,17 | .65 | $.63 \times 10^6$
▽ | UHM BLADES ON RTS | 6.1 FT | .0597 | FEB '69 | 37 | .642 | $.65 \times 10^6$
○ | UHM ISOLATED FWD ROTOR | 5.5 FT | .067 | BWT 620 | 43-48 | .59 | $.61 \times 10^6$
▽ | CH-47B ROTOR (FULL SCALE) | 60 FT | .067 | ASD '67 | - | .645 | 7.5×10^6
GORMONT 4-22-70
SHEET

THE BOEING COMPANY ENCLOSURE 5 NUMBER REV LTR 8-7441-1-410

REYNOLDS NUMBER EFFECT ON MODEL - FLT TEST CORRELATION

$N/\sqrt{\theta} = 245$
GW/δ = 30000 LB

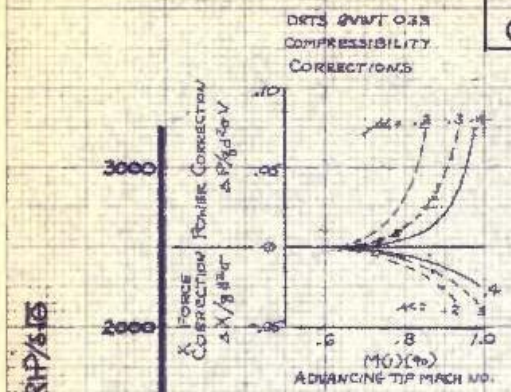

$M_{T_0} = \frac{\Omega R}{a}$

$M_{T(R)} = \frac{\Omega R + V}{a}$

UHM FWD ROTOR & DRTS COMPRESSIBILITY CORRECTION $M_{T_0} = 0.69$

UHM FWD ROTOR TEST $M_{T_0} = 0.45$

CH-47C FWD ROTOR FLT TEST DATA $M_{T_0} = 0.69$

UHM FWD ROTOR & DRTS COMPRESSIBILITY CORRECTION $M_{T_0} = 0.69$

UHM FWD ROTOR TEST $M_{T_0} = 0.45$

UHM FWD ROTOR PLUS DRTS COMPRESSIBILITY CORRECTION & FIRST APPROXIMATION REYNOLDS NUMBER CORRECTION

FORWARD ROTOR POWER - RHP/δ

3000
2000
1000

0 40 80 120 160 200

AIRSPEED, $V/\sqrt{\theta}$ ~ KT

NOTES:
1. CH-47C FLT TEST DATA PER 114-FT-712 REF (E)
2. UHM DATA PER D210-10077 AND USING A-97 TRIM ANALYSIS REF (G)
3. COMPRESSIBILITY CORRECTIONS PER 8WT 033 DRTS DATA REF (K)
4. REYNOLD'S NO. CORR. DERIVED FROM ENGL. / AND PSING $\Delta C_{P_{Re}} = \frac{\sigma^{.2} \Delta C_{d_{R_0}} (1 + 4.85 \mu^4)}{8}$

GORMONT 4-23-70

SHEET

ENCLOSURE 6

THE BOEING COMPANY

NUMBER 8-7441-1-410
REV LTR

REYNOLDS NUMBER EFFECT ON MODEL - FLT TEST CORRELATION

$N/\sqrt{\theta} = 245$

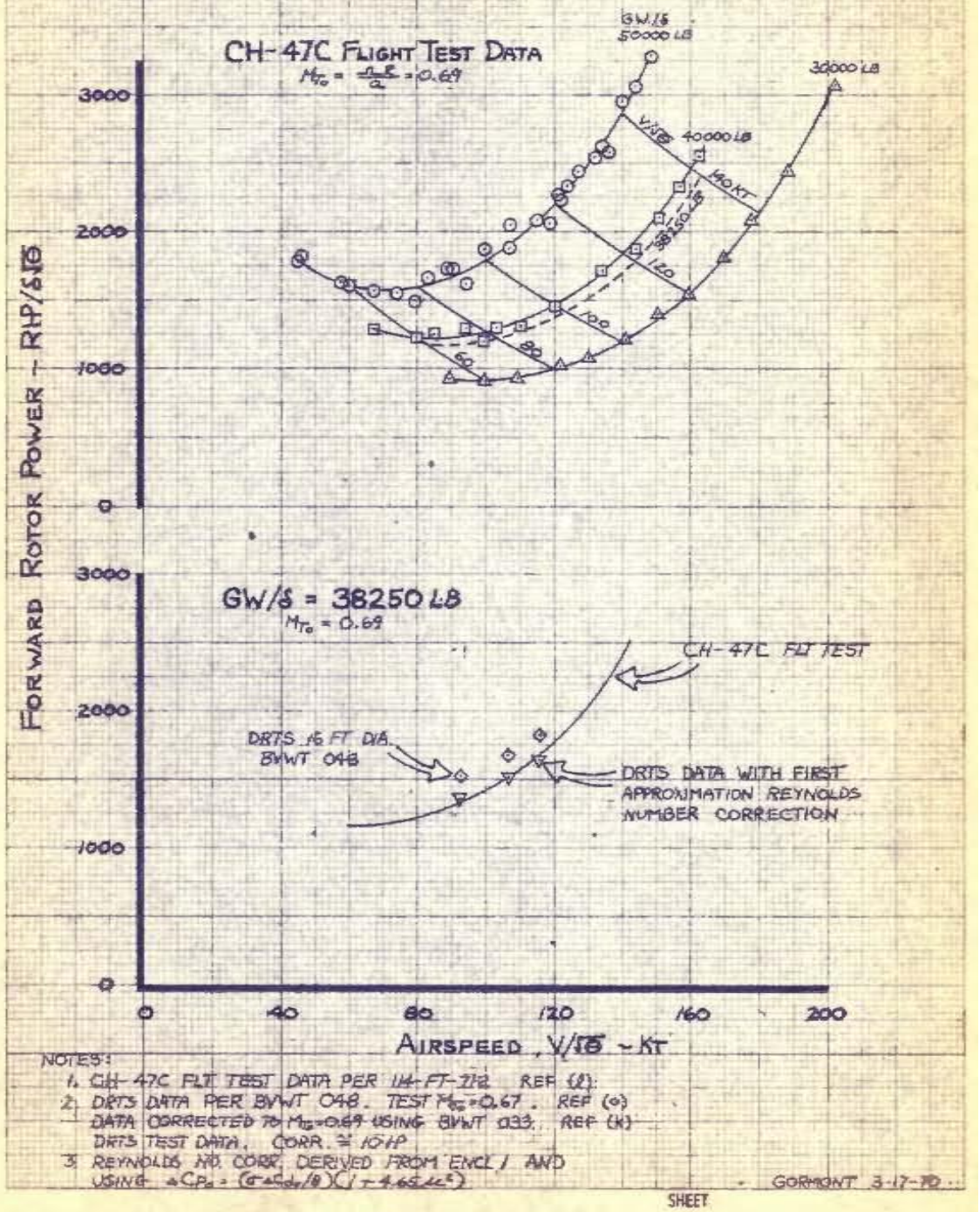

NOTES:
1. CH-47C FLT TEST DATA PER 114-FT-212 REF (L).
2. DRTS DATA PER BWT 048. TEST M_{T_o}=0.67. REF (O)
   DATA CORRECTED TO M_{T_o}=0.69 USING BWT 033. REF (K)
   DRTS TEST DATA. CORR. ≈ 10 HP
3. REYNOLDS NO. CORR. DERIVED FROM ENCL 1 AND USING $\Delta C_{P_o} = (\sigma a^2 c_{d_0}/8)(1 + 4.65\mu^2)$

GORMONT 3-17-70

SHEET

APPENDIX A - REYNOLDS NUMBER DISCUSSION

The drag coefficients of airfoil sections have been demonstrated to be significantly affected by operating Reynolds Number. Enclosure (A-1) contains a collection of available section data which illustrate the effect of Reynolds number on drag coefficient. The trends established by the data can be broken down to several distinct phases, paraphrasing from Hoerner (Ref. a):

- At R_e below 10^5 the sections exhibit high drag coefficients which are attributed to completely laminar boundary layer flow with flow separation from the rear.

- In the area near $R_e = 10^5$ there is a critical drop in drag level due to transition from laminar to turbulent flow along the airfoil sections.

- In a range of R_e above 10^5 the transition point remains relatively fixed at the minimum pressure point with laminar flow on the forebody. The drag coefficient varies as the laminar skin friction drag coefficient.

- Near $R_e \approx 10^6$ the transition point moves forward causing a larger portion of the boundary layer to be turbulent and resulting in an increase in drag. (In Enclosure (A-1) the drag levels tend to level off for $R_e \approx 1.$ to $2. \times 10^6$ due to the forward movement of the transition point. The data shown at $C_l = .7$ evidently eliminates any major contribution due to laminar flow for the R_e range from 10^5 to 10^6 and these drag levels more closely approximate the turbulent skin friction drag.)

- At R_e above approximately 2×10^6 the drag coefficient varies essentially in proportion to the turbulent skin friction drag, indicating that practically all the flow is turbulent.

The data presented in Enclosure (A-1) is shown for a C_l of .7 to eliminate laminar flow variations and for future reference it is appropriate to illustrate here that the established Reynolds Number trends are valid at $C_l = 0$, also. Enclosure (A-2) has data at $C_l = 0$ superimposed on the preceding data and the $C_l = 0$ data confirms the previously established trends. The 0012 section data shown in Enclosure (A-2) evidently has a significant laminar flow component since the overall levels are lower, however the trend of drag coefficient with Reynolds Number is in substantial agreement with the other data.

The majority of data depicted in Enclosures (A-1) and (A-2) are representative of the Reynolds number trends for essentially turbulent flow. These trends are judged to be applicable for estimating effects on helicopter rotor blades due to their turbulent environment.

In order to extend the results of this study to rotor applications, it is necessary to take a simplified approach to rotor test data since the local environment is not constant over the rotor disc. For the purposes of this study it was concluded that the rotor profile power coefficient in hover, expressed by $C_{P_o} = \sigma C_{d_o}/8$, could be used to determine equivalent effective drag coefficients for rotor test data. Data from several model hover tests as well as ASD full scale CH-47B rotor data were utilized to obtain the data shown in Enclosure (A-3). The rotor data shown is taken at thrust coefficients of zero so that the power coefficient is due entirely to profile losses. From the figure it is obvious that the rotor data is in excellent agreement with the section data, again verifying the Reynolds number trends previously established.

Application of Reynolds Number Correction:

To formulate a methodology which would properly account for the Reynolds Number trends shown above, the following approach was taken:

- The drag rise due to decreased Reynolds Number is manifested as an increase in rotor profile power.
- The drag increments (verified by rotor profile power measured at $C_T/\sigma = 0$) are applied independent of C_T/σ. This procedure is valid provided operation is limited to the region where linear aerodynamics apply. The Reynolds Number corrections are essentially constant, independent of C_l, in this range. The sketch illustrates a typical section drag polar and indicates that the Reynolds Number correction increases when operating outside the linear aero range. This effect is due to flow separation (which is highly sensitive to R_e).

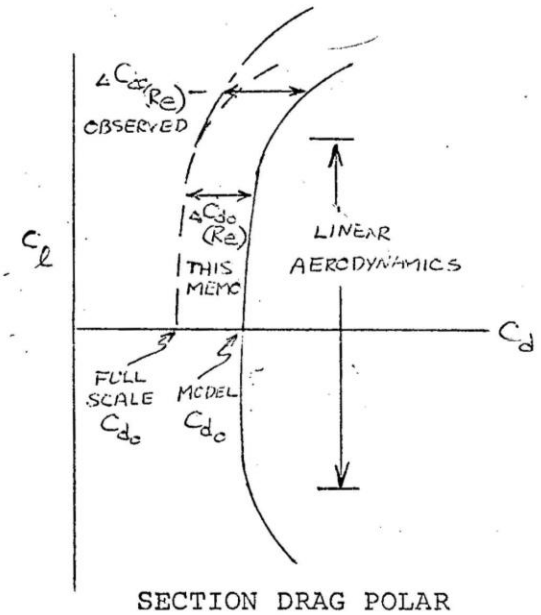

SECTION DRAG POLAR

. The first approximation for the profile power increments are of the form:

$$\frac{\Delta C_{P_{Re}}}{\sigma} = \frac{\Delta C_{d_{Re}}}{8} \text{ for hover}$$

and

$$\Delta \overline{P}_{Re} = \frac{\pi}{2\mu^3} \frac{\Delta C_{dRe}}{8} (1 + 4.65\mu^2) \text{ for forward flight.}$$

Rotor Correlation - Hover

The hover correlations previously discussed in the summary are again presented in Enclosures (A-4) and (A-5). As a first appriximation the Reynolds Number at 75% radius is chosen to be representative of the rotor as a whole and is utilized as a basis for comparison. The B-92 hover analysis uses airfoil section characteristics which were obtained at full scale CH-47B Reynolds Numbers and the figure illustrates that the full scale CH-47B test data and B-92 estimates are in good agreement throughout the range shown. The model test data indicates a power requirement considerably above the full scale data. At a C_T/σ of 0.10 the maximum data variation is on the order of 10%. Enclosure (A-5) contains the same test data but with a first approximation Reynolds Number correction applied to the model test data. The Re correction was applied using $\Delta C_{P_{Re}} = \sigma \Delta C_{d_{Re}}/8$ and obtaining $\Delta C_{d_{Re}}$ from Enclosure (A-1). With the corrections applied, the correlation is considerably improved and is within acceptable data scatter.

The tip Mach Numbers for the hover data are all below drag divergence levels indicated by airfoil data, thus compressibility effects are not present and the small variation in tip Mach Number can be ignored.

Rotor Correlation - Forward Flight

Enclosures (A-6) and (A-7) illustrate typical UHM rotor performance test data. Due to hardware restrictions the UHM test vehicle is generally limited to tip speeds of 500 fps. Consequently full scale tip Mach Numbers cannot be achieved. To overcome this problem, the UHM data have been corrected to the desired tip Mach Number by utilizing Dynamic Rotor Test Stand (DRTS) data (see insert on Enclosure A-6). The resulting model performance level was then adjusted using the first approximation Reynolds Number correction. For forward flight the correction takes the form:

$$\Delta C_{P_{Re}} = \frac{\sigma \Delta C_{d_{Re}}}{8} (1 + 4.65\mu^2)$$

and the $\Delta C_{d_{Re}}$ is again obtained from Enclosure (A-1). The Reynolds Number is based on .75 V_{TO} which represents the average velocity around the azimuth of the rotor disc at 75% radius. The corrected model data is in close agreement with the CH-47C full scale test data.

The data in Enclosure (A-7) indicate that the correlation at minimum power speed deteriorates at increased gross weights. This may be attributed to two factors: 1) stable flight test data is more difficult to obtain at high weight, which is evident from the increased data scatter at G.W./δ = 50000 lb, and 2) the rotor blade angle of attack may be entering an area where linear aerodynamics no longer apply and flow separation phenomena require a larger Reynolds Number correction. The latter factor is an area requiring further investigation.

A similar comparison was made with DRTS test data and is presented in Enclosure (A-8). The DRTS data were obtained at near full scale tip speeds, therefore, the required compressibility correction was only on the order of ten horsepower. Again the first approximation Reynolds Number correction brings the model and full scale data into close agreement.

The DRTS trim conditions correspond to a CH-47C forward rotor at a gross weight of 38250 lb and the CH-47C forward rotor flight test data were obtained from the carpet plot at the top of Enclosure (A-8). The DRTS test schedule called for an airspeed sweep, however, an equipment malfunction precluded running to speeds higher than the 116 kt point shown.

Estimated Reynolds Number Corrections:

Based on the above analysis, estimated Reynolds Number corrections have been calculated and are presented in Enclosure (A-9) and (A-10). The corrections are based on the $C_{d_{Re}}$ from Enclosure (A-1) and using

$$\frac{\Delta C_{P_{Re}}}{\sigma} = \frac{\Delta C_{d_{Re}}}{8} \quad \text{for hover}$$

and

$$\Delta \overline{P}_{Re} = \frac{\pi}{2\mu^3} \cdot \frac{C_{d_{Re}}}{8} (1 + 4.65\mu^2) \quad \text{for forward flight.}$$

The corrections are shown as increments from the full scale Reynolds Number of the CH-47C rotor operating at 245 RPM.

Rotor Thrust Limits:

An attempt was made to determine the possible effect of Reynolds Number on rotor $C_{T/\sigma\ MAX}$, however this effort was hindered by the lack of available full scale rotor test data at extreme thrust coefficients.

Furthermore, it is not obvious that such a comparison could be made anyway since the $C_{l_{max}}$ condition is probably a local phenomena for a rotor and may not be observable when viewing total rotor thrust parameters. The Reynolds Number effect could probably only be detected if the working section of the rotor was operating at $C_{l_{max}}$ over most of the disc which would be the case in hover for instance.

APPENDIX B - REFERENCES

a. Hoerner, Dr. S. F., Fluid-Dynamic Drag, 1965.

b. von Doenhoff, A. E., NACATN-1283, The Langley Two-Dimensional Low-Turbulence Pressure Tunnel, May 1947.

c. Boeing Report D2-23280, BTWT 833. A low Speed Two Dimensional Vertol Rotor Blade Test, 29 April 1964.

d. Boeing Report D2-24066-1, Boeing Wind Tunnel Test No. 927 - High Speed Force Tests to Determine Section Characteristics of VR-910M-1, Full Scale Airfoil Sections, For Product Improvement of Vertol Divisions CH-47, 22 February 1966.

e. Jacobs, E. N., and Sherman, A., NACA R-586, Airfoil Section Characteristics as Affected by Variations of the Reynolds Number, 1937.

f. Boeing-Vertol Report 114-ET-608, Models CH-47B and CH-47C Aft Rotor System 500 Hour Whirl Test Report, June 1967.

g. Jewel, J. W., Jr., NASA TND-245, Compressibility Effects on the Hovering Performance of a Two-Bladed 10-Foot Diameter Helicopter Rotor Operating at Tip Mach Numbers up to 0.98, April 1960.

h. University of Maryland Wind Tunnel Test 516, Unpublished test data, March 1968.

i. Boeing-Vertol Report D210-10077, Summary of Universal Helicopter Model Wind Tunnel Test Results November 1968 to December 1969; 19 December 1969.

j. Boeing-Vertol IOM 8-7441-1-400, Hover Performance of UHM Blades on Rotor Test Stand (RTS), February 1970.

k. Boeing-Vertol IOM 8-7458-1-293,'Quick-Look'Presentation Model 347 Flight Demonstrator DRTS Wind Tunnel Test (BVWT033), July 1969.

l. Boeing-Vertol Report 114-FT-712, Analysis of CH-47C Performance Flight Test; 20 January 1969.

m. Boeing Report D6-4781, Model 727 Cruise Performance Substantiation as of May 1, 1964, Release Date 1965.

n. Boeing Report D6-22318, Wake Survey Measurements on the 727 Wing and Calibration of an In-Flight Wake and Boundary Layer Probe (BTWT 1166) Release Date 1969.

o. Boeing-Vertol Wind Tunnel Test 048, Unpublished test data, January 1970.

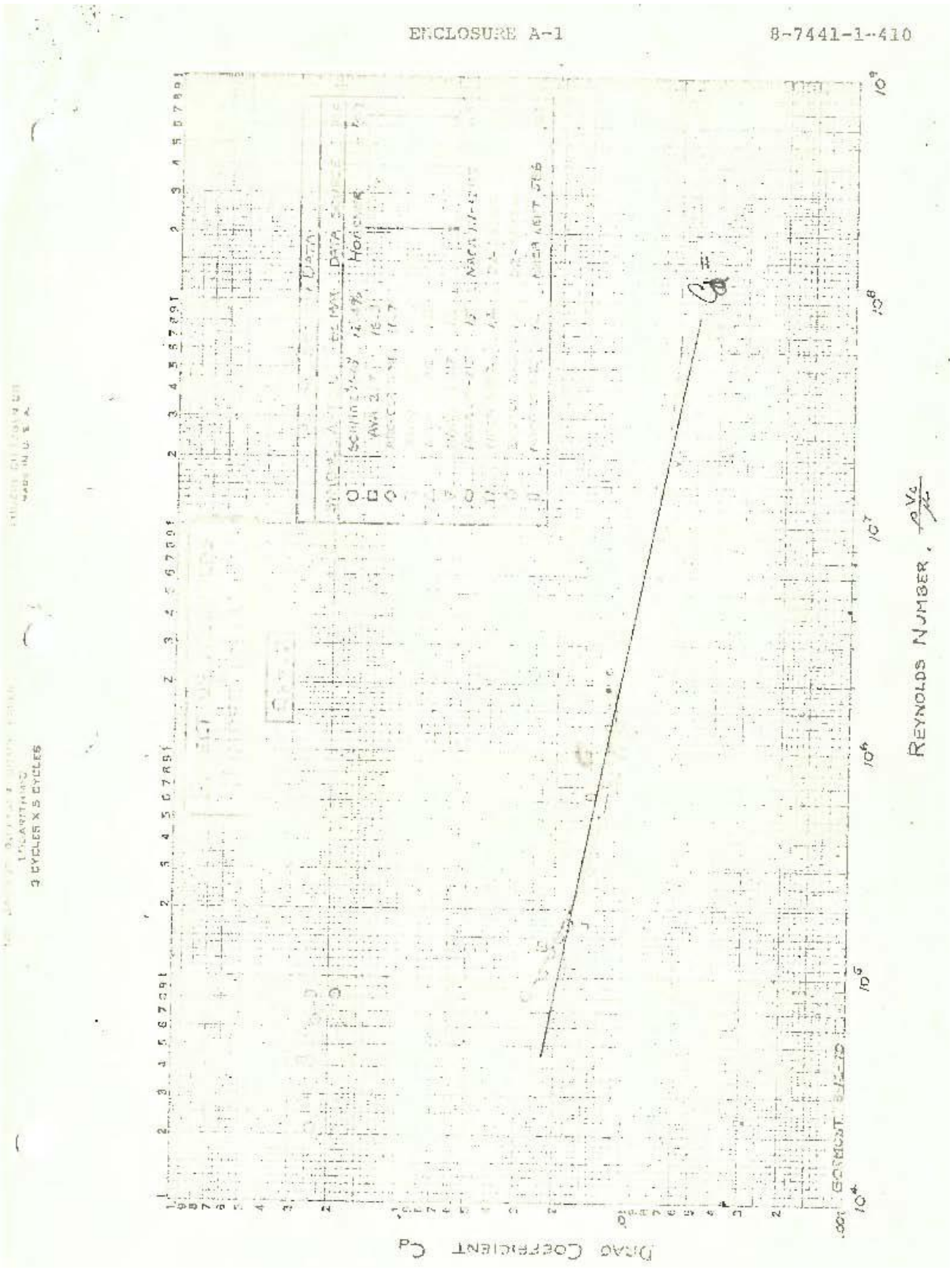
DRAG COEFFICIENT C_D
REYNOLDS NUMBER, $\frac{\rho V d}{\mu}$
3 CYCLES X 5 CYCLES

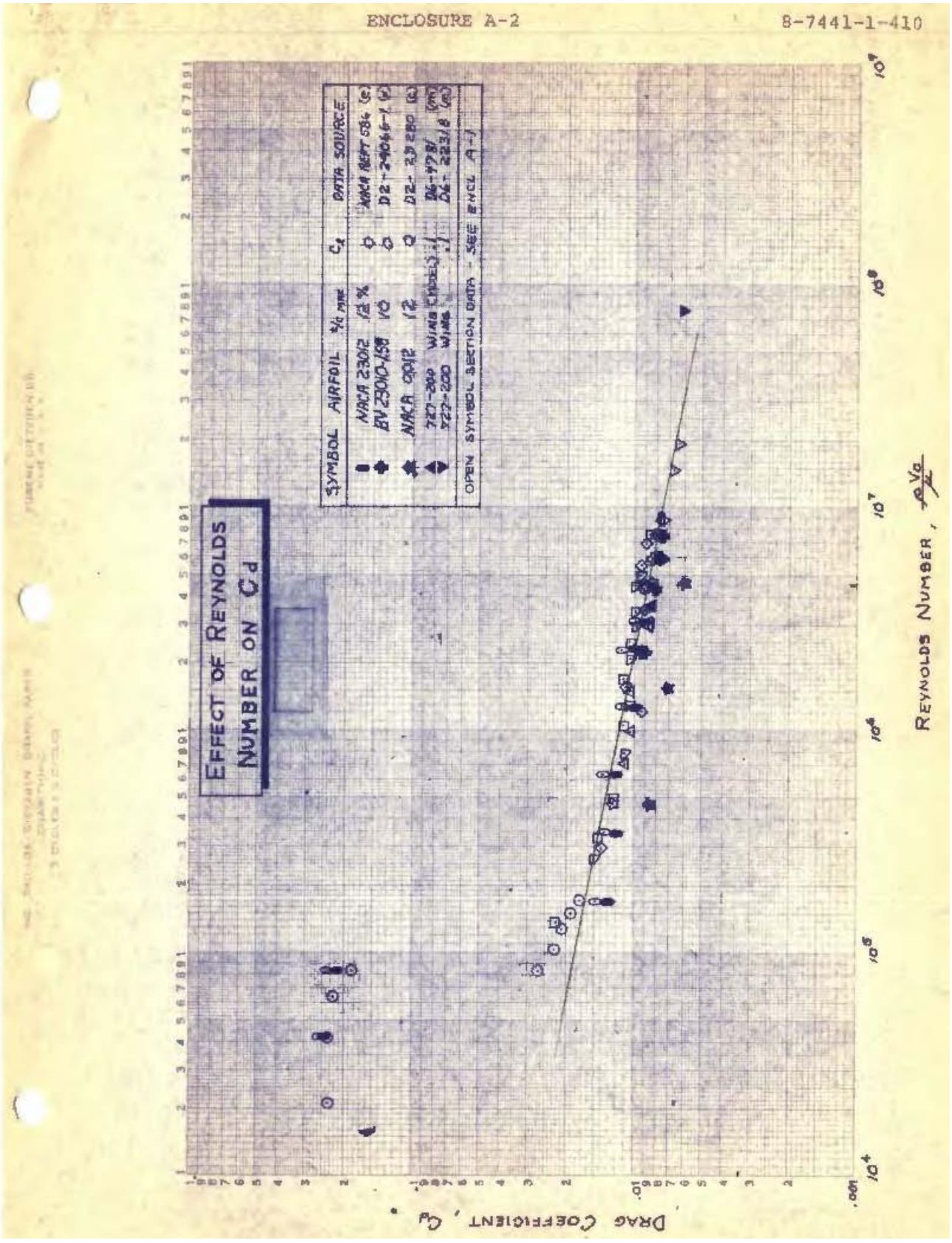
EFFECT OF REYNOLDS NUMBER ON C_d
SYMBOL AIRFOIL t/c mm C_d DATA SOURCE
NACA 23012 12 % NACA REPT 586 (a)
BV 230Q-158 10 D2-24046-1 (b)
NACA 0012 12 D2-23280 (c)
727-200 WING CRUISE D6-9738 (dm)
727-200 WING D6-22318 (dm)
OPEN SYMBOL SECTION DATA - SEE ENCL A-1
DRAG COEFFICIENT, C_d
REYNOLDS NUMBER, $\rho V_0 / \mu$

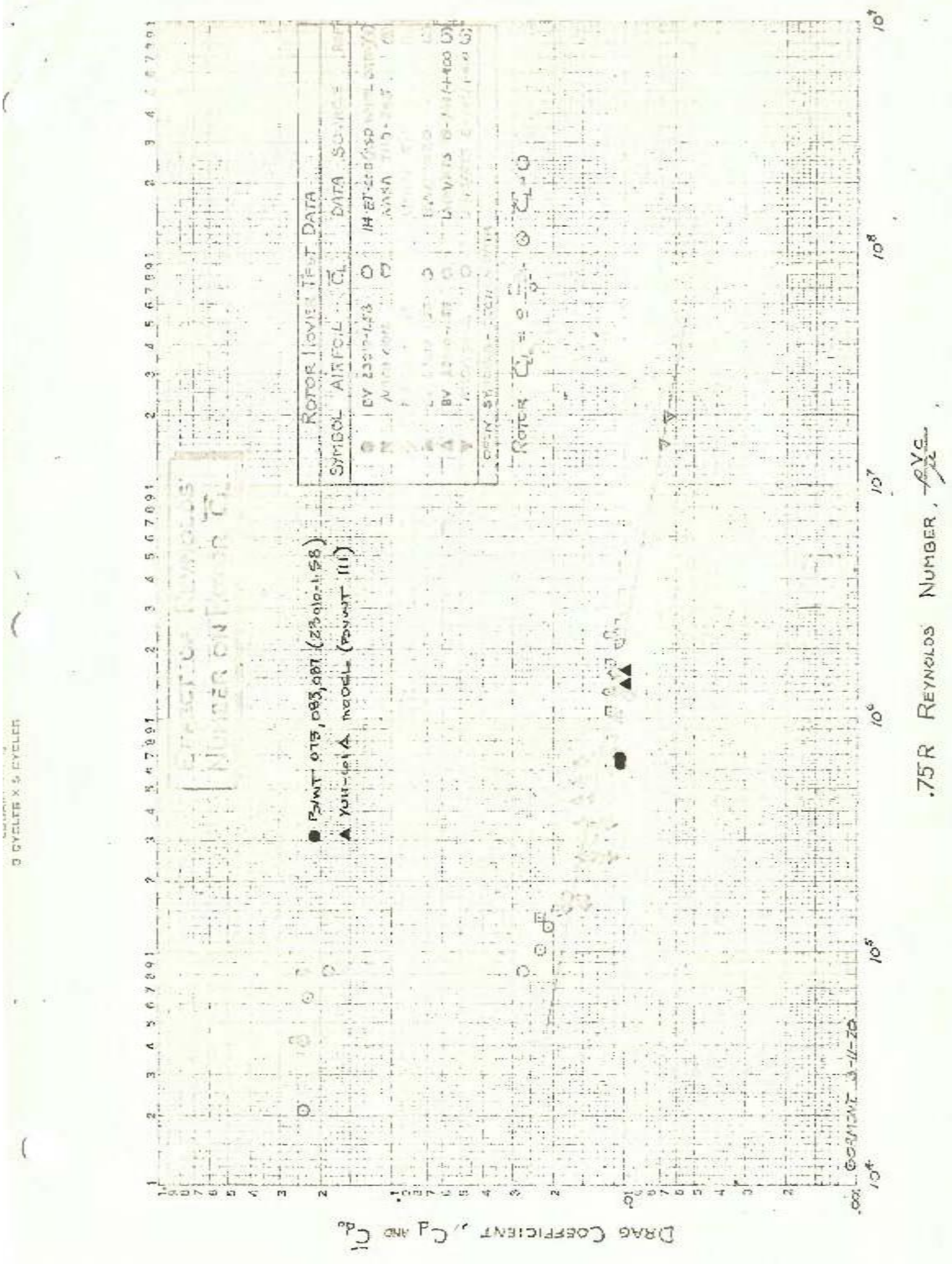
Rotor Hover Test Data
Symbol Airfoil C̄L Data Source
.75R Reynolds Number, ρVc/μ
Drag Coefficient, Cd, and Cd0

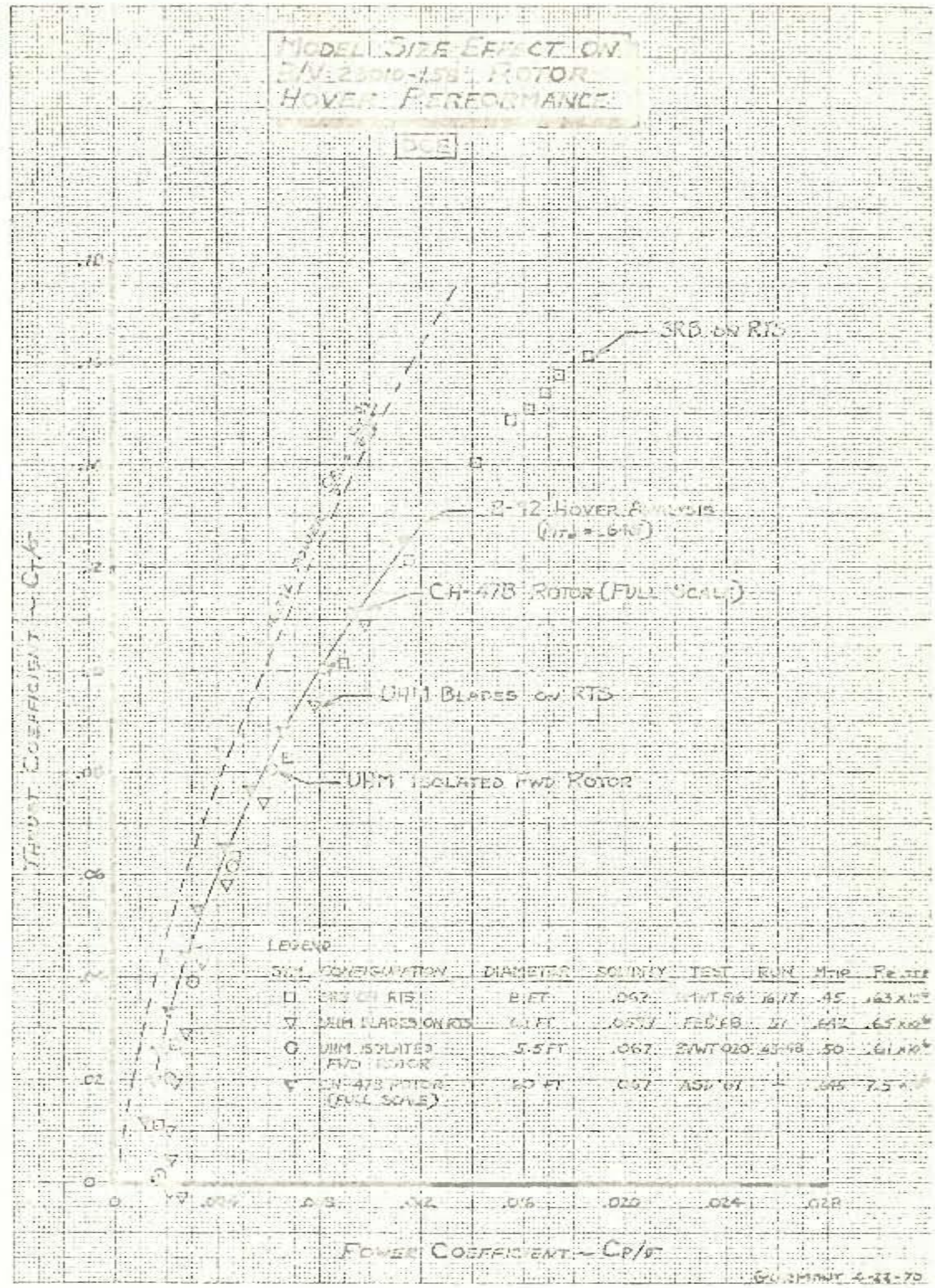
MODEL SIZE EFFECT ON
HOVER PERFORMANCE
3RB ON RTS
2-92 HOVER ANALYSIS
CH-47B ROTOR (FULL SCALE)
UH-1 BLADES ON RTS
UBM ISOLATED FWD ROTOR
THRUST COEFFICIENT ~ CT/σ
POWER COEFFICIENT ~ CP/σ
LEGEND
CONFIGURATION
DIAMETER
TEST
RUN
5.5 FT
.067
.50
(FULL SCALE)
.10
.08
.02
0
.004
.020
.024
.028

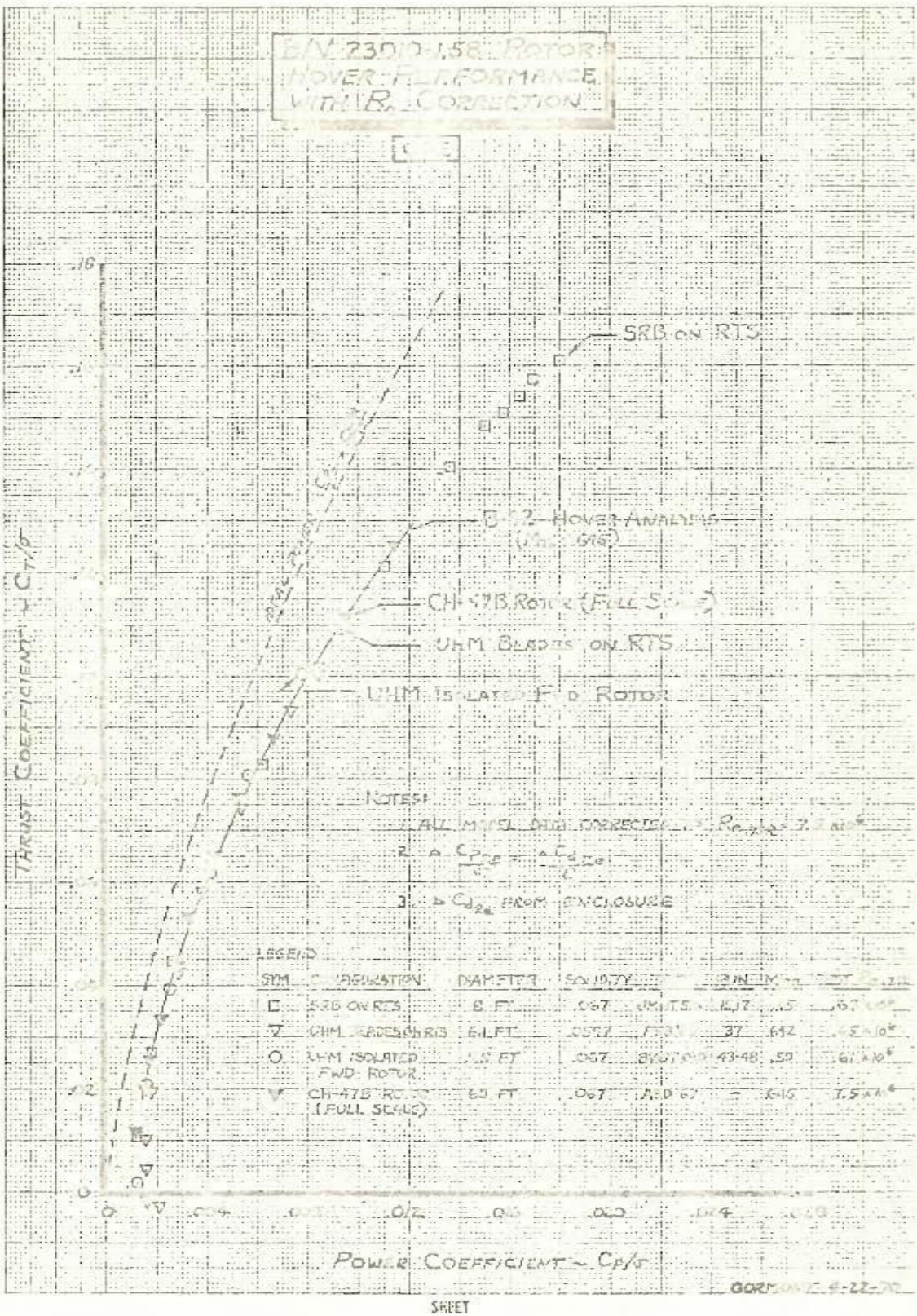

SHEET

ENCLOSURE A-6 NUMBER 8-7441-1-410

REYNOLDS NUMBER EFFECT ON MODEL-FLT TEST CORRELATION

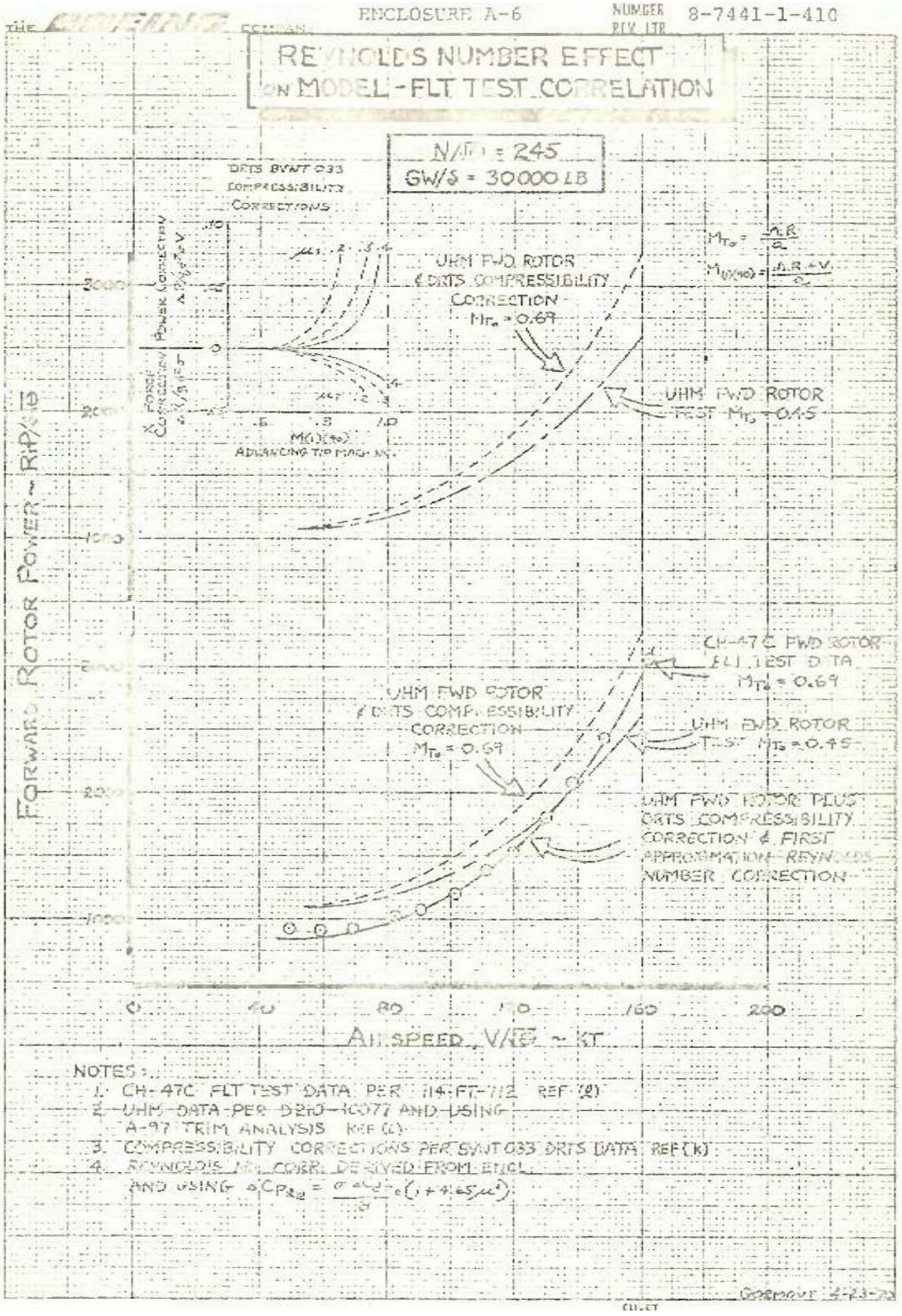

NOTES:
1. CH-47C FLT TEST DATA PER 114-FT-712 REF (g)
2. UHM DATA PER D210-10077 AND USING A-97 TRIM ANALYSIS REF (i)
3. COMPRESSIBILITY CORRECTIONS PER SVWT 033 DRTS DATA REF (k)
4. REYNOLDS NO. CORR. DERIVED FROM ENCL AND USING $\Delta C_{P_{R_e}} = \frac{\sigma a}{8} C_{T_0} \left(1 + 4.65 \mu^2\right)$

THE BOEING COMPANY ENCLOSURE A-7 NUMBER D-7441-1-410 REV LTR

REYNOLDS NUMBER EFFECT ON MODEL-FLT TEST CORRELATION

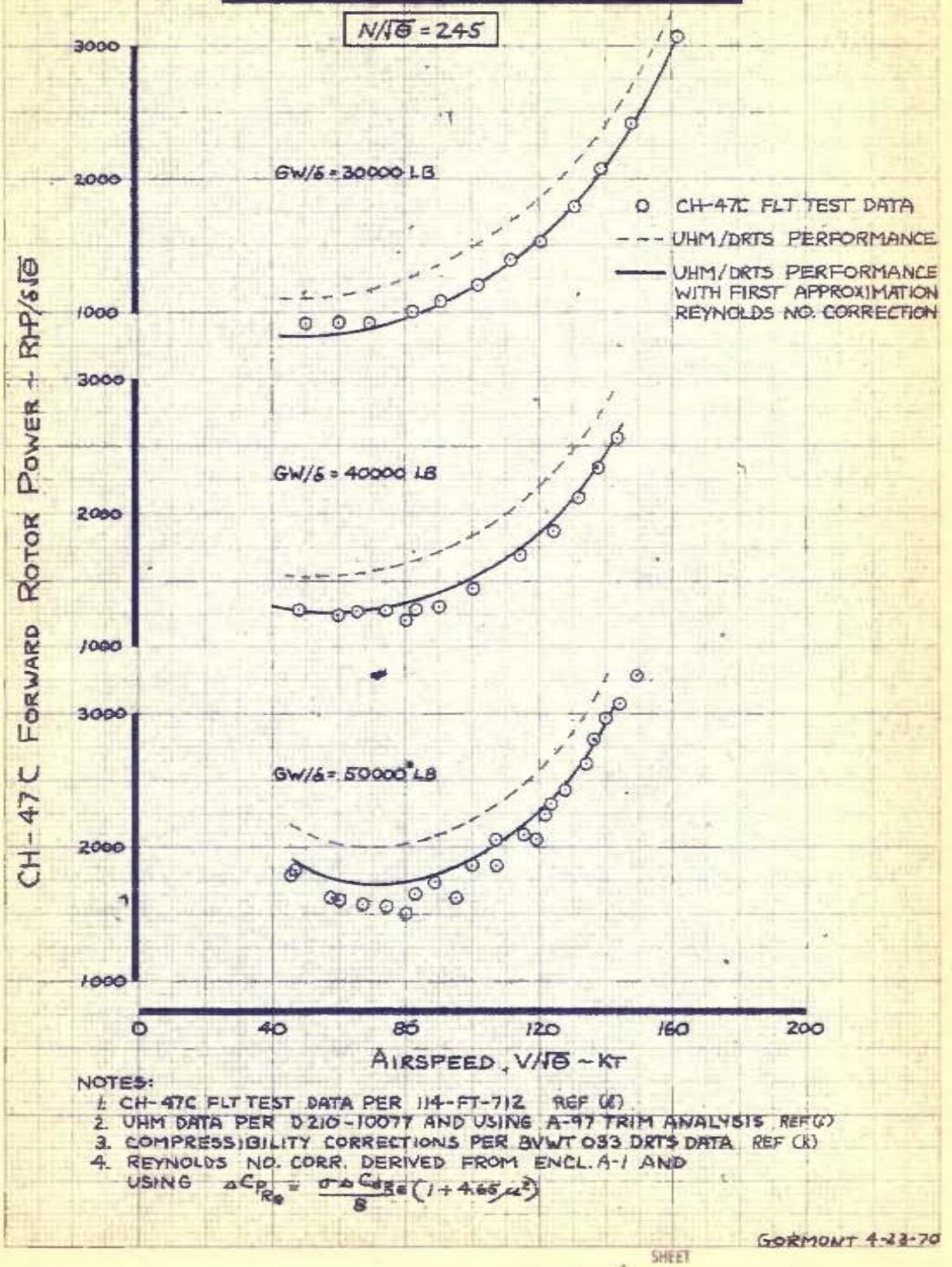

NOTES:
1. CH-47C FLT TEST DATA PER 114-FT-712 REF (A)
2. UHM DATA PER D 210-10077 AND USING A-97 TRIM ANALYSIS REF (C)
3. COMPRESSIBILITY CORRECTIONS PER BVWT 033 DRTS DATA REF (B)
4. REYNOLDS NO. CORR. DERIVED FROM ENCL. A-1 AND USING $\Delta C_{P_{R_e}} = \frac{\sigma \Delta C_{d_{R_e}} (1 + 4.65\mu^2)}{8}$

GORMONT 4-23-70

SHEET

ENCLOSURE A-8 NUMBER 8-7441-1-410

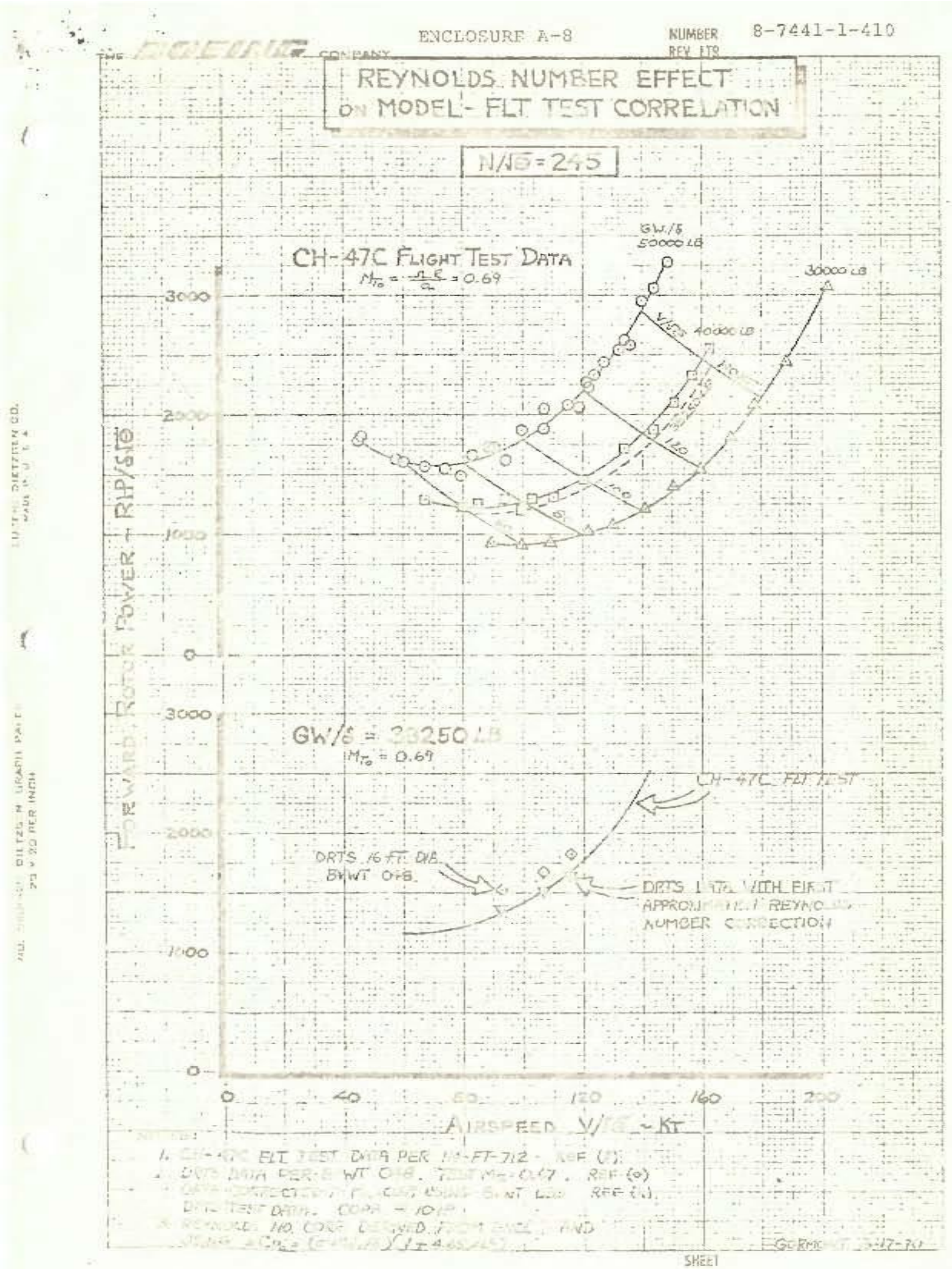

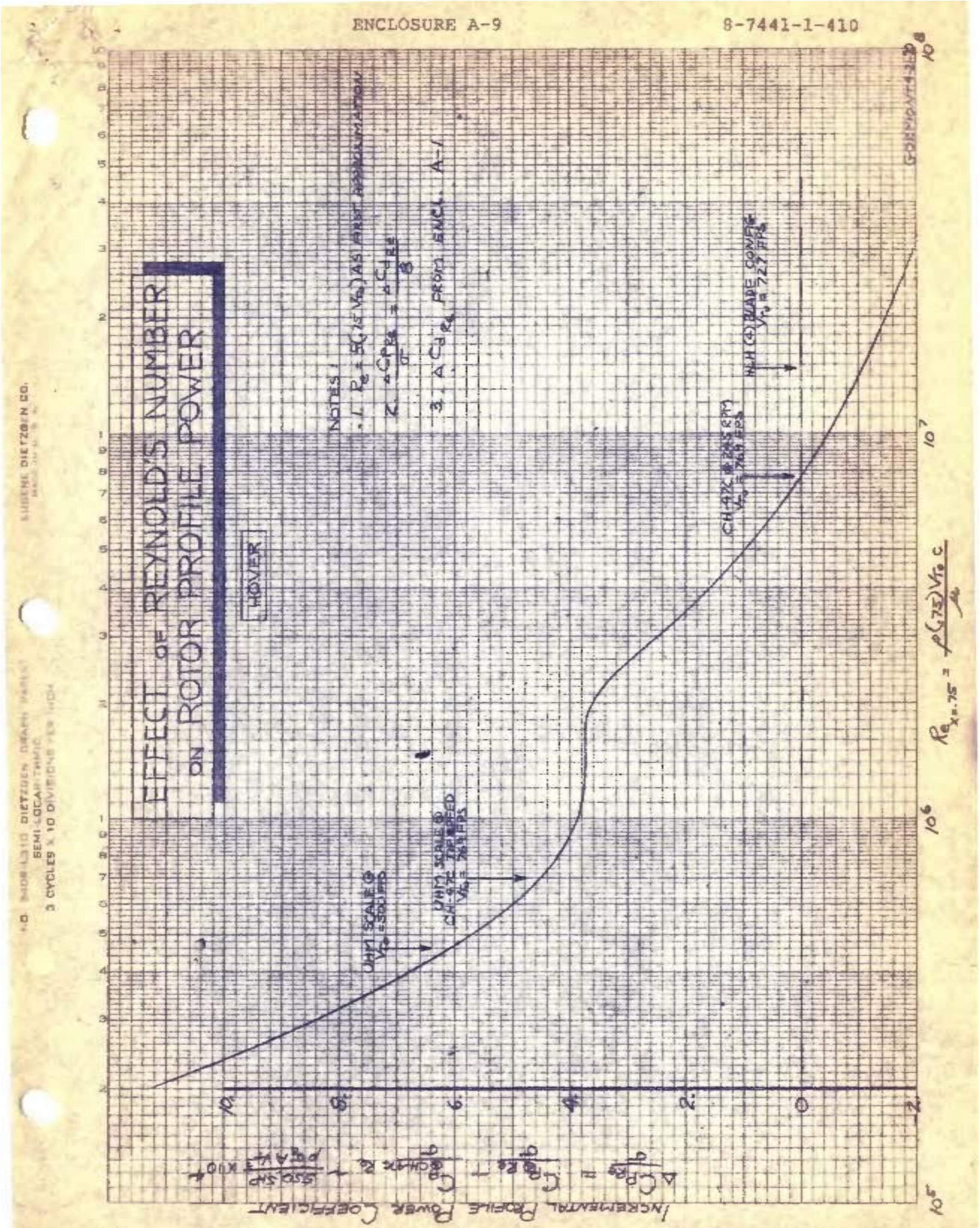
EFFECT OF REYNOLD'S NUMBER ON ROTOR PROFILE POWER
HOVER
NOTES:
3. Δ $C_{d_{Re}}$ FROM ENCL. A-1
INCREMENTAL PROFILE POWER COEFFICIENT
10.
8.
6.
4.
2.
0
-2
10^5
10^6
10^7
10^8

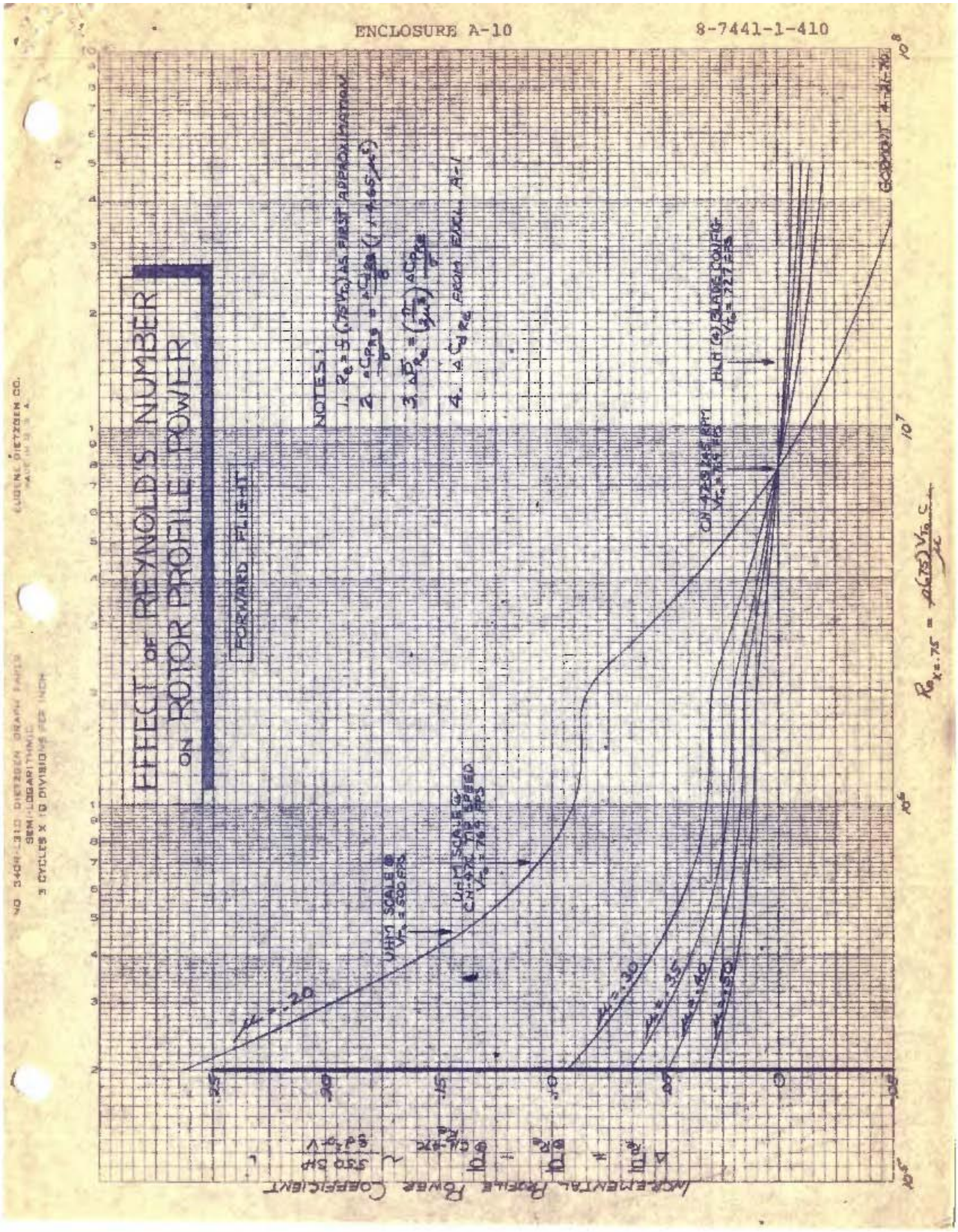
EFFECT OF REYNOLD'S NUMBER ON ROTOR PROFILE POWER
FORWARD FLIGHT
NOTES:
1. $Re = \frac{\rho}{\mu}(V_{TIP})(AS\ FIRST\ APPROXIMATION)$
2. $\frac{\Delta C_{P_{PROFILE}}}{\sigma} = \frac{\pm C_{D_{BASIC}}}{8}(1 + 4.65\mu^2)$
3. $\Delta P_{Re} = \left(\frac{\rho}{\mu V_{TIP}}\right)^{.2} \Delta C_{P_{PROFILE}}$
4. $\pm C_D$ R_e FROM FIGURE A-1
$M_A = .20$
$M_A = .30$
$M_A = .35$
$M_A = .40$
$M_A = .50$
INCREMENTAL Profile Power Coefficient
$\Delta C_{P_{PROFILE}} = \frac{\Delta P_{PROFILE}}{\rho A (\Omega R)^3} \sim \frac{550\,\Delta HP}{\rho A V^3}$
GEORGE W. ZUCKERT 4-24-56